

Assessment of the effects of stretch-injury on primary rat microglia.

by

Michael Christopher Shaughness

Dissertation submitted to the Faculty of the
Neuroscience Graduate Program
Uniformed Services University of the Health Sciences
In partial fulfillment of the requirements for the degree of
Doctor of Philosophy 2021

Distribution Statement

Distribution A: Public Release.

The views presented here are those of the author and are not to be construed as official or reflecting the views of the Uniformed Services University of the Health Sciences, the Department of Defense or the U.S. Government.



UNIFORMED SERVICES UNIVERSITY
 SCHOOL OF MEDICINE GRADUATE PROGRAMS
 Graduate Education Office (A 1045), 4301 Jones Bridge Road, Bethesda, MD 20814



APPROVAL OF THE DOCTORAL DISSERTATION IN THE NEUROSCIENCE GRADUATE PROGRAM

Title of Dissertation: "Assessment of the effects of stretch-injury on primary rat microglia"
 Name of Candidate: Michael C Shaughness
 Doctor of Philosophy
 August 3rd, 2021

DISSERTATION AND ABSTRACT APPROVED:

DATE:

Dr. Yumin Zhang
 DEPARTMENT OF ANATOMY, PHYSIOLOGY, AND GENETICS

8/17/21

Dr. Kimberly R. Byrnes
 DEPARTMENT OF ANATOMY, PHYSIOLOGY, AND GENETICS
 Dissertation Advisor

8/17/21

Dr. Ann Marini
 DEPARTMENT OF NEUROLOGY
 Committee Member

8/18/21

Dr. Zygmunt Galdzicki
 DEPARTMENT OF ANATOMY, PHYSIOLOGY, AND GENETICS
 Committee Member

8/17/21

Dr. Thomas Flagg
 DEPARTMENT OF ANATOMY, PHYSIOLOGY, AND GENETICS
 Committee Member

8/17/21

Date and time of Private Defense:

August 17th, 2021 2:00pm

Date and time of Public Defense:

The author hereby certifies that the use of any copyrighted material in the dissertation entitled:

“Assessment of the effects of stretch-injury on primary rat microglia”

is appropriately acknowledged and, beyond brief excerpts, is with the permission of the copyright owner.



8/22/2021

Michael Shaughness
NEUROSCIENCE PROGRAM
Uniformed Services University
8/19/2021

ACKNOWLEDGMENTS

The successful completion of this dissertation is the combination of an incredible amount of hard work, support and patience. I would first like to thank my advisor, Dr. Kimberly R. Byrnes, whose expertise was invaluable in formulating the research questions and challenging methodology. Your insightful feedback and mentorship guided me to refine my thought process and elevated my writing and scientific fecundity to a previously unimagined level. I want to individually thank the members of my dissertation committee. Thank you Dr. Yumin Zhang, committee chair, your guidance and patience during this journey was greatly appreciated. I knew that I could rely on you to help navigate the challenges that come with getting a Ph.D. and provide encouragement when things (experiments) were not going well. To Dr. Ann. Marini, thank you for sharing your experiences regarding the cell culture technique and life lesson in academia. This was a new technique and I greatly appreciated all of the insight you provided. Last but not least, I am truly grateful that you allowed me to use your cell culture lab. I want to thank Dr. Flagg for his early encouragement and belief in my project and the assistance with preparing my proposal. And last but not least, Dr. Zygmunt Galdzicki, thank you for all the hallway meetings that started with a neuroscience question and invariably ended with discussing football (soccer). I will miss our discussions and will forever know where I buy Accutase.

To the members of the Byrnes' lab past and present, you have been unconditionally supportive and a joy to work with. I will cherish and miss the times we shared- Ramona Von-Leden Ph.D., Col. John Yauger Ph.D., LTC John Reed Ph.D., Nicole Hockenbury, Sarah Bermudez, Deanna Acs, Sean Collier, Austin Smith and

Nathan Pierron and the entire graduate department. Your guidance and support has been exemplary.

A special thanks goes to the entire Burnett lab- Nikki McCormick Ph.D., Guzal Kharyrullina Ph.D., thank you for your patience with teaching me the RT-PCR assay. Additionally, I want to thank Ann Mae Dileonardi Ph.D. from the Army Research Lab (ARL) for providing the strain-rate information for the CIC II model.

I can confidently say that my journey would have been much more arduous if it wasn't for my fellow class mates Guzal Kharyrullina Ph.D., Donald (DJ) Bradshaw Ph.D., Kathleen Whiting, and Alexandra Yaszemski. Thank you for your kindness and thoughtful guidance throughout our journey.

This work would not have been possible without the support of the Center for the Study of Traumatic Stress (CSTS). The generous grant funded this project and provided the opportunity to travel and share my work with the neurotrauma community.

My decision to pursue graduate school was motivated and supported by the good Dr. Ahlers Ph.D., who's patience and mentoring greatly influenced my decisions to attend USU. Additionally, I want to extend my gratitude to Dr. Grunberg Ph.D. for providing his insight and sharing his experience in academia and guiding me through the admission process.

Finally, I want to thank my loving family and friends for their support.

DEDICATION

This dissertation is dedicated to my family. To my wife and best friend, Rania Abutaraboush Ph.D., thank you for your unconditional support through the highs and lows of my journey. Thank you to my Mom and Dad who supported, encouraged and inspired me.

ABSTRACT

Assessment of the effects of stretch-injury on primary rat microglia

Michael C Shaughness, Doctor of Philosophy in Neuroscience, 2021

Thesis directed by: Kimberly R. Byrnes, Ph.D., Professor, Department of Anatomy, Physiology, and Genetics

Mechanical stretch-injury is a prominent force involved in the etiology of traumatic brain injury (TBI). It is known to directly cause damage and dysfunction in neurons, astrocytes, and endothelial cells. However, the deleterious effects of stretch-injury on microglia, the brain's primary immunocompetent cell, are currently unknown. The Cell Injury Controller II (CICII), a validated model of cellular neurotrauma, induced a mechanical stretch-injury in primary rat microglia. Statistical analysis utilized student t-test and one and two way-ANOVAs with Tukey's and Sidak's multiple comparisons, respectively. Cells exposed to stretch-injury showed no signs of membrane permeability, necrosis, or apoptosis, as measured by media-derived lactate dehydrogenase (LDH) and cleaved-caspase 3 immunocytochemistry, respectively. Interestingly, injured cells displayed a functional deficit in nitric oxide (NO) production, identified by a media assay, at 6, 12, 18, and 48 hours post-injury. Coinciding with the decreased media levels of NO, iNOS (inducible nitric oxide synthase) protein expression was significantly decreased at twelve hours after injury. Furthermore, gene expression analysis revealed the expression of inflammatory cytokines IL-6 and IL-10 and enzyme arginase-1 was significantly down-regulated at 12 hours post-injury. Using a cell exclusion zone assay,

time-course evaluation of microglial cell migration showed stretch-injured cells display decreased migration into the exclusion zone at 48 and 72 hours post-stretch. Lastly, coinciding with the functional immune deficits was a significant change in morphology, with process length decreasing and cell diameter increasing following an injury at 12 hours. Taken together, the data demonstrate that stretch-injury produces significant alterations in microglial morphology and function, which may have a marked impact on their response to injury or their interaction with other cells. The $\alpha 5\beta 1$ integrin mediates microglial attachment to fibronectin via the RGD binding peptide. We found that blocking the $\alpha 5\beta 1$ integrin with a commercially available RGD peptide mimicked the stretch-induced morphological alterations and functional deficits in primary rat microglia. Like injured cells, RGD treatment resulted in significant decreases in media nitric oxide (NO) levels, iNOS expression and migration deficits. The integrin-associated signaling enzyme, focal adhesion kinase (FAK), autophosphorylates tyrosine residue 397 upon integrin ligation and mediates multiple downstream cellular processes. Phosphorylation of the tyrosine 397 residue on FAK is significantly decreased following a stretch-injury and when treated with an RGD peptide. Post-injury treatment with 20nM of ZINC 40099027, an activator specific to the tyrosine 397 residue, rescued the stretch-induced decrease in FAK phosphorylation without affecting the total expression of FAK. Furthermore, treatment of stretch-injured cells with ZINC 40099027 ameliorated the injury-induced decrease in media NO levels, iNOS expression and inflammatory associated gene expression. Additionally, treatment alleviated morphological changes observed after stretch-injury and restored normal migratory behavior to control groups. In

conclusion, these data suggest that the $\alpha 5 \beta 1$ integrin/FAK pathway partially mediates the stretch-injured phenotype in microglia.

TABLE OF CONTENTS

LIST OF TABLES.....	xii
LIST OF FIGURES	xiii
CHAPTER 1: Introduction	17
What is Traumatic Brain Injury (TBI)	17
Microglia and TBI.....	17
Microglial activation.....	18
Morphology.....	19
Soluble factors and receptor expression	20
Microglia M1/M2 polarization	21
Microglia in human TBI	22
Microglia in <i>in vivo</i> models of TBI.....	24
Stretch-injuries.....	26
In vitro models	27
Neurons	27
Astrocytes	28
Endothelial cells.....	29
Integrins and mechanotransduction	31
$\alpha 5 \beta 1$ integrin and fibronectin.....	32
FAK pathway	34
Hypothesis and specific aims.....	34
Chapter 2: Assessment of the effects of stretch-injury on primary rat microglia.....	36
Abstract.....	36
Introduction.....	37
Methods.....	39
Cell culture.....	39
Stretch-injury	39
Lipopolysaccharide (LPS) and Etoposide treatment.....	40
Reactive oxygen species (ROS) assays.....	40
Cell death assays.....	41
Nitric oxide (NO) measurement.....	41
Immunocytochemistry	41
RNA isolation and gene analysis	42
Migration assay and morphological evaluation	43
Phagocytosis assay.....	44
Statistical analysis.....	45
Results.....	46
Stretch-injury does not increase LDH at multiple time points or cleaved caspase-3 at 12 hours post-injury	46

NO release and iNOS expression is significantly down-regulated following stretch-injury	48
ROS is unaffected by stretch-injury.....	49
Genes associated with microglia activation are significantly down-regulated or unaffected following exposure to stretch-injury	51
Morphology is significantly altered in response to stretch-injury	52
Migration is impaired substantially following stretch-injury	53
Phagocytosis is not affected by injury	54
Stretch-injury does not prime or depress microglial NO release or alter LDH release when exposed to a subsequent LPS challenge.....	55
Discussion	58
Stretch-injury does not affect microglial viability	58
NO production is impaired following injury	59
ROS production is unaffected by injury	61
Inflammatory gene expression is significantly decreased after stretch-injury.....	62
Migration is impaired after a stretch-injury	63
Stretch-injury alter microglia morphology	63
Injury does not affect phagocytosis	64
Injury does not prime microglia to a subsequent LPS challenge.....	65
Conclusions:.....	66
Chapter 3: The $\alpha 5\beta 1$ integrin/FAK pathway partially mediates stretch-induced deficits in primary rat microglia	67
Abstract.....	67
Introduction.....	67
Methods.....	70
Cell culture.....	70
Stretch-injury	70
RGD peptide and FAK activator treatment	71
Nitric oxide (NO) measurement.....	71
Immunocytochemistry	72
Protein quantification.....	72
RNA isolation and gene analysis	73
Migration assay and morphological evaluation	74
Statistical analysis.....	75
Results.....	76
$\alpha 5\beta 1$ integrin protein and gene expression of primary rat microglia are unaffected following stretch-injury.	76
RGD-blocking peptide reduces media NO levels, iNOS expression and FAK phosphorylation.....	77
Blocking integrin-binding with an RGD blocking peptide alters inflammatory gene expression.	80
Migration is significantly impaired following the administration of an RGD blocking peptide.....	81
Treatment with FAK activator rescues media NO levels, iNOS expression and FAK phosphorylation.....	82

.....	85
Injury-induced morphological alterations are ameliorated with 20nM FAK activator treatment.	85
Migration impairments following injury are ameliorated following treatment with FAK activator.....	87
Gene expression of stretch-injured microglia returns to control levels following treatment with 20nM of FAK activator.	88
Discussion.....	90
Conclusions:.....	99
Chapter 4: Discussion.....	100
Introduction:.....	100
REFERENCES	113

LIST OF TABLES

Table 1. Selected gene sequences for RT-PCR	42
Table 2. Selected gene sequences for RT-PCR	73

LIST OF FIGURES

- Figure 1. $\alpha 5\beta 1$ attachment to fibronectin. Following ligation, -associated FAK autophosphorylates and assembles with other structural proteins linked to the actin cytoskeleton. 31
- Figure 2. Stretch-injury does not affect primary microglia viability. A) Primary microglia exposed to a stretch-injury of 5psi show no significant difference in media LDH compared to control cells. Injured condition normalized to controls (set as 1.0). B) Representative sample of one trial presented. Scale bar is 50 μ m. C) Immunocytochemistry evaluation of cleaved caspase-3 indicates no significant difference between injured and control cells. Points represent individual data points. N=3/group. Error bar represents \pm SD. 47
- Figure 3. Stretch-injured primary microglia display decreased NO production and iNOS expression. A) Media assays show injured cells produce significantly less NO when compared to uninjured cells at 6, 12, 18, and 48 hours after injury. Injured condition normalized to controls set at 1.0. All groups were compared using two-way ANOVA with Sidak's post-test. * $p < 0.05$, ** $p < 0.01$. N=3/group. Error bars represent \pm SD. B) Stretch-injury does not significantly alter iNOS gene expression twelve hours post-injury. Points represent individual data points. C) Representative sample of one trial presented. Scale bar is 50 μ m. D) Quantification of pixel density shows stretch-injury significantly down-regulates iNOS protein expression at 12 hours post-injury. N = 3/group. Points represent individual data points. Error bars represent \pm SD. Groups were compared using an unpaired t-test, ** $p < 0.01$ 49
- Figure 4. ROS production is not altered by stretch-injury. A) Cellular and media ROS production is not altered at 12 or 24 hours after stretch-injury. All groups were compared using one-way ANOVA. N=3/group. Experimental groups were normalized to control values. B) Oxidative stress, measured by 3-NT, is not significantly altered at twelve hours following stretch-injury. C) Representative blots for 3NT. D) Stretch-injury does not alter the expression of NOX2/gp91 twelve hours after injury. E) Representative blots for gp91. N=3/group. All groups were compared using an unpaired t-test. Points represent individual data points. Error bar represents \pm SD. 50
- Figure 5. Injured cells display decreases in both pro and anti-inflammatory genes. Stretch-injury decreased expression of pro-inflammatory associated gene IL-6 (A) and reduced expression of anti-inflammatory associated gene ARG1 (B) and IL-10 (C) at 12 hours after injury. Gene expression of experimental groups normalized to controls set as 1.0. Stretch-injury did not alter anti-inflammatory genes TGF β (D) and CD206 (E) or pro-inflammatory genes CD86 (F) and IL-1 β (G). H) Representative sample of one trial presented. Scale bar is 50 μ m. I) Quantification of pixel density shows stretch-injury, compared to control cells, significantly down-regulates arginase-1 protein expression at 12 hours post-injury. N = 3/group. Points represent individual data points. Error bars represent \pm SD. Groups were compared using an unpaired t-test, * $p < .05$, ** $p < 0.01$ 52
- Figure 6. Stretch-injury significantly alters microglia morphology at 12 hours post-injury. A) Representative images of phase contrast micrographs twelve hours post-injury.

- Scale bar is set to 50 μ m. The total cell count (B) and average process number per cell (C) are unaffected following stretch-injury. D) Injured cells display a significantly larger cell body area compared to controls. E) The average process length is significantly decreased compared to controls. N=3/group. All groups were compared using unpaired t-test, * $p < .05$, ** $p < .01$. Bars represent mean \pm SD. 53
- Figure 7. Migration is significantly decreased following a stretch injury at 48 and 72 hours after injury. A) Representative phase-contrast micrographs of the cell exclusion zone assay. B) Stretch-injury significantly decreases the number of cells that migrate into the exclusion zone at 48 and 72 hours post-injury compared to the control group. N=3/group. Two-way ANOVA with Sidak's multiple comparison test, *** $p < .001$, **** $p < .0001$. Bars represent mean \pm SD 54
- Figure 8. Stretch-injury does not alter phagocytic activity. A) Representative images of latex beads conjugated with FITC-IgG (green) were incubated for 4 hours with control, stretch-injured and LPS treated primary microglia cells. Scale bar set to 50 μ m. B) Quantitation of phagocytosed beads demonstrated that stretch-injury did not alter phagocytic activity compared to control, uninjured cells at 12 hours post-injury (8 hours following stretch-injury cells were treated with FITC-IgG for 4 hours). The LPS positive control (100ng/mL) displayed a strong trend towards phagocytosing significantly more beads when assessed at 48 hours post-treatment (44 hours after LPS treatment cells were incubated with FITC-IgG for 4 hours). ... 55
- Figure 9. Stretch-injury does not alter microglia NO or LDH responses to subsequent LPS stimulation. A) Stretch-injury before LPS treatment does not induce a significant difference in LDH release between LPS treated and stretch-injury plus LPS treatment. Both LPS and LPS plus stretch-injury significantly increase LDH release at 24, 48, and 72 hours post-treatment. B) Pre-stretch-injury does not alter NO responses when subsequently exposed to LPS. LPS and stretch-injury plus LPS both significantly upregulate NO at 48 and 72 hours post-treatment. N=3/group. One-way ANOVA with Dunnett's post-test. * $p < 0.05$, ** $p < 0.01$, *** $p < 0.001$, **** $p < 0.0001$. Experimental groups are normalized to the control group set at 1.0. Error bars represent mean \pm SD..... 57
- Figure 10: Stretch-injury does not alter $\alpha 5\beta 1$ integrin gene or protein expression twelve hours after injury. A) There is no effect of stretch-injury on $\alpha 5$ protein expression. B) Representative $\alpha 5$ western blot image. C) Stretch-injury does not alter the expression of $\beta 1$ protein expression. D) Representative $\beta 1$ western blot image. E) Gene expression of $\alpha 5$ does not change following injury. F) Stretch-injured microglia $\beta 1$ gene expression is unchanged following injury. Unpaired student's t-test. N=3. Bar represents standard deviation. 77
- Figures 11. Treatment with RGD peptide reduces media NO and iNOS expression. A) Treatment with .1mg/mL, .2mg/mL and .3mg/mL significantly reduced NO media levels forty eight hours after stretch-injury. Absorption values of the injured condition were normalized to controls (set as 1.0). B) iNOS expression is significantly downregulated forty-eight hours after treatment with .2mg/mL RGD peptide. C) Representative images of immunocytochemistry for iNOS expression forty-eight hours after treatment. All groups were compared using two-way ANOVA with Dunnett's post-test. * $p < 0.05$, ** $p < .01$. N=3/group. Error bars represent \pm SD..... 79

- Figure 12. Treatment with .2mg/mL RGD peptide significantly decreases phosphorylation of tyrosine residue 397 forty-eight hours post-treatment. A) Representative images of pFAK western blot. B) Representative images of FAK western blot. C) Blocking integrin-binding with .2mg/mL of an RGD peptide significantly decreases FAK phosphorylation forty-eight hours after treatment. D) Treatment does not alter FAK expression. E) The ratio of pFAK to total FAK has significantly decreased post-treatment at forty-eight hours. All groups were compared using a one-way ANOVA with Tukey's post-test. * $p < 0.05$. N=3/group. Error bars represent \pm SD. 79
- Figures 13. RGD peptide treatment significantly down-regulated iNOS gene expression 48 hours after treatment. Treatment with .2mg/mL RGD peptide altered inflammatory associated gene expression at 48 hours post-treatment. Treatment decreased expression of pro-inflammatory associated gene iNOS. A) 48 hours after treatment. Gene expression of experimental groups normalized to controls set as 1.0. Treatment did not alter anti-inflammatory genes Arg1 (E), IL-10 (F), CD206 (G) and TGF β (H) or pro-inflammatory genes IL-6 (B), CD86 (C), and IL-1 β (D). N = 3/group. Points represent individual data points. Error bars represent \pm SD. Groups were compared using an unpaired t-test, * $p < 0.05$ 81
- Figure 14. Migration is significantly decreased following RGD peptide treatment at 48 and 72 hours after injury. A) Representative phase-contrast micrographs of the cell exclusion zone assay. Black arrows indicate quantifiable cells. B) RGD peptide treatment significantly decreases the number of cells that migrate into the exclusion zone at 48 and 72 hours post-injury compared to the control group. N=3/group. Two-way ANOVA with Sidak's multiple comparison test, * $p < 0.05$. Bars represent mean \pm SD. Scale bar is set to 200 μ m. 82
- Figure 15. Six-hour post-injury treatment with 20nM FAK activator rescues reduction in FAK phosphorylation. A) Representative western blot images for pFAK. B) Representative images for FAK. C) Stretch-injury significantly reduces FAK phosphorylation twelve hours post-injury and six-hour post-injury treatment with a FAK activator rescue FAK phosphorylation. Treatment only does not significantly alter FAK phosphorylation. D) FAK expression is unaffected by injury or treatment at twelve hours post-injury. E) The ratio of pFAK to total FAK is not significantly altered by injury, treatment or combination. However, there is a strong trend of injury decreasing the ratio and treatment restoring it. All groups were compared using a one-way ANOVA with Tukey's post-test. * $p < 0.05$. N=3/group. Error bars represent \pm SD. 84
- Figure 16. Treatment with a 20nM FAK activator rescues the stretch-induced down-regulation of iNOS. A) Representative iNOS immunocytochemistry images. B) Stretch-injury significantly reduces iNOS expression 12 hours after injury compared to controls. Treatment with 20nM FAK rescues the stretch-induced reduction in iNOS expression compared to injured cells twelve hours after injury. C) Stretch-injured cells display less NO media than controls, and treatment with 20nM of a FAK activator six hours post-injury rescues the injury-induced decrease of NO media levels. FAK treatment only did not alter media NO levels compared to control cells. Absorption values of the injured condition were normalized to controls (set as

1.0). All groups were compared using a one-way ANOVA with Tukey's post-test. * $p < 0.05$. N=3/group. Error bars represent \pm SD. 85

Figure 17. Treatment with 20nM of a FAK activator, six hours after injury, restores stretch-injured morphological deficits. A) Representative phase-contrast microscopy images at 20x. Scale bar represents 50um B) Cell diameter significantly increases after injury, and treatment with 20nM FAK activator rescues the injury-induced increase. C) Stretch-injury significantly reduces average process length compared to controls. Treatment with a 20nM FAK activator does not significantly increase process length following injury. However, there is a strong trend towards increasing process length. N=3/group. All groups were compared using a one-way ANOVA with Tukey's post-test, * $p < 0.05$. Bars represent mean \pm SD..... 86

Figure 18. Treatment with 20nM of FAK activator rescues stretch-induced migratory deficits. A) Representative phase-contrast microscopy images of cell exclusion zone assay. B) Stretch-injury significantly reduces the number of cells in the exclusion zone 72 hours post-injury. Treatment with 20nM of FAK activator ameliorates injury-induced reduction of cells migrating into the exclusion zone compared to controls. N=3/group. Two-way ANOVA with Tukey's multiple comparison test, * $p < 0.05$, ** $p < 0.01$. Bars represent mean \pm SD. Scale bar is 200um. 88

Figure 19. Treatment with 20nM FAK treatment rescues stretch-induced down-regulation of inflammatory gene expression. Stretch-injury significantly reduced pro-inflammatory and anti-inflammatory associated genes IL-6 (A) and IL-10 (B) expression, respectively. Notably, injured cells displayed a non-significant decreased expression of Arg1 (C). Injured cells treated with 20nM of a FAK activator restored the stretch-injured suppressed gene expression of IL-6 and Arg1. N=3/group. One-way ANOVA with Tukey's post-test. * $p < 0.05$, ** $p < 0.01$. Experimental groups are normalized to the control group. For gene expression analysis, all experimental group changes are represented as fold changes compared to the control group. Error bars represent mean \pm SD. 90

Figure 20. Standard integrin binding and integrin signaling after injury. Binding activates intracellular FAK phosphorylation and facilitates canonical gene expression, NO production, migration and morphology. After a stretch-injury, FAK phosphorylation and gene expression, NO production and migration are decreased; additionally, morphology is altered. 108

CHAPTER 1: Introduction

What is Traumatic Brain Injury (TBI)

There are nearly 2.5 million annual traumatic brain injury cases (TBI) in the United States, and this is associated with a reported economic burden of almost 78 billion dollars (198). TBI is defined as an event in which an external force acts on the skull, either directly or indirectly, resulting in a rapid redistribution of forces that produce an immediate mechanical deformation of sensitive brain parenchyma. The resulting mechanical deformation subjects the brain tissue to damaging strain and compressive strengths, leading to heterogeneous outcomes depending on the individual mechanical properties that vary by brain region, cell type, and sub-cellular structure (98). TBI is composed of two injury phases, the primary and secondary. The primary injury results from the initial traumatic force and is immediate, irreversible and unamenable to conventional therapies. Within minutes to hours, secondary injury cascades are initiated, including ischemia, hypoxia, edema, blood-brain barrier (BBB) permeability, excitotoxicity, apoptosis/necrosis and neuroinflammation. The majority of deaths resulting from a TBI are due to the secondary injury phase and represent an opportunity for therapeutic intervention (171).

Microglia and TBI

A secondary injury process that has garnered interest in recent years is neuroinflammation. This process is mediated by astrocytes, microglia, endothelial cells and infiltrating peripheral immune cells that produce factors, such as cytokines, chemokines, reactive oxygen and nitrogen species and secondary messengers, that

orchestrate the immune response to restore the brain to pre-insult homeostasis (174). Microglia, the brain's innate immune cell, initiate and mediate the neuroinflammation response to neurotrauma. It is initiated by interacting with soluble factors released from damaged and dying cells and directly interacting with compromised and dead cells (50). In the context of neurotrauma, the initial function of the immune response is to contain the damage site and remove, via phagocytosis, dead and damaged cells, cellular debris and toxic byproducts to minimize the expansion of the injury site. Following this initial phase, immunomodulatory, neurotrophic and extracellular matrix (ECM) remodeling factors are produced to resolve the immune response and restore cellular viability and matrix integrity to the affected area (204). The degree of neuroinflammation depends on the primary injury, duration, and mode. Microglia are chronically activated after a single insult in humans (160) and multiple animal models of TBI (13; 42; 122). The persistent activity of the inflammatory response is associated with secondary processes such as apoptosis and necrosis, glutamate excitotoxicity, ischemia, mitochondrial dysfunction and electrolyte imbalances (128). Furthermore, their chronic activation contributes to the harmful effects of prolonged inflammation in the post-TBI brain (20; 105; 108). Currently, the mechanism(s) that mediate persistent microglial activation is unknown (174).

Microglial activation

Microglia are derived from primitive yolk sac myeloid progenitors that migrate to the brain at the early stages of embryonic development before maturation of the BBB (66). The brain's microglial population is maintained through a self-renewal process, without contributions from the peripheral monocyte population (64; 73). In the healthy,

non-injured brain, microglia have a small cell body with multiple long slender processes that survey the extracellular environment for homeostatic disruptions through cell surface receptors (12). During development, they support neural maturation through two processes: phagocytosis and the release of diffusible factors. Studies in mice show two main periods where microglia phagocytose synapses in the dorsolateral geniculate nucleus of the thalamus (dLGN). The first is during the early neonatal period after synapses are initially formed, and the second is in the juvenile phase, where fine connections are pruned (173). Microglia phagocytose ECM proteins in the adult mouse brain via an IL-33 receptor mechanism that facilitates plasticity and maintains synapse integrity (151). Microglia support neurogenesis and promote cellular viability via the production and release of insulin-like growth factor (IGF1) and cytokines such as TNF- α , IL-1 β and IL-6 (71; 206). Additionally, they promote synaptic spine formation by producing and releasing IL-10 and brain-derived neurotrophic factor (BDNF) (119; 156). Lastly, microglia mediate vascular network development via proangiogenic TGF- β signaling (52).

Morphology

Following activation, microglia retract their processes and transform from a small, rounded cell diameter to a more extensive, irregular, amoeboid morphology with few to no processes and a significantly increased soma diameter (48; 185). A standard marker used to identify microglial activation and provide exceptional visualization of morphological changes is the ionized calcium-binding adaptor molecule -1 (IBA1), which is involved in membrane ruffling and phagocytosis (85; 152; 153). The new cytoskeleton architecture allows for efficient migration to the injury site to contain the

damage site and initiate and facilitate an immune response (164). The increased cell membrane area and cytoplasmic area allow for increased expression of lysosomal enzymes, such as CD68, that support phagocytosis, an essential process that enables microglia to remove debris, toxic factors and dead, damaged or dying cells from the damaged area environment (101).

Soluble factors and receptor expression

Microglia produce cytokines and chemokines that attract and act on other immune cells to facilitate the immune response, respectively (33). Additionally, there is an upregulation of functional immune enzymes such as NADPH oxidase 2 (NOX2), inducible nitric oxide synthase (iNOS) and arginase-1 (Arg-1), which are commonly used as markers for microglia activation. The NOX2 enzyme produces reactive oxygen species (ROS) by oxidizing NADPH and converting molecular oxygen to a superoxide anion that can then interact with reactive nitrogen species (RNS) and nitric oxide (NO), produced primarily by iNOS in microglia, to form cytotoxic peroxynitrite (20; 42). Arg-1 is associated with cytoskeleton remodeling and acts on its substrate arginine to produce L-ornithine that is metabolized to produce polyamines used for ECM protein production during tissue remodeling. Briefly, both iNOS and Arg-1 compete for arginine as their substrate to produce nitric oxide and polyamines, respectively (24). In peripheral macrophages, there is an inverse relationship between the expression and function of the two enzymes and are associated with pro and anti-inflammatory activation, respectively, classically referred to in the macrophage literature as M1/M2 polarization (87). However, this classification system does not always apply concerning microglia activation in the injured brain and will be discussed below. Furthermore, activated microglia upregulate

immune cell surface receptors CD86 (12), CD206 (12), CR3/43 (68), CD11b (42; 68), and CD45 (25) to aid in antigen presentation and serve to identify activated microglia. While the initial immune response is hypothesized to be beneficial (150), by containing the injury site, removing deleterious factors and orchestrating a therapeutic immune response, persistent activation, also known as chronic neuroinflammation, is associated with slower recovery, persistent neurocognitive and behavioral deficits and neurodegeneration (15; 20; 158). To date, the mechanism(s) that contribute and drive persistently reactive microglia in the TBI brain is unknown.

Microglia M1/M2 polarization

The coordinated physiological response to brain injury is, in part, initiated, mediated and propagated by activated microglia by releasing an array of soluble cellular constituents in the injured parenchyma (114). The interaction with resident astrocytes, infiltrating immune cells and altered cytoarchitecture produces a complex networked response. Much of the field investigating neuroinflammation is devoted to defining this multifaceted immune response in limiting, dichotomous, M1 or M2 polarization phenotypes. The classification of innate immune polarization was born out of *in vitro* experiments evaluating the differential effects of inflammogens (LPS, IL-4 and IFN- γ) on macrophage inflammatory gene expression (183). These findings were adopted by researchers characterizing microglia because they are generated from yolk-sac (YS) erythromyeloid precursors (EMPs), which also produce YS macrophages and perform similar biological functions in their respective anatomical locations (67; 99; 114; 176).

Given their similar origins and function, microglia activation was defined using a classification system adapted from the macrophage literature (208). Activated cells are

characterized as either M1, classically activated (iNOS, NOX2, MHC I & II, CD86, IL-6, IL-1 β , TNF- α), or M2, alternatively activated (Arg-1, CD206, Ym1, IL-10, IL-4, TGF- β), which is further stratified into M2a-d. In contrast to macrophage activation, microglial activation phenotypes have been shown to present on a spectrum simultaneously presenting M1 and M2 cells surface markers, functional enzymes and the release of soluble factors (145; 183). This is demonstrated in animal models of TBI, where mice that are exposed to a single controlled cortical impact injury (CCI) display increased microglia activation as indicated by significantly increased expression of immune-related enzymes iNOS (108; 192; 199) and Arg-1 (84; 192; 199) acutely and chronically after injury. Other researchers using CCI injured mice highlight this difference where CD86 and CD206 are co-expressed following an injury at both the acute and chronic post-injury time points (92; 193; 199). The mixed presentation between traditional M1 and M2 cytokines is also observed in TBI mouse and rat models. Kumar et al. (103) showed a varied display of M1 (IL-6 and IL-1 β) and M2 (IL-4 and TGF- β) associated cytokines up to seven days after a single CCI injury in a mouse model (105). These studies showed that microglia activation is similar to macrophage activation in expressing immune-associated receptors and enzymes and cytokines/chemokines used during an immune response, yet distinctly different in the temporal presentation.

MICROGLIA IN HUMAN TBI

Clinical evaluation of reactive microglia *in vivo* has proven difficult due to limited technical procedures and microglia-specific markers. However, studies of neuroinflammation using positron emission tomography (PET) imaging have provided inroads in this elusive field of study. Ramlackhansingh et al. (160) showed persistent

neuroinflammation up to seventeen years following a single TBI in their seminal work. They showed this by using [¹¹C]-PK11195 (PK) PET imaging for the radioligand Translocator protein (TSPO), a cholesterol transporter located on the outer mitochondrial membrane of glial cells whose expression and activity is increased during microglial activation, where TBI patients had significantly increased PK binding potential (BP_{ND}) compared to healthy age-matched controls. This work was the first to show that persistently reactive microglia are detectable in human beings decades after a single TBI. A limitation of this study was that no other information regarding their cognitive, emotional or mental state was available to correlate with the imaging studies. Researchers showed an association between chronic neuroinflammation and white matter damage by combining the PET imaging technique with magnetic resonance imaging (MRI) T1 and diffuse tensor imaging (DTI). They identified the thalamocortical axonal tracks in patients with a history of a single moderate to severe TBI, had significantly less fractional anisotropy (FA), a measure of white matter integrity, compared to healthy controls and negatively correlated with PK binding potential (BP_{ND}) (175). These are significant findings because they demonstrate that white matter tract damage and chronic neuroinflammation are closely associated with living individuals with TBI. This report did not provide patient data correlating the imaging results to recovery status or symptomology similar to the prior study. However, other studies evaluating patients with a single moderate to severe TBI showed that patients displayed impairments in thalamic associated functions, such as sensory dysfunction, including tingling, numbness, and hypersensitivity to light (16), disruptions in cognition, including attention and memory, (17) and insomnia (40). Before these studies, most of the literature evaluating chronic

microglial activation in humans was conducted using histopathological stains for microglia from post-mortem brain tissue (93). Johnson et al. (93) evaluated reactive microglia in post-mortem brain tissue of individuals with a single TBI using immunohistochemical staining for reactive microglia, defined as amoeboid morphology and CR3/43 and CD68 positive staining. They showed that reactive microglia are 30% more prevalent in injured patients than in age-matched non-TBI controls at the sub-acute, two weeks to a year, and long-term, > one year, post-injury time points. Interestingly, this was not observed in the acute time point (less than two weeks post-injury). Furthermore, the reactive microglial phenotype was associated with increased uptake of myelin fragments, as shown by localization of reactive microglia and myelin essential protein via immunohistochemical staining. Lastly, corpus callosum thickness was significantly decreased only in the long-term TBI group compared to age-matched controls (93). Another post-mortem study evaluated microglia activation in post-mortem human thalamic nuclei and found that activated microglia, stained with CR3/43, are more numerous in white matter tracks in patients with a severe TBI. Taken together, these results show the association between persistently reactive microglia and chronic white matter neuropathology in the TBI brain.

MICROGLIA IN *IN VIVO* MODELS OF TBI

To better understand microglia in the injured brain, animal models of TBI have been developed that are consistent, reproducible and biofidelic to the human condition. Further, they reproduce the biomechanical and pathophysiological patterns observed in TBI and allow for identifying pathological mechanisms, developing therapeutic agents, and testing treatment strategies. Typically, these models employ porcine, murine, or

recently, mustelid species exposed to a single or repeated parenchymal injury. The most commonly used experimental model of TBI is a single injury using the CCI injury model, where the injury is caused by a metal piston directly impacting the cortex (20; 108). The CCI model TBI directly damages the brain parenchyma and replicates multiple aspects of microglia activation such as amoeboid morphology, increased cell surface expression of IBA1, CD86, and CD11b expression (1), demonstrating that microglia responses are similar to those observed in human cases of TBI.

The fluid percussion injury (FPI) model is a widely used model that produces a diffuse strain field exposing the entire brain to shearing forces by applying a momentary fluid pressure pulse on the exposed dura, and similar to the CCI model requires the animal to be anesthetized and have a craniotomy (129). The FPI model of TBI produces injuries that result from diffuse forces that are observed in inertial injuries. This is demonstrated by mildly and severely injured animals having significantly increased IBA1 and CD45 reactive microglia in areas of the brain distal to the force-generating site, such as the thalamus, compared to sham-injured controls (25).

The closed-head impact model of engineered rotational acceleration (CHIMERA) injures anesthetized animals by allowing unconstrained head movement following a piston striking at the skull base (131). It mimics the biomechanical acceleration events during a TBI, with injured mice showing IBA1 activated microglia localized to multiple white matter tracts, such as the corpus callosum (CC), optic tract, olfactory nerve tract and branches of the superior colliculus (149).

Lastly, custom-made models allow for a range of impact-less head rotational kinematics. However, these models are reserved for higher-order species and are more

challenging to employ, requiring highly specialized and skilled teams for medical management, biomechanics and neurological recovery. However, they mimic multiple aspects of human TBI, including activated microglia, with porcine injured animals displaying significantly increased IBA1 in the periventricular white matter (69).

An important conclusion to take away from this discussion is that models that produce direct tissue damage, such as the CCI, and inertial induced injury, such as the FPI, CHIMERA and rotational models, all result in activated microglia and mimic the human TBI population. The utility of these models in characterizing the pathophysiological process is immense; there are limitations to the kinds of questions that can be addressed, such as the effects of primary injury forces on individual cells. To examine and address these questions, *in vitro* models are necessary since factors from other cells types, such as debris from the initial injury and secondary injury cascades, can mask the effect of the primary injury.

STRETCH-INJURIES

Stretch is a prominent force involved in the inertial component of a TBI (177). The brain is a viscoelastic material and one of the softest tissues in the body, rendering it highly susceptible to mechanical insults (143) with inertial and impact forces acting on the sensitive brain parenchyma (133). For example, TBIs resulting from falls, sports injuries and motor vehicle accidents account for over 50% of TBI cases. They are characterized by an impact followed by a cranial acceleration-deceleration event or an acceleration event followed by an impact in the case of falls. Acceleration events lead to injuries resulting from the head rotating or accelerating, straining the tissue beyond functional or structural tolerance (154). To illustrate this, a 2008 study showed that strain

fields were observed in healthy individuals following a mild angular head acceleration, roughly equivalent to 10% of the force experienced by voluntary heading a soccer ball, demonstrating the ability of the non-injurious cranial movement to induce mechanical deformations (167). Due to obvious ethical limitations, the direct evaluation of stretch injuries during a TBI is unexplored. Therefore, *in vitro* and *in vivo* models of experimental TBI have been developed and utilized to model the injury biomechanics.

IN VITRO MODELS

To investigate the individual cellular pathophysiological mechanism(s) that mediate inertial induced injuries, *in vitro* models have been developed. These models are necessary due to the heterogeneous cellular and cytoarchitecture environment found in the brain. Furthermore, immediately following injury, innumerable factors, such as ATP, damage-associated molecular patterns (DAMPS), and damaged cells contribute to secondary injury, thus making the evaluation of the primary injury challenging if not impossible. The advantages of *in vitro* models are exquisite control over experimental conditions, reproducibility and the ease in evaluating cellular-level changes following injury.

Neurons

Using primary rat cortical neuronal cultures, investigators evaluated the intrinsic response of neurons to a mechanical injury. The injury model produced a bilateral stretch-injury with a strain rate of 20% and resulted in neurophysiological, neurochemical and morphological alterations following a single injury (191). Cultured cortical neurons displayed stretch-induced delayed depolarization (SIDDD) one hour after injury and recovered to pre-injury baseline levels at twenty-four hours. In a different study, using

the same cell type and parameters, damage led to a significant increase of intracellular calcium and glutamate that lasted for twenty-four hours (203), both of which are observed in *in vivo* models of TBI (166) (57). These results show that strain-induced injury in cultured neurons results in neurophysiological and neurochemical changes that are observed in *in vivo* models of TBI. Recent *in vitro* work from Dileonardi et al. (56) from the Army Research Laboratory (ARL) showed that stretching cultured rat hippocampal neurons produced morphological alterations. They showed a single injury-induced neuronal morphological alterations in cultured rat hippocampal neurons, indicated by injured cells displaying increased fragmentation and decreased arborization (branching) patterns compared to non-injured controls twenty-four hours after injury. These results showed that a single injury produced structural damage that may underlie neuronal dysfunction. Lastly, using a unilateral-stretch injury and beta-III tubulin immunocytochemistry, Hemphill et al. (75) found that cortical rat neurons exposed to a single injury displayed focal axonal swellings, a cellular hallmark reminiscent of DAI, twenty-four hours post-injury. Interestingly, the degree and diffusivity of the stretch-injured focal axonal swelling were substrate-dependent, with neurons cultured on fibronectin displaying significantly more beta-III tubulin staining than injured cells cultured on poly-D lysine. This study showed that cellular pathologies commonly observed in humans and animal models of TBI could be modeled and induced by primary injury forces alone. Additionally, the substrate-receptor complex involved in cellular attachment contributes, in part, to the magnitude of the injury.

Astrocytes

Astrocytes play a vital role in maintaining the neurovascular unit, neuronal support and synaptic transmission (126). Cullen et al. (44) showed that cultured primary rat astrocytes were more resistant to stretch-induced cell death than neurons. Furthermore, Cullen and others (55; 113) showed that stretch-injury induced a significant increase in the number of hypertrophic processes at forty-eight hours and five days post-injury (44). Consistent with the stretch-induced morphological changes, astrocyte reactivity, as shown by a significant increase in the expression of glial fibrillary acidic protein (GFAP), an intermediate filament and generic astrocyte marker, is also significantly upregulated as early as thirty minutes (113), twenty-four (80; 136) and forty-eight hours following a mechanical injury (44). Research from Jayakumar et al. (89) confirmed the injury-induced morphological findings, with injured primary rat astrocytes having significantly more swelling than uninjured controls twenty-four hours after injury. Furthermore, swollen cells displayed a significant increase in mitochondrial permeability transition, characterized by a sudden disruption of the inner mitochondrial membrane that is associated with bioenergetics failure in astrocytes following a TBI (3).

Endothelial cells

Endothelial cells form a monolayer that lines blood vessels, creating a restrictive barrier between blood and CNS (196). These layers regulate the transfer of gases, glucose, and ions from the blood to the surrounding tissues and are a fundamental component of the BBB. During a TBI, primary injurious forces lead to BBB breakdown, allowing for secondary injuries such as edema, hyperexcitability and inflammation (4). Studies evaluating primary stretch-injury forces on endothelial cells showed that rat-derived endothelial cells are more resistant to stretch-induced membrane disruptions than

neurons and astrocytes, as indicated by fewer cells taking up the membrane-impermeable dye propidium iodide (PI) twenty-four hours after injury (130). A study utilizing mouse endothelial cells showed that compared to uninjured controls, injured cells displayed significant morphological and structural alterations two hours after injury indicated by increased F-actin stress fibers and reduced, or ectopic, distribution of ZO-1 (5). Another study using mouse endothelial cells replicated the stretch-induced morphological alterations and found that expression of other tight junction proteins, claudin-5 and occluding, were significantly decreased twenty-four hours after injury (168). Furthermore, they discovered that injury significantly increased inflammation associated gene transcripts, IL-6, I-1 α , TNF- α and CCL2 twenty-four hours and was associated with a strong, non-significant, trend of increased permeability with an increase in the number of FITC—labeled avidin-bound to the biotinylated gelatin-coated membrane twenty-four hours after injury.

These results from the *in vitro* neurotrauma literature demonstrate the validity of *in vitro* models to replicate cellular pathologies and associated dysfunction in the case of BBB disruption that is observed in *in vivo* models of TBI. To date, the effects of primary injurious forces on microglia are currently unknown. This question is essential because chronic microglial activation is a prominent and deleterious secondary injury process prevalent in multiple animal models and humans with TBI. Given the literature demonstrating that primary forces induce pathologies and dysfunction in other brain cells types, we asked the question, what are the effects of the direct injury on microglia and how does this affect their immune response? Based upon the literature, we hypothesized that injury would alter microglial morphology and function. We anticipated that the effect

of the mechanical forces causing morphological changes following injury would be less compared to the other cells types in the brain. This is primarily due to the difference in size, motility and function of the different cell types in the brain. For neurons, astrocytes, endothelial cells are much larger than microglia; for example, some neuronal soma areas range between 3-100 μm^2 and have up to 50 dendritic branches with lengths totaling 6000 μm long (19). The increase in surface area renders the cells more susceptible to physical injuries and morphological disruptions. Additionally, all three cells types are inherently stationary and non-motile compared to the highly migratory and motile microglia.

Adherent cells have markedly more focal adhesion complex (FAC) to anchor the cells and thus have an increased probability of mechanotransduction signaling. Lastly, the immune surveillance function of microglia may lead to different effects of the primary injury on their function and morphology because while migrating, they are constantly turning over FAC, and the opportunity for mechanotransduction may not be as frequent.

INTEGRINS AND MECHANOTRANSDUCTION

The use of *in vitro* models to study the effects of inertial generated forces allows for the unadulterated investigation into stretch-induced cellular dysfunction and pathology.

Additionally, the *in vitro* setting is free from confounding cellular constituents that can obscure the evaluation of the

molecular mechanism underlying the force-induced cellular changes. The process of converting mechanical forces into biochemical signals is mechanotransduction (146).

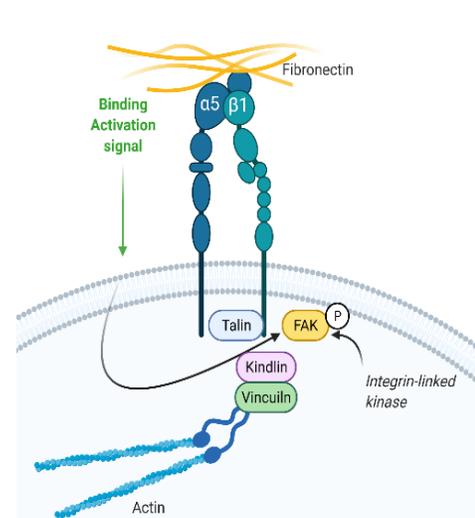


Figure 1. Attachment of $\alpha 5 \beta 1$ subunits of Integrin to fibronectin. Following ligation, membrane associated FAK autophosphorylates and assembles with other structural proteins that link to the actin cytoskeleton.

Most of the literature assessing the impact of primary forces on brain cells is conducted with brain cells cultured on appropriate ECM protein found in the brain. The primary cell-to-ECM adhesion receptor is the integrin. Integrins are transmembrane heterodimeric glycoproteins that create a physical link to the extracellular environment. The extracellular component consists of alpha and beta subunits that assemble the binding site for the cognate ECM ligand. The cytosolic aspect contains the tail of the integrin that forms a complex to the actin cytoskeleton, forming a focal adhesion complex. (FAC) (214). The FAC comprises structural and enzymatically functional proteins that facilitate signaling from the extracellular space through the actin cytoskeleton and mediates cell signaling cascades (Figure 1). Through this adhesion complex, cells can sense changes in the extracellular environment, such as substrate rigidity and the ECM composition that indicates injury and disease states. Furthermore, these adhesion receptors mediate multiple cellular processes such as cell survival (187), proliferation (144), motility (134), cytoskeletal organization (63), and inflammation (139).

$\alpha 5\beta 1$ integrin and fibronectin

Among the limited literature on microglia integrin substrate interactions, the $\alpha 5\beta 1$ fibronectin interaction is the most studied and well-characterized in microglia. Microglia express the $\alpha 5\beta 1$ integrin during resting and upregulate it during activation (72; 137-140). Smolders et al. (182) showed the $\alpha 5\beta 1$ integrin-mediated microglial migration during development. Milner et al. (140) demonstrated that the $\alpha 5\beta 1$ integrin mediates MHC class I expression in microglia when cells are cultured on fibronectin. They identified fibronectin's binding motif as the arginine glycine aspartate (RGD) peptide using functional blocking peptides. These findings are consistent with the literature

demonstrating that $\alpha 5\beta 1$ integrin mediates attachment to fibronectin through the RGD binding motif in other immune cells(14). In studies utilizing mouse macrophages, the peripheral immune cells similar to microglia in embryonic origin and function, researchers showed that the $\alpha 5\beta 1$ integrin-mediated attachment to fibronectin, and the production and secretion of cytokines TGF- α & β and IL-1 (180). Fibronectin cultured mouse bone marrow-derived macrophages (BMDMs), compared to polydimethylsiloxane (PDMS) cultured, displayed a high degree of cell elongation, expressed significantly more arginase-1, CD206 YM1 and anti-inflammatory cytokines IL-4 & IL-13. While the immune responses differ between microglia and macrophages, these results demonstrated a substrate-dependent relationship between morphology and immune function (132).

Fibronectin is a relevant brain ECM since it is present in the developing (117) and adult (94) brains. Interestingly, the role of plasma fibronectin in the post-injured brain suggests that it is neuroprotective (190). Mice subjected to a CCI showed a significant increase in fibronectin after injury. Researchers showed that, compared to wild-type mice, conditional plasma fibronectin knockout mice performed considerably worse on motor and cognitive tasks, had substantially greater lesion volume and apoptotic cell death and significantly fewer phagocytic microglia in the injured cortex. Interestingly, intravenous injection of fibronectin before CCI in pFN knockout mice rescued the deficits found in pFN injured mice, demonstrating the neuroprotective effect of plasma-derived fibronectin (190). These results suggested that fibronectin is neuroprotective; however, how newly incorporated hepatocyte-derived fibronectin and healthy brain-derived fibronectin may differ is unknown. Given that fibronectin is a neuroprotective brain-associated ECM protein, could disrupting the binding between microglia and

fibronectin contribute to dysfunctional microglial states after a TBI? The interesting question is, how are microglia affected by primary injury forces when attached to fibronectin.?

FAK pathway

FACs are associated with many effector signaling molecules that mediate cellular processes. Upon ligation with its cognate ligand focal adhesion kinase (FAK), a membrane-associated tyrosine kinase, auto-phosphorylates at Y397. This initiates a cascade of events that creates docking sites for structural and signaling proteins that facilitate other downstream pathways involved in adhesion, motility, morphology and inflammation. Fibroblasts from FAK-null mice display morphological alterations and migration deficits (120). Researchers identified that the deficiencies in FAC disassembly in the protrusive and rear end of FAK null fibroblast lead to migratory and morphological deficits (202). Microglia migration towards amyloid- β ($A\beta$) pathology is impaired in mice with mutations for triggering receptors expressed on myeloid cells 2 (TREM2) (163). Researchers showed that FAK phosphorylation in microglia from TREM2 mutant mice was significantly decreased compared to wild-type cells *in vitro* following oligomeric $A\beta$ 42 treatment. The migratory deficits and FAK phosphorylation were restored when treated with a CD04, a downstream activator of FAK. Primary rat microglia stimulated with LPS increased gene and protein expression of inflammatory cytokines IL-6, IL-1 β and correlated with a significant increase in FAK expression (8). The literature regarding the FAK pathway in microglia is a vital field of study, and the contributions of FAC signaling enzymes are becoming more prevalent in the literature.

HYPOTHESIS AND SPECIFIC AIMS

The work presented here examined two unexplored aspects of microglia biology in TBI, 1) the mechanical injury and 2) the $\alpha 5\beta 1$ integrin/FAK signaling. These are essential questions to address due to the prevalence of dysfunctional microglia observed in the injured brain. The literature shows primary injury forces produce cellular pathologies in neurons, astrocytes, and endothelial cells, which are observed in humans and experimental models of TBI. Determining if stretch-injury forces similarly affect microglia will identify novel signaling pathways for therapeutic targeting. Additionally, this work will contribute to the growing literature addressing multiple integrin-mediated inflammation processes. We hypothesized that stretch-injury alters microglia function, and the $\alpha 5\beta 1$ integrin partially mediates it. We will test our hypothesis with the following specific aims:

Aim one: Assess the effects of stretch-injury on primary rat microglia.

Aim two: Determine the role of $\alpha 5\beta 1$ integrin in injured primary rat microglia.

Chapter 2: Assessment of the effects of stretch-injury on primary rat microglia

ABSTRACT

Mechanical stretch-injury is a prominent force involved in the etiology of traumatic brain injury (TBI). It is known to directly cause damage and dysfunction in neurons, astrocytes, and endothelial cells. However, the deleterious effects of stretch-injury on microglia, the brain's primary immunocompetent cell, are currently unknown. The Cell Injury Controller II (CICII), a validated model of cellular neurotrauma, induced a mechanical stretch-injury in primary rat microglia. Statistical analysis utilized student t-test and one and two way-ANOVAs with Tukey's and Sidak's multiple comparisons, respectively. Cells exposed to stretch-injury showed no signs of membrane permeability, necrosis, or apoptosis, as measured by media-derived lactate dehydrogenase (LDH) and cleaved-caspase 3 immunocytochemistry, respectively. Interestingly, injured cells displayed a functional deficit in nitric oxide (NO) production, identified by media assay, at 6, 12, 18, and 48 hours post-injury and immunocytochemistry for iNOS (inducible nitric oxide synthase) at 12 hours. Furthermore, gene expression analysis revealed the expression of inflammatory cytokines IL-6 and IL-10 and enzyme arginase-1 was significantly down-regulated at 12 hours post-injury. Time course evaluation of migration, using a cell exclusion zone assay, showed stretch-injured cells display decreased migration into the exclusion zone at 48 and 72 hours post-stretch. Lastly, a significant change in morphology coincided with the functional immune deficits, with process length decreasing and cell diameter increasing following an injury at 12 hours. Taken together, the data demonstrate that stretch-injury produces significant alterations in

microglial function, which may have a marked impact on their response to injury or their interaction with other cells.

INTRODUCTION

Traumatic brain injury (TBI) is a growing severe public and military health concern, with 1.7 million cases accruing an economic burden near 76.8 billion annually (23). TBI is divided into two injury phases, primary and secondary (103). The primary injury results from the impact or acceleration events generating mechanical forces that act upon the sensitive brain tissue, resulting in immediate, irreparable damage and dysfunction. Secondary injury processes resulting from the initial injury evolve over a period of time and contribute to the destruction of brain tissue. A prominent secondary injury process is the inflammatory response, primarily mediated by activated microglia, the brain's immunocompetent cell (12). The initial immune response is thought to be a protective and restorative process; however, multiple experimental models (65; 77; 107; 197) and human (43; 160) cases of TBI implicate prolonged microglia activation in deleterious outcomes. Currently, the mechanism causing prolonged microglial activation is unknown.

Mechanical strain produced from the primary injury generates shearing forces that stretch and deform the cytoarchitecture and cells, contributing to death and dysfunction. Stretch-injury *in vitro* models allows for the study of the effects of primary injury forces on individual cells. To date, *in vitro* models of neurotrauma show neuronal (75; 124), astrocyte (7), and endothelial (6) pathologies that mimic those injuries observed in *in vivo* TBI models. For example, rat primary cortical neurons exposed to a uniaxial stretch-injury with a strain of 10% displayed focal axonal swellings, similar to swellings

observed in diffuse axonal injury (DAI) in experimental models and human cases of TBI (75). Human astrocytes exposed to a biaxial stretch-injury with a strain of 20% displayed retracted end-feet processes and activation c-Jun NH₂-terminal kinase (JNK), replicating astrocyte associated dysfunction in blood-brain barrier (BBB) integrity. Furthermore, murine endothelial cells exposed to a stretch-injury with a 20% strain displayed markedly retracted, swollen and deformed morphology with notable intercellular spaces between cells (6). To date, the effects of stretch-injury on microglia viability, phenotype, and function are currently unknown.

Following the initial trauma, microglia interact with trauma associated-factors and become activated; this transformative process is necessary to mediate an inflammatory response. This is characterized by a morphological and phenotypic transformation known as activation (209). The morphological changes involve a transition from a ramified to amoeboid shape, and functional changes such as up-regulation of nitric oxide (NO) (12) and reactive oxygen species (ROS) production (209), the release of chemokine/cytokines (104), alteration in cell surface immune receptors and functional enzymes, and an increase in phagocytic and migratory behavior (159). Unactivated or resting microglia present with small cell bodies with multiple long slender processes, a significantly decreased production and expression of the previously mentioned factors, reduced phagocytic capacity and reduced migration. Persistent, or chronic activation of microglia following a TBI can occur if the initial response is left unresolved, leading to functional deficits and neurodegeneration (58). To date, the mechanism(s) underlying chronic post-traumatic microglia activation remain elusive, and given that the primary insult can

induce cellular pathologies in other cell types, an investigation into the effects of primary forces on microglia function is warranted.

This study aimed to evaluate the impact of stretch-injury on microglial viability, function, and morphology. Additionally, the effect of stretch-injury on microglial priming was examined by examining microglia viability and function after microglia were treated with a known inflammogen after a stretch-injury. First, time-course studies were conducted using media assays to assess viability (LDH) and function (NO). From this, we focused on a single post-injury time point to evaluate inflammatory associated cytokines and enzymes, reactive oxygen species and morphology analysis. Lastly, a time-course study assessed the priming effect of stretch-injury on microglial viability and function. This study is the first to comprehensively study the impact of stretch-injury on microglial viability, morphology, and function.

METHODS

Cell culture

Primary microglia cultures were isolated from 2-day-old Sprague-Dawley rat pups by shaking mixed glia cultures at 100 RPM for 1 hour at 37 °C yielding 90% purity as previously described (188). Cells were maintained at 37 °C in a humidified atmosphere augmented with 5% CO₂ in media containing Dulbecco's modified Eagle medium (Gibco), 1% L-glutamine (Gibco), 1% sodium pyruvate (Gibco), 10% FBS (Hyclone), and 1% penicillin and streptomycin (Thermo Fisher Scientific). Media replacement occurred every 3–5 days. What is the purity of your microglial cultures?

Stretch-injury

Cells were seeded at a density of 3×10^5 cells/mL on Pronectin coated silicone-based deformable membrane BIOFLEX® culture plates (BF-3001P Flexcell International, Hillsborough, NC). Cells were incubated for 24 hours in growth media to allow for adherence (37°C, 5% CO₂), after which a stretch-injury was administered, as previously described (125). Briefly, a stretch-injury was produced using the Cell injury controller II (CIC II), which utilizes nitrogen gas to pressurize a BIOFLEX® well individually. The CIC II regulates the duration and pressure of gas delivered to the well by using a rubber tube that feeds through a plastic circular well adaptor plug that attaches to the top of the well, creating a hermetically sealed system. Upon discharging the gas, the well becomes pressurized, and a bi-axial deformation of the flexible membrane, resulting in the cultured cells experiencing a stretch-injury. All stretch-injury experiments used identical parameters with 60psi regulator pressure for a duration of 50 mSec, resulting in a 5psi pressurization of the well that created a 20% stretch event in the center of the well.

Lipopolysaccharide (LPS) and Etoposide treatment

To evaluate the potential priming effect of stretch-injury, primary microglia were treated with 100 ng/mL concentration of LPS (Sigma, L8274) 15 minutes after stretch-injury (12). Additionally, an LPS treated-only group served as an activation control group. A dose of 15 μ M of Etoposide (catalog no. E1383; Sigma) was used to induce apoptosis and elicit a robust cleaved caspase-3 response to serve as a positive control (39).

Reactive oxygen species (ROS) assays

To detect ROS intermediates, cells were treated with 10 μ M of 2',7'-dichlorodihydrofluorescein diacetate (H₂DCFDA, Thermo Fisher); a separate experiment was conducted to evaluate ROS intermediates at 12 hours post-injury. Before treatment with H₂DCFDA, cells were washed with warm PBS, then incubated for 45 min with the assay components, and fluorescence emission was measured on a FLUOstar (BMG LABTECH Inc., Cary, NC) plate reader.

Cell death assays

Cell culture media was assessed for lactate dehydrogenase (LDH) at 1, 6, 12, 18, 24, 48, and 72 hours post-injury using the Cytotox 96 assay (Promega) according to the manufacturer's instructions. Absorbance at 496nm was measured using a ChroMate microplate reader (Awareness Technology Inc., Palm City, FL).

Nitric oxide (NO) measurement

NO was measured in primary microglia exposed to stretch-injury at 1, 6, 12, 18, 24, 48, and 72 hours post-injury. NO content in the media was quantified using a Griess reagent assay kit (Invitrogen). The assay was performed per the manufacturer's recommendations and as previously described (21). Colorimetric changes in 96-well plates were quantified with a Chroma Plate Reader (Midwest Scientific, St. Louis, MO, USA) at 545 nm.

Immunocytochemistry

Cells were fixed with 4% paraformaldehyde for 10 minutes and rinsed twice with 1 \times PBS. Primary antibodies included rabbit anti-arginase-1 (20 μ l/ml; Abcam), rabbit anti-NOS (10 μ l/ml; Abcam, Cambridge, MA) and rabbit anti-cleaved caspase-3

(10 µl/ml; Abcam). Also, cell nuclei were stained with DAPI (0.5 µl/ml; Life Technologies, Carlsbad, CA). Fluorescently tagged secondary antibodies (Invitrogen) were visualized with an Olympus BX43 fluorescent microscope with a CellSens Standard imaging program. Five randomly selected images were taken per sample, and each image was qualitatively assessed for pixel density and normalized to the total number of DAPI stained cells. Images were taken from the center of the membrane.

RNA isolation and gene analysis

TRIzol® (Invitrogen, Carlsbad, CA) was used to extract mRNA from the cells, and mRNA concentrations were measured by a Nanodrop system (Thermo Scientific). A Veriti thermal cycler (Applied Biosciences) and a complementary DNA (cDNA) conversion kit (Applied Biosciences, Waltham, MA) were used to convert 1 µg of mRNA into cDNA, according to the manufacturer’s suggested protocol. According to the manufacturer's recommended protocol, all quantitative real-time PCR (qRT-PCR) data was procured through the StepOnePlus Real-Time PCR System (Applied Biosciences). All primers were designed by Sigma-Aldrich (Darmstadt, Germany) and listed in Table [1](#).

Table 1. Selected gene sequences for RT-PCR

Gene	Symbol	Forward (5'-3')	Reverse (5'-3')
Transforming growth factor-beta 1	TGF-β-1	GGAAATCAATGGGATCAGTC	CTGAAGCAGTAGTTGGTATC

Interleukin-1, beta	IL-1 β	TAAGCCAACAAGTGGTATTC	AGGTATAGATTCTTCCCCTTG
Interleukin-4	IL-4	GAACCAGGTCACAGAAAAAG	GGGAAGTAAAATTTGCCAAG
Interleukin-6	IL-6	CAGAGTCATTCAGAGCAATAC	CTTTCAAGATGAGTTGGATGG
Interleukin-12	IL-12	CTTCTTTGATGATGACCCTG	AATAGCCATCAGCATGTTTC
Interleukin-10	IL-10	TCTCCCCTGTGAGAAATAAAAG	GAAAGGAAAGTTCCCAGATG
Cluster of differentiation 86	CD86	CACAAGCTTTGATAGGGATAAC	TTCTTGTTTCATTCTGAGCC
Mannose receptor	CD206	GGAGTTGTGGAGCAGATGGAAG	CTTGAATGGAAATGCACAGAC
Arginase-1	Arg1	GAAGGAAAGTTCCCAGATG	CTTGTCCACTTCAGTCATTG
Inducible nitric oxide synthase	iNOS	TTCCTCAGGCTTGGGTCTTGT	GAGGAACTGGGGGAAACCATT
Phosphoglycerate kinase 1	PGK1	GGAGATGTCTATGTCAATGATG	TTTAGCTCCTCCCAAGATAG

Migration assay and morphological evaluation

A cellular exclusion zone assay was used to quantify migration. Cells were seeded at a density of 3×10^5 /mL on Proectin coated BioFlex well plates with a 1.4 cm x .1 cm strip of silicone membrane placed in the center of the well and allowed to attach for 24 hours. A graded grid was drawn onto the underside of the membrane as a reference. Microphotographs were taken using a phase-contrast microscope (Zeiss, PrimoVert) with a USB adapted ocular (Swiftcam 5.0-megapixel digital camera microscopes, Amazon.com) for capturing images. Images were captured at pre-injury baseline and 12, 24, 48, and 72 hours post-injury. ImageJ (NIH, open-access software) was used to quantify cell exclusion zone diameter. Twenty-four hours after plating, the barrier strip of silicone was removed, and a baseline image was taken to define the cell exclusion zone. Then a stretch-injury was administered, and cells were returned to the incubator. Cells were counted in the exclusion zone at pre-stretch, 12, 24, 48, and 72 hours post-injury time points. Cells were counted if they matched criteria, 1) dark coloring, 2) circular or branched phenotype. In some experiments, cells were able to attach underneath the silicone barrier in the exclusion zone. These cells were counted and subtracted from the total number of migrating cells in subsequent post-injury assessment time points, 12, 24, 48, and 72 hours.

Morphology was evaluated using the same devices, and images were taken at pre-injury and twelve hours post-injury. ImageJ (NIH, open-access software) was used to quantify cellular characteristics, i.e., number and length of processes and cell diameter.

Phagocytosis assay

At 12 hours after stretch-injury, cells were assessed for phagocytic activity using the Phagocytosis Assay Kit (Cayman Chemical, Ann Arbor, MI). Briefly, at 8 hours after

injury, latex beads with rabbit IgG-FITC conjugates (1:500) were incubated with control and injured cells for 4 hours, followed by a 1-minute incubation with trypan blue to quench non-phagocytosed bead fluorescence and cell fixation with 4% paraformaldehyde. Cells were counterstained with DAPI, and five images at 20X magnification were collected from each coverslip. The number of DAPI cells containing FITC labeled beads was counted and normalized to the total number of DAPI-positive cells. This assay was repeated in triplicate.

Statistical analysis

Statistical analysis was conducted using Graphpad Prism Software version 6.01. (GraphPad Software, San Diego, CA). NO, and LDH assays were performed in triplicate for each trial, and the trials were replicated four times to generate a sample size of $n = 4$ per group. A two-way ANOVA with Sidak's multiple comparisons test was conducted on the groups whose controls were set to 1.0. The stretch-injured values were normalized to control values for each trial for NO and LDH assay measures. ROS assays were conducted singly for each trial, and the trials were replicated three times to generate a sample size of $n=3$. A one-way ANOVA with Tukey's multiple comparisons test was conducted. Western blot analysis was performed in pooled samples from triplicates for each trial, and the trials were replicated three times to generate a sample size of $n=3$. Immunocytochemistry experiments were conducted singly and repeated three times to create a sample size of $n=3$. Western blot and immunocytochemistry results were analyzed using an unpaired student's t-test. The migration assay was conducted singly for each trial and replicated three times for an $n=3$. The total number of migrating injured cells was normalized to control cells at each time point. A two-way ANOVA with

Sidak's multiple comparisons test was conducted for assay measures. The morphology analysis was assessed from five images per trial, and each trial was replicated three times to generate a sample size of $n=3$. A total of 15 images were analyzed for the control and stretch-injured condition. Percent averages for each group were assessed using a two-way ANOVA with Sidak's multiple comparisons. For all statistical tests described, a p -value < 0.05 was considered statistically significant. Data are presented as mean \pm standard deviation (SD).

RESULTS

Stretch-injury does not increase LDH at multiple time points or cleaved caspase-3 at 12 hours post-injury

Media levels of the intracellular enzyme LDH are an indicator of compromised membrane integrity and necrosis (9; 55). A time-course study of media-derived LDH was conducted to determine the effect of stretch-injury on microglial viability and membrane permeability at acute and long-term time points. LDH is typically confined in the cytosol and is detectable in the event of cell lysis, necrosis, or compromised membrane permeability. Following a 20% stretch-injury, media was assayed for LDH at 1, 6, 12, 18, 24, 48, and 72 hours post-injury and showed no significant differences in media LDH content between stretch-injured and control cells at any time point (Figure 2A, two-way ANOVA). To further assess microglia viability, an immunocytochemistry evaluation of cleaved caspase-3, a marker of apoptosis, was conducted on fixed cells at the 12 hours post-injury time-point and revealed no significant difference between injured and non-injured cells (Figure 2C, unpaired student's t -test). The observation that LDH media levels were unchanged between controls and injured cells suggests that a 20% stretch-injury does not alter microglia viability or membrane permeability. Furthermore, there

was no significant difference between control and injured cells of cleaved caspase-3 expression, a marker of apoptosis, demonstrating that 20% stretch-injury does not induce apoptosis. Taken together, these results suggest that a 20% stretch-injury does not significantly affect microglia viability or membrane permeability at 12 hours post-injury.

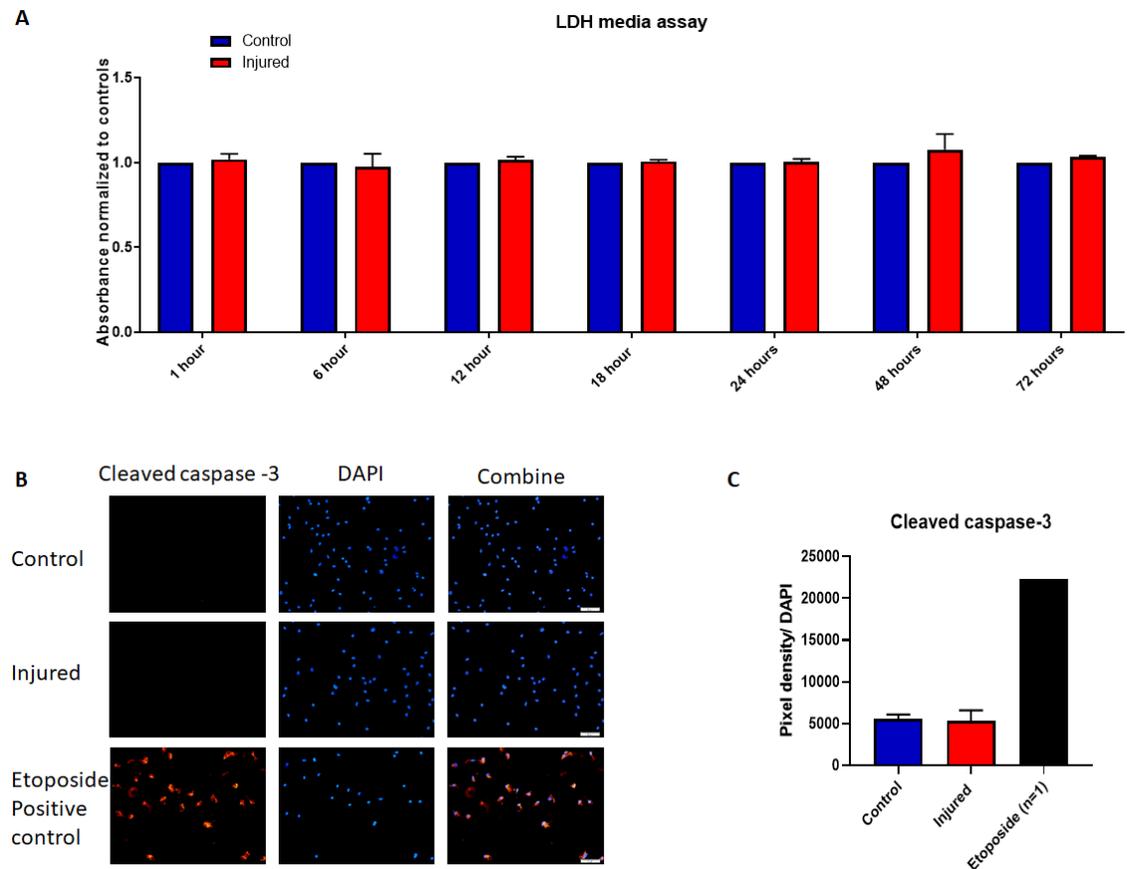


Figure 2. Stretch-injury does not affect primary microglia viability. A) Primary microglia exposed to a stretch-injury of 5 psi show no significant difference in media LDH compared to control cells. Injured condition normalized to controls (set as 1.0). B) Representative sample of one trial presented. Scale bar is 50 μ m. C) Immunocytochemistry evaluation of cleaved caspase-3 indicates no significant difference between injured and control cells. Points represent individual data points. N=3/group. Error bar represents \pm SD.

NO release and iNOS expression is significantly down-regulated following stretch-injury

To examine the acute and long-term effect of stretch-injury on microglia function, a -course study was conducted using NO assessment in the media at 1, 6, 12, 18, 24, 48, and 72 hours post-injury. Stretch-injury significantly down-regulated release of NO at 6, 12, 18, and 48 hours post-injury (Fig 3A; 6 p=0.0143, 12 p=0.0191, and 18 p=0.0338 and 48 hours p=0.0040, two way ANOVA, Sidak's multiple comparisons post-test).

Immunocytochemistry evaluated the primary enzyme responsible for catalyzing NO production, iNOS, at 12 hours post-injury and showed that stretch-injury significantly decreased iNOS expression compared to non-stretched control cells (Fig 2B; p=0.0015 unpaired student's t-test). Compared to controls, stretch-injury did not alter gene expression of iNOS at 12 hours post-injury. The observed decreases in NO release and iNOS protein expression following a 20% stretch-injury suggest that a mechanical stimulus can reduce microglia function. This reduction is not related to a decrease in cellular viability.

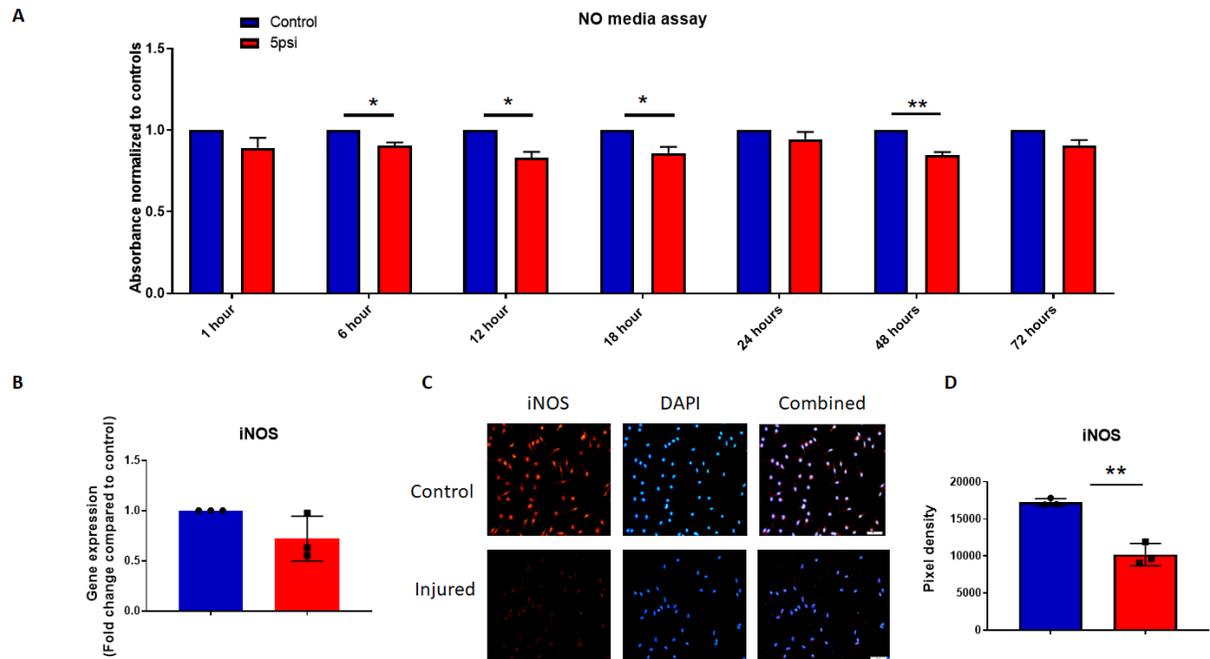


Figure 3. Stretch-injured primary microglia display decreased NO production and iNOS expression. A) Media assays show injured cells produce significantly less NO when compared to uninjured cells at 6, 12, 18, and 48 hours after injury. Injured condition normalized to controls set at 1.0. All groups were compared using two-way ANOVA with Sidak's post-test. * $p < 0.05$, ** $p < 0.01$. $N=3$ /group. Error bars represent \pm SD. B) Stretch-injury does not significantly alter iNOS gene expression twelve hours post-injury. Points represent individual data points. C) Representative sample of one trial presented. Scale bar is 50µm. D) Quantification of pixel density shows stretch-injury significantly down-regulates iNOS protein expression at 12 hours post-injury. $N = 3$ /group. Points represent individual data points. Error bars represent \pm SD. Groups were compared using an unpaired t-test, ** $p < 0.01$.

ROS is unaffected by stretch-injury

ROS production was assessed at 12 and 24 hours post-stretch to determine if this microglial activation product and subsequent oxidative stress aligned with NO release. Evaluation of ROS at 12 and 24 hours post-injury showed no significant effect of stretch-injury on ROS production at either time point compared to control cells (Fig 4A, one-way ANOVA). There was no effect of stretch-injury on microglia-mediated oxidative stress,

evaluated using western blot analysis for 3-NT, at 12 hours post-injury (Fig 4B, unpaired student's t-test). To further investigate ROS production, the expression of the NOX2 membrane-bound enzyme component, gp91, was evaluated at 12 hours post-injury using western blot, and its expression, compared to controls cells, was not significantly altered (Fig 4C, unpaired student's t-test). The data shows that ROS production and oxidative stress do not track with decreases in NO release.

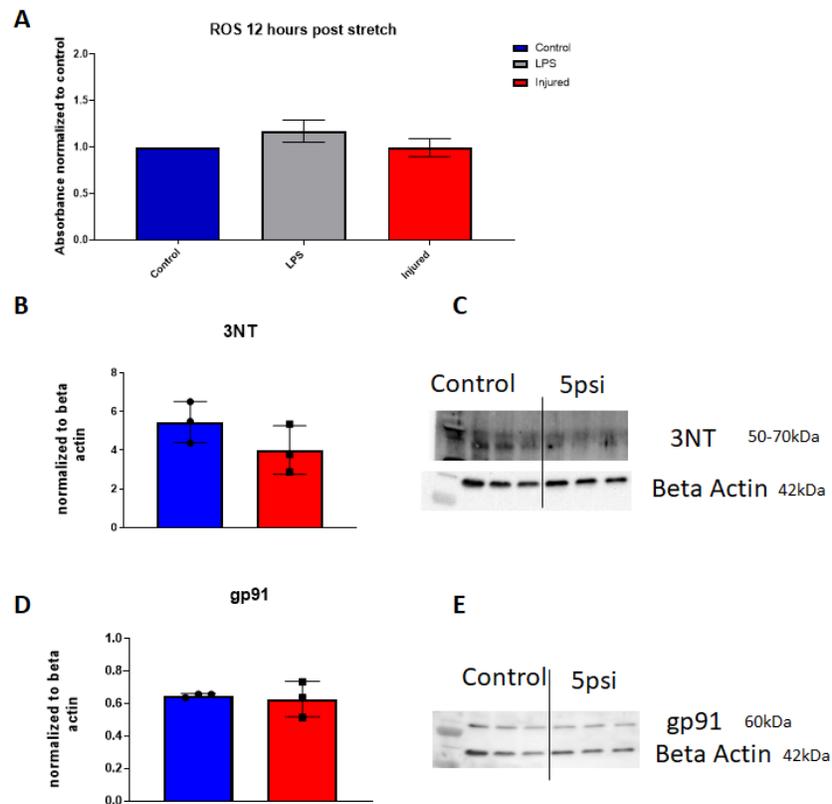


Figure 4. ROS production is not altered by stretch-injury. A) Cellular and media ROS production is not altered at 12 or 24 hours after stretch-injury. All groups were compared using one-way ANOVA. N=3/group. Experimental groups were normalized to control values. B) Oxidative stress, measured by 3-NT, is not significantly altered at twelve hours following stretch-injury. C) Representative blots for 3NT. D) Stretch-injury does not alter the expression of NOX2/gp91 twelve hours after injury. E) Representative blots for gp91. N=3/group. All groups were compared using an unpaired t-test. Points represent individual data points. Error bar represents \pm SD.

Genes associated with microglia activation are significantly down-regulated or unaffected following exposure to stretch-injury

The expression of genes associated with microglial activation in TBI was evaluated using RT-PCR at 12 hours post-injury. The 12 hour time point was chosen based on preliminary data identifying it as the first time point after post-injury to display a significant decrease in microglia function, NO release. Pro-inflammatory associated genes, IL-6 (107), CD86 (88) and IL-1 β (107), were selected for their observed up-regulation in activated microglia in the secondary injury cascade in experimental models of TBI. Anti-inflammatory associated genes were chosen for their microglia-associated roles in TBI: immunomodulation (IL-10), tissue repair (arginase-1), homeostatic maintenance (TGF β) and pathogen recognition and capture (CD206). Pro-inflammatory associated cytokine gene IL-6 was significantly down-regulated compared to controls 12 hours after stretch-injury (Fig 5A; $p=0.0142$ unpaired student's t-test). Interestingly, the anti-inflammatory associated gene coding for the enzyme arginase-1 was also significantly down-regulated at the 12 hour post-injury time point (Fig 5B $p=0.0233$ unpaired student's t-test). Immunocytochemistry analysis of arginase-1 confirmed the gene expression results (Fig. 5I; $p=0.0491$ unpaired student's t-test). The gene expression of IL-10 was significantly decreased following stretch-injury (Fig. 5C; $p=0.0431$ unpaired student's t-test). There was no significant difference in gene expression of pro-inflammatory associated genes, CD86 and IL-1 β (Fig 5F-G) or anti-inflammatory associated genes CD206 and TGF β (Fig 5C-E) between injured and control cells at 12 hours post-injury. Interestingly, both pro and anti-inflammatory genes were significantly down-regulated at 12 hours post-injury, suggesting suppression of basal level gene expression.

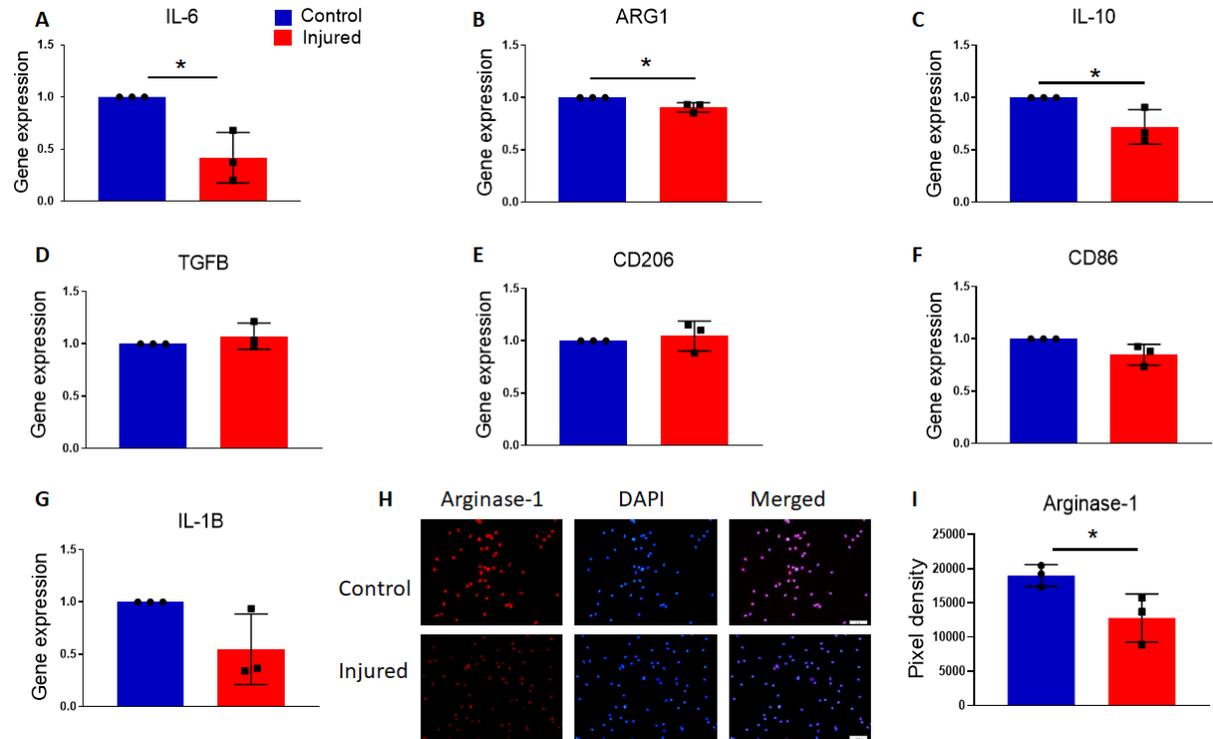


Figure 5. Injured cells display decreases in both pro and anti-inflammatory genes. Stretch-injury decreased expression of pro-inflammatory associated gene IL-6 (A) and reduced expression of anti-inflammatory associated gene ARG1 (B) and IL-10 (C) at 12 hours after injury. Gene expression of experimental groups normalized to controls set as 1.0. Stretch-injury did not alter anti-inflammatory genes TGFβ (D) and CD206 (E) or pro-inflammatory genes CD86 (F) and IL-1β (G). H) Representative sample of one trial presented. Scale bar is 50μm. I) Quantification of pixel density shows stretch-injury, compared to control cells, significantly down-regulates arginase-1 protein expression at 12 hours post-injury. N = 3/group. Points represent individual data points. Error bars represent ±SD. Groups were compared using an unpaired t-test, * $p < .05$, ** $p < 0.01$.

Morphology is significantly altered in response to stretch-injury

Following a TBI, microglia undergo a morphological transformation from a small, ramified cell body to a broader, rounded amoeboid phenotype. To determine the effect of mechanical strain on morphology, phase-contrast microscopy images were taken from the center of the well twelve hours post-injury. The cell count, cell body area, number, and length of processes were evaluated using Image J analysis software. Following stretch-

injury, microglia display a significant increase in their cell body area, which is defined by the total area of the cell except for their processes, compared to controls at twelve hours after injury (Figure 6D $p=0.0049$ unpaired student's t-test). Furthermore, stretch-injured cell processes length is significantly decreased compared to control cells twelve hours following injury. (Figure 6E $p=0.0141$ unpaired student's t-test).

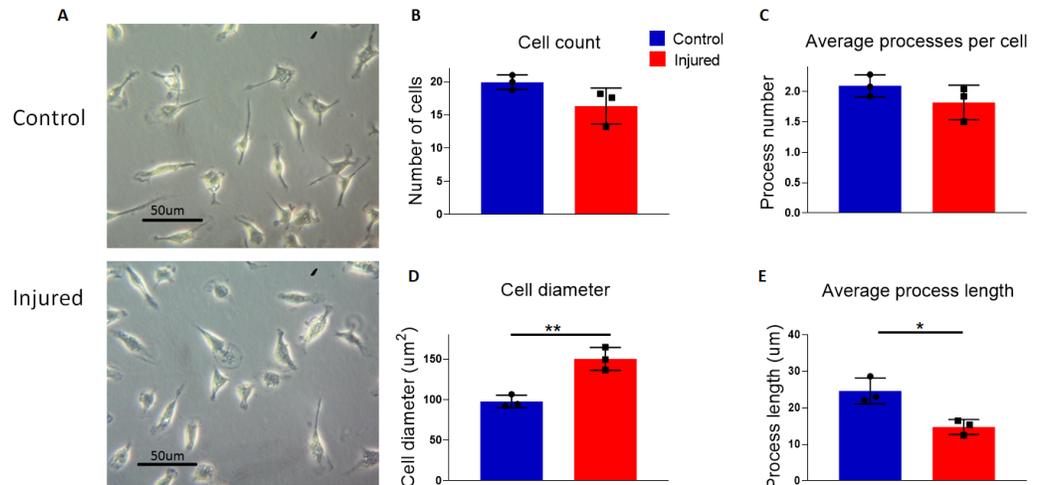


Figure 6. Stretch-injury significantly alters microglia morphology at 12 hours post-injury. A) Representative images of phase contrast micrographs twelve hours post-injury. Scale bar is set to 50µm. The total cell count (B) and average process number per cell (C) are unaffected following stretch-injury. D) Injured cells display a significantly larger cell body area compared to controls. E) The average process length is significantly decreased compared to controls. N=3/group. All groups were compared using unpaired t-test, * $p<.05$, ** $p<.01$. Bars represent mean \pm SD.

Migration is impaired substantially following stretch-injury

Microglia localizes to the site to help contain the damage and mediate the immune response in response to injury. We developed and conducted a longitudinal examination of migratory behavior using a cell exclusion zone assay to assess this behavior following injury. The exclusion zone assay assesses migration based upon the cell's propensity to migrate to areas void of other cells. The silicone stripe was placed in the center of the

well before seeding to create an area void of cells. The results showed significantly fewer cells migrated into the exclusion zone in the injured condition at forty-eight and seventy-two hours after injury than control cells (Figure 7B $p=0.0002$ and $p=0.00001$ two-way ANOVA with Sidak's multiple comparisons).

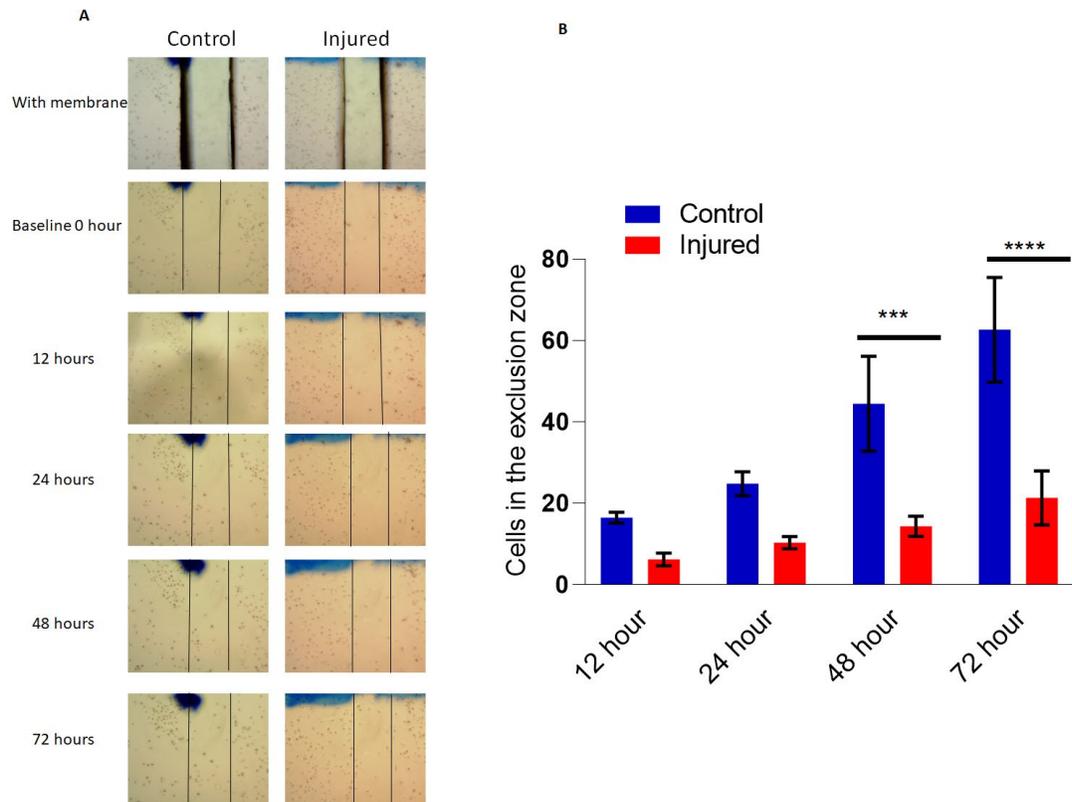


Figure 7. Migration is significantly decreased following a stretch-injury at 48 and 72 hours after injury. A) Representative phase-contrast micrographs of the cell exclusion zone assay. B) Stretch-injury significantly decreases the number of cells that migrate into the exclusion zone at 48 and 72 hours post-injury compared to the control group. $N=3/\text{group}$. Two-way ANOVA with Sidak's multiple comparison test, *** $p<.001$, **** $p<.0001$. Bars represent mean \pm SD

Phagocytosis is not affected by injury

To assess the phagocytic activity of microglial cells in response to injury, primary cells were exposed to a stretch-injury, and eight hours after the measurement of

phagocytosis of FITC-IgG conjugated latex beads was assessed. Interestingly, there was no difference between bead uptake between the control and injured cells, demonstrating that stretch does not affect phagocytosis. Culture dishes treated with LPS (100 ng/mL) were included as a positive control. Briefly, cells were incubated with LPS for 44 hours and treated with identical conditions to control and injured cells. Compared to controls, the LPS treated group increased bead uptake (Figure 8B. $p=.0501$ one-way ANOVA with multiple comparisons).

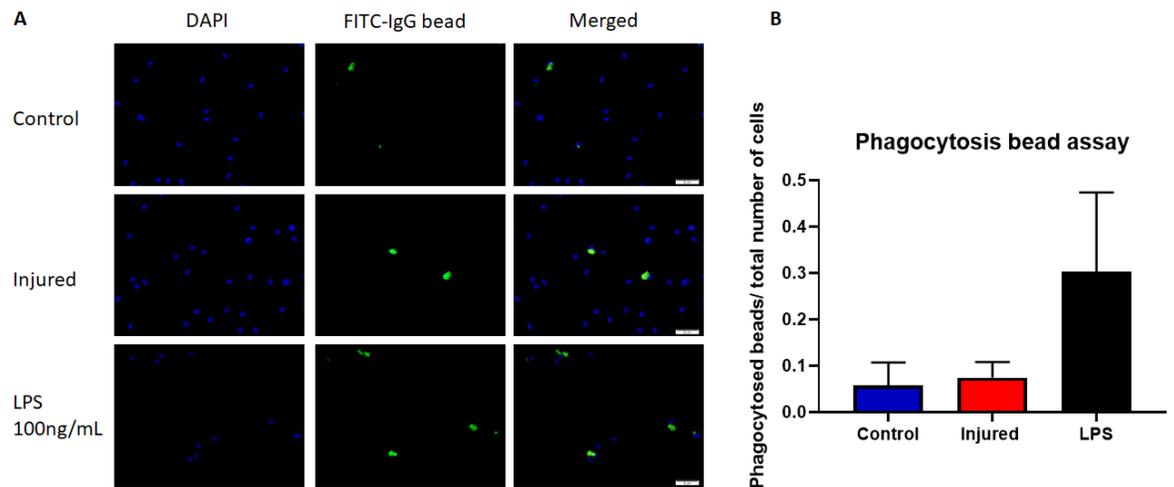


Figure 8. Stretch-injury does not alter phagocytic activity. A) Representative images of latex beads conjugated with FITC-IgG (green) were incubated for 4 hours with control, stretch-injured, and LPS treated primary microglial cells. Scale bar set to 50 μm . B) Quantitation of phagocytosed beads demonstrated that stretch-injury did not alter phagocytic activity compared to control, uninjured cells at 12 hours post-injury (8 hours following stretch-injury cells were treated with FITC-IgG for 4 hours). The LPS positive control (100ng/mL) displayed a strong trend towards phagocytosing significantly more beads when assessed at 48 hours post-treatment (44 hours after LPS treatment cells were incubated with FITC-IgG for 4 hours).

Stretch-injury does not prime or depress microglial NO release or alter LDH release when exposed to a subsequent LPS challenge

To evaluate the potential priming effect of stretch-injury, primary microglia were exposed to a stretch-injury then treated with LPS (100 ng/mL) fifteen minutes after the injury. Following treatment, cells were assayed for viability and function using LDH and NO media assays, respectively. Compared to LPS only treated cells, stretch-injury did not significantly alter viability when subsequently treated with LPS at 24, 48, or 72 hours post-injury (Fig 9A, one-way ANOVA). There was a significant increase in media LDH in both the LPS treated only and LPS plus stretch-injury at 24, 48 and 72 (Figure 9A $p=0.0007$, $p=0.0008$ and $p=0.004$) hours compared to control cells. Stretch-injury does not prime or depress NO release when treated with LPS fifteen minutes after injury compared to LPS treated only cells at 24, 48, or 72 hours post-injury (Fig 9B, one way ANOVA). Cells exposed to a stretch-injury plus LPS and LPS treated only displayed a significant increase in NO release at 48 (Figure 9B $p=0.0001$ one-way ANOVA with Dunnett's post-test) and 72 hours after LPS treatment ($p=0.0091$ one-way ANOVA with Dunnett's post-test). Surprisingly, stretch-injury antecedent to LPS treatment did not affect NO release at any post-injury time point, despite the finding that stretch-injury decreases NO release at 48 hours. However, several factors may have contributed to this observation, such as the potency of LPS, schedule of subsequent treatment, and outcome measure of microglia function.

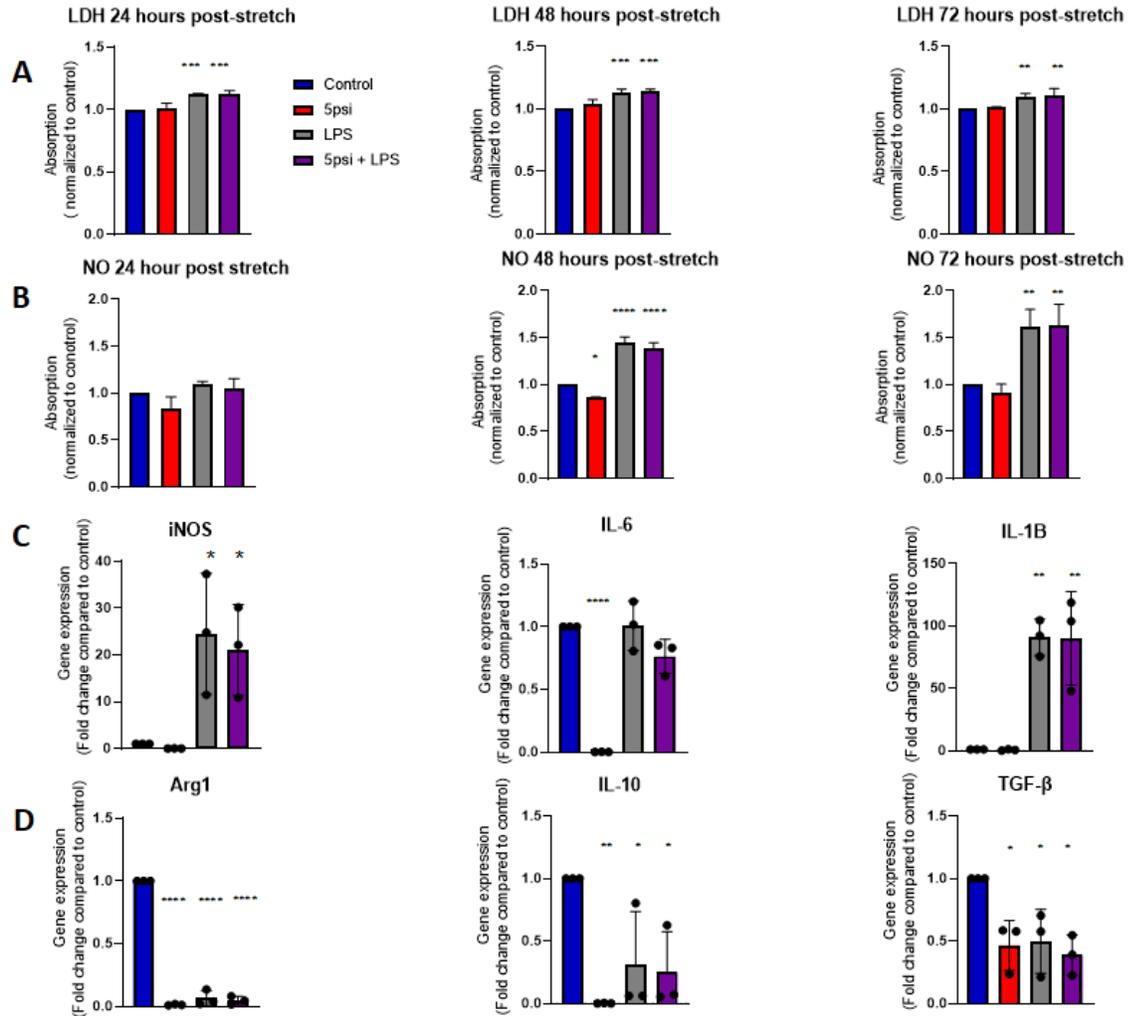


Figure 9. Stretch-injury does not alter microglia NO or LDH responses to subsequent LPS stimulation. A) Stretch-injury before LPS treatment does not induce a significant difference in LDH release between LPS treated and stretch-injury plus LPS treatment. Both LPS and LPS plus stretch-injury significantly increased LDH release at 24, 48, and 72 hours post-treatment. B) Pre-stretch-injury does not alter NO responses when subsequently exposed to LPS. LPS and stretch-injury plus LPS both significantly upregulate NO at 48 and 72 hours post-treatment. C) Post-injury treatment with LPS does not alter pro-inflammatory associated gene expression twenty-four hours after treatment. D) Post-injury treatment with LPS does not alter anti-inflammatory associated gene expression twenty-four hours after treatment. N=3/group. One-way ANOVA with Dunnett's post-test. * $p < 0.05$, ** $p < 0.01$, *** $p < 0.001$, **** $p < 0.0001$. Experimental groups are normalized to the control group set at 1.0. Error bars represent mean \pm SD.

DISCUSSION

The findings presented here address a significant gap in the microglia literature in the context of TBI, specifically the consequences of the primary-injury on microglia viability, morphology, and function. We demonstrate that rat primary microglia remain viable while displaying significant functional and morphological perturbations in response to a stretch-injury with a 20% strain magnitude.

Stretch-injury does not affect microglial viability

The longitudinal assessment of media LDH from stretch-injured cells showed no significant changes at any post-injury time point examined compared to controls, demonstrating that stretch-injury does not result in altered membrane integrity or necrosis. For example, stretch-injured rat cortical astrocytes exposed to injury parameters similar to those used in this study exhibit increased media LDH up to twenty-four hours after injury, suggestive of injury-induced membrane permeability (55). Additionally, stretch-injury does not induce apoptosis, as indicated by no changes in cleaved caspase-3 expression between injured and control cells. These findings counter what is found in stretch-injured astrocytes (7) and neurons (207). They can be attributed to differences in cellular size, morphology, and functional roles in the brain. Astrocytes are significantly larger than microglia and, consequently, have more surface area exposed to the strain forces, leading to increased membrane alterations (195). Like astrocytes, neurons vary significantly in cell diameter and morphology compared to microglia, with a larger cell body and long, delicate axons susceptible to damaging strain forces (75). Furthermore, microglia may be less sensitive to harmful strain forces than astrocytes and neurons because they are constantly surveying the brain through migratory and motile behavior.

In contrast, astrocytes and neurons are adherents, stationary and non-migratory in non-pathological conditions, rendering them more susceptible to mechanical deformations. Taken together, these results suggest that stretch-injury does not alter viability or membrane permeability.

NO production is impaired following injury

Stretch-injury significantly downregulated iNOS expression and decreased media levels of NO. These findings contrast to what is observed in patients and experimental models of TBI. They can be attributed to fundamental modeling differences and may indicate an innate response of microglia to the injury itself. To assess the effects of primary injurious forces on microglia, monolayer cultures are exposed to an injury in a sterile environment, free from other damaged cells and DAMPS. Because of this unique environment, microglia activation and subsequent up-regulation of iNOS and NO production are not observed. Microglia upregulate the immune-response enzyme iNOS increasing the production of NO, an inflammatory mediator. Multiple experimental models of TBI (61; 106; 109; 110) show a significant upregulation of iNOS gene and protein expression following injury. Through increased iNOS expression and activity, continuous production of NO can lead to cytotoxic oxidants, such as peroxynitrite, that contribute to oxidative stress (42; 70; 178). Multiple aspects of the process involved in NO production were evaluated in the current study. Contrary to what is observed in the *in vivo* injured brain, media NO levels were significantly down-regulated at six, twelve, eighteen, and forty-eight hours after injury compared to uninjured cells. The absence of DAMP and soluble inflammogens can account for these interesting findings. Our priming study showed that injured cells treated with LPS responded identically to uninjured LPS-

treated cells. Demonstrating that a physical injury produces a unique phenotype, unobserved in the literature.

Consistent with the decreased NO in the media, the expression of iNOS protein was significantly down-regulated twelve hours following injury. However, mRNA transcripts were unaffected by injury at the same time points compared to non-stretched cells. Interestingly, a rat model using a controlled cortical impact (CCI) showed that tissue NO is significantly decreased at two, six, and twelve hours following injury near the injury site. However, opposite to our iNOS findings, there was a significant increase in NADPH-diaphorase-positive cells, indicative of NOS activity, in the same regions where the NO decrease was detected. The authors attributed the reduction in NO to it being converted into peroxynitrite (217). Additionally, consistent with the findings of the *in vivo* study, we observed a significant decrease in media NO levels following injury; however, in contrast to the animal model, we found that the protein expression of iNOS is significantly decreased. This can be explained by the context of the *in vitro* environment, which lacks damaged associated factors that lead to microglial activation and increase iNOS expression. Future studies will evaluate the mechanism underlying the marked reduction in iNOS expression and determine if stretch-injury alters NO production in activated microglia. Our findings show that a stretch-injury suppresses media NO levels and down-regulates iNOS protein expression, suggesting that basal level NO production is affected by stretch-injury

The finding that stretch alters media NO and iNOS expression, but not iNOS mRNA transcription, is puzzling. A possible explanation could be that stretch-injury disrupts protein synthesis by inducing endoplasmic reticulum stress, observed in animals

TBI model of blast injury (127) and fluid percussion injury (189). Additionally, rats exposed to a CCI model of TBI showed differentially methylated mRNA transcripts (213), a prominent post-transcriptional modifier of RNA, and has been shown to inhibit translation (28). Collectively, the data indicate that stretch-injury significantly down-regulated NO media production at multiple time points. This is mediated by a significant decrease in iNOS expression, demonstrating that stretch-injury produces functional deficits in immune function.

ROS production is unaffected by injury

Experimental models of TBI show that chronically activated microglia contribute to neuronal damage and dysfunction by producing free radical oxygen species that lead to cytotoxic oxidative stress (42; 76; 78). Following activation, microglia upregulate NOX2 and increase ROS production, which can form cytotoxic factors, such as peroxynitrite, that lead to protein nitrosylation, resulting in protein cellular dysfunction or death. To evaluate the effect of stretch-injury on microglial ROS generation and oxidative stress, assessments of ROS, oxidative stress and the NOX2 enzyme were performed. Production of ROS was conducted by evaluating media and cellular levels twelve hours after injury. Interestingly, there was no effect of stretch-injury on ROS production compared to control cells. Next, western blot analysis showed that the expression of gp91, the membrane-bound component of the NOX2 complex, was unaffected by stretch-injury. Lastly, western blot evaluated oxidative stress for 3-NT, a marker of protein nitrosylation, specifically tyrosine residues. Consistent with the other ROS-related outcome measures, stretch-injury did not affect the oxidative stress response; specifically, protein nitrosylation, indicated by no changes between control and injured cells using

western blot analysis of 3-NT. These results are surprising, given that multiple lines of research show both NO and ROS production are increased following microglial activation (18; 35; 38). Contrary to the RNS data, ROS does not appear to be affected by stretch-injury.

Inflammatory gene expression is significantly decreased after stretch-injury

Following a TBI, activated microglia release both pro and anti-inflammatory-associated cytokines (45). Multiple converging lines of research show that the post-insult inflammatory response in the brain presents with a pro and anti-inflammatory phenotype, and this duality varies temporally. For example, a rodent model of diffuse brain injury, where strain-induced injuries are prevalent, showed an increase in both pro (IL-1 β , CD14 and iNOS) and anti (arginase-1) inflammatory mRNA transcripts at twenty-four hours post-injury (62). The effect(s) of the primary forces on the expression of microglial inflammatory-related genes is undefined. To address this gap in the literature, mRNA transcripts of inflammatory-associated genes were evaluated using RT-PCR at twelve hours post-stretch-injury. Interestingly, we found that both pro-inflammatory (IL-6) and anti-inflammatory (IL-10 and arginase1) associated genes were down-regulated following injury. This is counter to what is observed in experimental models and patients with TBI, where these genes are commonly upregulated. For example, plasma levels of IL-6 are significantly elevated acutely in patients who sustain an mTBI (53). In a rat model of experimental TBI, there was an immediate increase in brain IL-10 mRNA transcripts, peaking at four hours post-injury and continuing to rise until 20 hours post-injury (95). In a mouse model of TBI, arginase-1 mRNA transcripts were significantly upregulated twenty-four hours following injury in both young (three-month old) and old (24-months

old) animals (108). However, an important distinction between our findings and these in vivo observations is that, in our study, 1) only microglia are exposed to the stretch-injury, and 2) they do not interact with DAMPs or damaged cells and do not appear to be activated, either morphologically or functionally. Therefore, the upregulation of inflammatory genes would not be expected. Stretch-injury suppresses multiple genes associated with the inflammatory response following injury; the consequence and long-term ramifications on microglial inflammatory response are important since dysfunctional inflammatory responses are observed in the chronically injured brain.

Migration is impaired after a stretch-injury

Stretch-injury decreases basal level microglial migration. Following the initial injury, microglia sense factors from the trauma and migrate to the injury site to remove debris and damaged cells (79). To date, the effect of stretch-injury on migration in the biomechanically injured brain is unexplored in the literature. To address this gap in the literature, we assessed migration following stretch-injury by using a cell exclusion assay and found that stretch-injury significantly reduced the number of cells that migrated into the exclusion zone at forty-eight and seventy-two hours post-injury. These findings show that a mechanical stimulus can reduce an essential functional behavior integral to the response to injury and necessary for homeostatic function. Future studies will elucidate the extent these migratory deficits play in a physiologically relevant setting.

Stretch-injury alter microglia morphology

Microglial morphology is significantly altered following exposure to stretch-injury. Following the primary injury, microglia undergo a morphological transformation characterized by a significant increase in soma diameter and reduced processes to take on

an amoeboid phenotype (26). Phase-contrast imaging showed that stretch-injury significantly increased cell diameter and reduced process length twelve hours after injury, demonstrating that a deformation event alone can rearrange the cytoskeleton. This is consistent with morphological alteration in neurons (90; 172), astrocytes (201), and endothelial (169) cells exposed to stretch-injury. The stretch-induced reduction in process length may contribute to the decreased number of cells migrated into the exclusion zone. Since migration involves remodeling of the cytoskeleton, one explanation could be that stretch-injury alters and impairs its remodeling during migration.

Injury does not affect phagocytosis

Phagocytosis is unaffected following stretch-injury. Multiple studies show that activated microglia significantly increase their phagocytic function compared to their resting cells (59; 82; 210). A critical role of activated microglia in the post-injured brain is phagocytosing debris and dead and damaged cells (121). The assessment of phagocytosis on stretch-injured cells showed no difference in fluorescently label conjugated beads uptake between the control and stretch-injured group, twelve hours post-injury. Given that basal level phagocytosis in resting microglia is already low, it was not expected to see an effect of a stretch injury. An interesting observation was the relatively low number of phagocytosed beads in the non-activated cells cultured on Pronectin. This finding is consistent with a study showing that when primary rat microglia are incubated with fibronectin, there is a reduction in phagocytosis, as measured by the engulfment of zymogen particles. Furthermore, the same study showed that morphological phenotypes were consistent with our control cells, with cells displaying a reduced cell body diameter and an increased number of processes (30).

Injury does not prime microglia to a subsequent LPS challenge

The microglial inflammatory response is not altered following treatment with LPS post-stretch-injury. To extend our model into a more physiologically relevant setting, where mechanical forces are followed by exposure to inflammatory challenges, stretch-injured microglia were treated with LPS, a potent microglial activator, fifteen minutes following injury. Then media levels of NO and LDH were assessed at twenty-four, forty-eight, and seventy-two hours post-treatment to determine viability and activation. Surprisingly, the suppressive effect of stretch-injury on NO media levels was not observed in the post-stretch, LPS treated cells. Consistent with the LDH results from the time course assessment, LDH media levels were unchanged between any groups. The unexpected NO media result could be attributable to multiple issues. The first could be the potency of LPS as an inflammatory challenge.

Given that LPS is an endotoxin found on the outer membrane of gram-negative bacteria, it is expected that LPS would elicit a more robust inflammatory response than factors that are released during a TBI. For example, primary rat microglia treated with interferon- γ (IFN γ) and tumor necrosis factor- α (TNF α), factors associated with brain trauma, display a varied inflammatory response compared to LPS. Compared to the IFN γ and TNF α treatment, LPS treated cells expressed more NOS and arginase-1 mRNA transcripts and protein expression. Additionally, media NO levels were also considerably higher. The second issue could be the timing of the challenge post-injury. The effects of stretch-injury may not have enough time to alter the response to LPS. Future studies will challenge stretch-injured cells at immediate and delayed time points. These results suggest that stretch-injury does not change microglial inflammatory response when

subsequently challenged; however, as noted above, multiple factors could account for these findings.

CONCLUSIONS:

The results presented here are the first to examine the consequences of the primary injury on microglia by characterizing the effects of stretch-injury on viability, morphology and function. The data shows that microglia remain viable after the injury and display morphological alterations, with decreased process length and functional deficits, reduced migration and nitric oxide production at twelve hours after injury. Additionally, stretch-injury significantly down-regulates inflammatory associated gene transcripts at 12 hours. These findings will contribute to the understanding of microglia in TBI, and future studies will elucidate the molecular mechanism(s) responsible for these deficits. Furthermore, studies will examine the effects of dysfunctional microglia response observed in experimental models and individuals with TBI.

Chapter 3: The $\alpha 5\beta 1$ integrin/FAK pathway partially mediates stretch-induced deficits in primary rat microglia

ABSTRACT

Stretch-injured primary rat microglia, cultured on a synthetic fibronectin substrate, display significantly altered morphology, function and inflammatory-associated gene expression. The $\alpha 5\beta 1$ integrin mediates microglial attachment to fibronectin via the RGD binding peptide. We now find that blocking the $\alpha 5\beta 1$ integrin with a commercially available RGD peptide mimics the stretch-induced morphological alterations and functional deficits in primary rat microglia. Like injured cells, RGD treatment resulted in significant decreases in media nitric oxide (NO) levels, iNOS expression and migration deficits. The integrin-associated signaling enzyme, focal adhesion kinase (FAK), autophosphorylates tyrosine residue 397 upon integrin ligation and mediates multiple downstream cellular processes. Phosphorylation of the tyrosine 397 residue on FAK is significantly decreased following a stretch-injury and when treated with an RGD peptide. Post-injury treatment with 20nM of ZINC 40099027, an activator specific to the tyrosine 397 residue, rescued the stretch-induced decrease in FAK phosphorylation without affecting the total expression of FAK. Furthermore, treatment of stretch-injured cells ameliorated the injury-induced decrease in media NO levels, iNOS expression and inflammatory associated gene expression. Additionally, treatment alleviated morphological changes observed after stretch-injury and restored normal migratory behavior to control levels. Taken together, these data suggest that the $\alpha 5\beta 1$ integrin/FAK pathway partially mediates the stretch-injured phenotype in microglia.

INTRODUCTION

A traumatic brain injury (TBI) occurs when an external mechanical force directly or indirectly acts on the skull, resulting in the brain experiencing a sudden and rapid distribution of force that leads to immediate and irreversible damage (171). Stretch injuries are a prevalent etiological force that contributes to the initial trauma. *In vitro* models of neurotrauma are commonly used to study the effects of primary force injuries because they provide greater control over the applied mechanical stimulus, improved reproducibility and an unadulterated cellular environment (98). Multiple *in vitro* models have faithfully reproduced the cellular pathophysiology in neurons (33; 96; 205), astrocytes (33; 54; 165), endothelial cells (6; 168; 169) and microglia (177) observed in patients and *in vivo* models of experimental TBI.

We have previously demonstrated that stretch-injured primary rat microglia, the brain's predominant innate immune cells, have significantly altered morphology and functional responses twelve hours after stretch (177). Further, we found that significantly fewer stretch-injured microglia migrated into an exclusion zone compared to uninjured controls. Injured cells also significantly decreased their expression of pro-inflammatory (IL-6) and anti-inflammatory (IL-10 and arginase-1) associated genes and displayed significant morphological alterations. Injured cells had a substantially larger cell body and shorter processes. Further characterization of this novel microglial phenotype and elucidating the molecular mechanism that mediates the stretch-injured induced alterations will contribute to understanding the dysfunctional microglia states observed in people and experimental animal models of TBI.

Pilot studies showed the injury-induced phenotype was only observed when cells were cultured on Pronectin, a synthetic substrate composed of the arginine-glycine-

aspartic acid (RGD) binding peptide found on fibronectin, and not collagen I or IV, laminin, poly-D-lysine, or uncoated Flexwell plates. Milner et al. identified the $\alpha 5\beta 1$ integrin as the primary integrin receptor that mediated mouse microglia attachment to fibronectin (141). Using an RGD blocking peptide or an alpha-5 antibody, they found that blocking $\alpha 5\beta 1$ integrin attachment to fibronectin significantly altered microglial morphology, reduced integrin expression, and down-regulated the expression of the immune receptor MHC I. These results showed that the $\alpha 5\beta 1$ integrin receptor/ fibronectin axis is present in microglia and that it mediates microglial morphology and function. Integrins are transmembrane heterodimeric glycoproteins that mediate cell adhesion to the extracellular matrix (ECM) and downstream signaling for cell survival, migration, morphology, cytokine production and immune function (138). Upon integrin ligation to its cognate ECM protein, an assembly of proteins attach the cytoplasmic tail of the integrin to the actin cytoskeleton to form a focal adhesion complex. (FAC). This dynamic protein complex serves as a mechanical linkage to the ECM and mediates signal transduction pathways (170). A prominent FAC-associated signaling molecule is focal adhesion kinase (FAK). Following ligation, FAK autophosphorylates tyrosine residue 397; this regulates catalytic activities of other FAC proteins and provides docking sites for phospho-tyrosine recognition domains, thus providing the formation of protein complexes control focal adhesion dynamics and cellular function (142). Inhibition of microglial FAK phosphorylation is associated with significantly reduced migration (163). The $\alpha 5\beta 1$ integrin receptor/ fibronectin axis is established in macrophages, and one study showed a relationship between FAK activity and immune function, where inhibiting FAK phosphorylation significantly reduced migration (49) and TNF- α and IL-1 β production

(147). The role of integrin binding and the involvement of the downstream cell signaling pathway in primary rat microglia is poorly understood. Additionally, the signaling mechanism that mediates the functional and morphological deficits following a stretch-injury is unknown.

This study sought to determine the cell signaling pathway that mediates the stretch-induced migration and morphological deficits and dysregulated gene expression following injury. Two approaches were used to elucidate the pathway; the first utilized a functional RGD-blocking peptide, and the second, a FAK activator. This study demonstrated that the $\alpha 5 \beta 1$ integrin/FAK axis was present in primary rat microglia and mediated the stretch-injured functional deficits and morphological alterations twelve hours after injury.

METHODS

Cell culture

Primary microglia cultures were isolated from 2-day-old Sprague-Dawley rat pups by shaking mixed glia cultures at 100 RPM for 1 hour at 37 °C yielding 90% purity as previously described (188). Cells were maintained at 37 °C and a humidified atmosphere augmented with 5% CO₂ in media containing Dulbecco's modified Eagle medium (Gibco), 1% L-glutamine (Gibco), 1% sodium pyruvate (Gibco), 10% FBS (Hyclone), and 1% penicillin and streptomycin (Thermo Fisher Scientific). Media replacement occurred every 3–5 days.

Stretch-injury

Cells were seeded at a density of 3×10^5 cells/mL on Pronectin coated silicone-based deformable membrane BIOFLEX® culture plates (BF-3001P Flexcell

International, Hillsborough, NC). Cells were incubated for 24 hours in growth media to allow for adherence (37°C, 5% CO₂), after which a stretch-injury was administered, as previously described (177). Briefly, a stretch-injury was produced using the Cell injury controller II (CIC II), which utilizes nitrogen gas to pressurize a BIOFLEX® well individually. The CIC II regulates the duration and pressure of gas delivered to the well by using a rubber tube that feeds through a plastic circular well adaptor plug that attaches to the top of the well, creating a hermetically sealed system. Upon discharging the gas, the well becomes pressurized, and a bi-axial deformation of the flexible membrane, resulting in the cultured cells experiencing a stretch-injury. All stretch-injury experiments used identical parameters with 60psi regulator pressure for a duration of 50 mSec, resulting in a 5psi pressurization of the well that created a 20% stretch event in the center of the well. The parameters used for this study were determined by a stretch-injury dose-response pilot study that established the CICII's highest setting, 60psi, resulted in functional deficits (177).

RGD peptide and FAK activator treatment

Primary rat microglia were treated two hours after plating with an RGD blocking peptide (Sigma-Aldrich CAS Number 99896-85-2) at a concentration of .2mg/mL (140). Treatment with 20nM of a commercially available FAK activator (Aoboius ZINC40099027 Cat No: A0B33456) was administered six hours after injury.

Nitric oxide (NO) measurement

Media NO was measured in injured primary microglia treated with a FAK activator 12 hours post-injury. NO content in the media was quantified using a Griess reagent assay kit (Invitrogen). The assay was performed per the manufacturer's

recommendations and as previously described (22). Colorimetric changes in 96-well plates were quantified with a Chroma Plate Reader (Midwest Scientific, St. Louis, MO, USA) at 545 nm.

Immunocytochemistry

Cells were fixed with 4% paraformaldehyde and rinsed twice with $1\times$ PBS. Primary antibodies included rabbit anti-iNOS (10 μ l/ml; Abcam, Cambridge, MA). Cell nuclei were stained with DAPI (0.5 μ l/ml; Life Technologies, Carlsbad, CA). Fluorescently tagged secondary antibodies (Invitrogen) were visualized with an Olympus BX43 fluorescent microscope with a CellSens Standard imaging program. Five randomly selected images were taken per sample, and each image was qualitatively assessed for pixel density and normalized to the total number of DAPI stained cells. Images were taken from the center of the membrane.

Protein quantification

Protein was collected from cells at twelve hours post-injury. Cells were lysed, treated with protease inhibitor (Halt Protease Inhibitor single-use cocktail, Thermo Scientific) then centrifuged for 10 minutes.. The supernatant was collected, and western blot analysis was performed as previously described (42). Briefly, 25 μ g of protein sample was run on a Mini-protean TGX precast gel then transferred to a nitrocellulose sheet (Trans-Blot Turbo Transfer System, Biorad, Hercules, CA, USA). The nitrocellulose sheet was blocked for one hour in 5% milk buffer then incubated overnight with the following antibodies: α 5 (1:100, Abcam), β 1 (1:100, Abcam) pFAK (1:1000, Abcam) and FAK (1:2000, Abcam). Individual blots were probed for the respective

antibodies. Resultant bands were quantified with Image J densitometry and normalized to a loading control protein, beta-actin (1:5000, Abcam).

RNA isolation and gene analysis

TRIzol® (Invitrogen, Carlsbad, CA) was used to extract mRNA from the cells, and mRNA concentrations were measured by a Nanodrop system (Thermo Scientific). RNA pellets were treated with RNAase. Select genes were normalized to the housekeeping gene PGK2. A Veriti thermal cycler (Applied Biosciences) and a complementary DNA (cDNA) conversion kit (Applied Biosciences, Waltham, MA) were used to convert 1 µg of mRNA into cDNA according to the manufacturer's suggested protocol. According to the manufacturer's recommended protocol, all quantitative real-time PCR (qRT-PCR) data was procured through the StepOnePlus Real-Time PCR System (Applied Biosciences). All primers were designed by Sigma-Aldrich (Darmstadt, Germany) and listed in Table 2.

Table 2. Selected gene sequences for RT-PCR

Gene	Symbol	Forward (5'-3')	Reverse (5'-3')
Transforming growth factor-beta 1	TGF-β-1	GGAAATCAATGGGATCAGTC	CTGAAGCAGTAGTTGGTATC
Interleukin-1, beta	IL-1β	TAAGCCAACAAGTGGTATTC	AGGTATAGATTCTTCCCCTTG
Interleukin-4	IL-4	GAACCAGGTCACAGAAAAAG	GGGAAGTAAAATTTGCGAAG

Interleukin-6	IL-6	CAGAGTCATTCAGAGCAATAC	CTTTCAAGATGAGTTGGATGG
Interleukin-12	IL-12	CTTCTTTGATGATGACCCTG	AATAGCCATCAGCATGTTTC
Interleukin-10	IL-10	TCTCCCCTGTGAGAAATAAAAG	GAAAGGAAAGTTCCCAGATG
Cluster of differentiation 86	CD86	CACAAGCTTTGATAGGGATAAC	TTCTTGTTTCATTCTGAGCC
Mannose receptor	CD206	GGAGTTGTGGAGCAGATGGAAG	CTTGAATGGAAATGCACAGAC
Arginase-1	Arg1	GAAGGAAAGTTCCCAGATG	CTTGTCCACTTCAGTCATTG
Inducible nitric oxide synthase	iNOS	TTCCTCAGGCTTGGGTCTTGT	GAGGAACTGGGGGAAACCATT
Phosphoglycerate kinase 1	PGK1	GGAGATGTCTATGTCAATGATG	TTTAGCTCCTCCCAAGATAG
Itga5	α 5	CAGATCTCGGAGTCCTAT	CCACAGAGTATCCCAAGT
Itgb1	β 1	AGCCTGTTTACAAGGAAT	GAAGAAAGGGAATTGTAG

Migration assay and morphological evaluation

A cellular exclusion zone assay was used to quantify migration as previously described (177). Briefly, cells were seeded at a density of 3×10^5 /mL on Pronectin coated

BioFlex well plates with a 1.4 cm x .1 cm strip of silicone membrane placed in the center of the well. Microphotographs were taken using a phase-contrast microscope (Zeiss, PrimoVert). Images were captured at pre-injury baseline and 12, 24, 48, and 72 hours post-injury. ImageJ (NIH, open-access software) was used to quantify cell exclusion zone diameter. Cells were counted in the exclusion zone if they matched criteria, 1) dark coloring, 2) circular or branched phenotype.

Morphology was evaluated using the same devices, and images were taken at pre-injury and twelve hours post-injury (177). ImageJ (NIH, open-access software) was used to quantify cellular characteristics, i.e., number and length of processes and cell diameter.

Statistical analysis

Statistical analysis was conducted using Graphpad Prism Software version 9.01. (GraphPad Software, San Diego, CA). NO and LDH assays were performed in triplicate for each trial, and the trials were replicated four times to generate a sample size of $n = 3$ per group. A two-way ANOVA with Sidak's multiple comparisons test was conducted on the groups whose controls were set to 1.0. The stretch-injured values were normalized to control values for each trial for NO and LDH assay measures. The trials were replicated three times to generate a sample size of $n=3$. A one-way ANOVA with Tukey's multiple comparisons test was conducted. Western blot analysis was performed in pooled samples from triplicates for each trial, and the trials were replicated three times to generate a sample size of $n=3$. Immunocytochemistry experiments were conducted singly and repeated three times to create a sample size of $n=3$. Western blot and immunocytochemistry results were analyzed using an unpaired student's t-test. The migration assay was conducted singly for each trial and replicated three times for an $n=3$.

The total number of migrating injured cells was normalized to control cells at each time point. A two-way ANOVA with Sidak's multiple comparisons test was conducted for assay measures. The morphology analysis was assessed from five images per trial, and each trial was replicated three times to generate a sample size of n=3. A total of 15 images were analyzed for the control, stretch-injured, stretch-injured treatment and treatment conditions. Percent averages for each group were assessed using a two-way ANOVA with Sidak's multiple comparisons. For all statistical tests described, a p-value < 0.05 was considered statistically significant. Data are presented as mean +/- standard deviation (SD).

RESULTS

$\alpha 5\beta 1$ integrin protein and gene expression of primary rat microglia are unaffected following stretch-injury.

Cells cultured on Pronectin, a synthetic fibronectin-mimicking substrate that primarily relies on $\alpha 5\beta 1$ for cellular attachment, displayed morphologic and functional deficits following a stretch injury (182). To determine whether injury alters the expression of the $\alpha 5\beta 1$ integrin, possibly mediating the injury-induced phenotype, western blot and RT-PCR techniques were used to evaluate protein and gene expression, respectively. Protein expression of the $\alpha 5$ and $\beta 1$ of injured microglia 12 hours after injury is equivalent to uninjured controls (Figure 10 A, C, unpaired student t-test). Consistent with the protein expression, $\alpha 5$ and $\beta 1$ mRNA gene transcripts remain at controls expression levels after injury (Figure 10 E, F, unpaired student t-test). These results show that the observed alterations following injury are not due to altered protein or gene expression of the $\alpha 5\beta 1$ integrin.

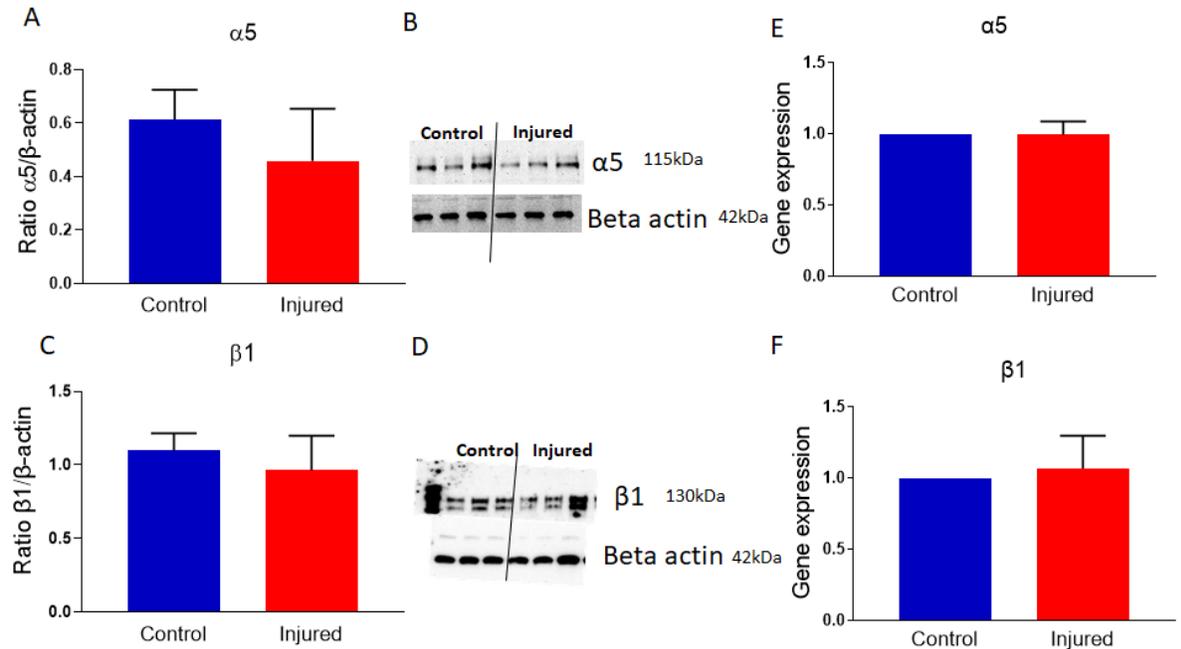


Figure 10: Stretch-injury does not alter $\alpha 5\beta 1$ integrin gene or protein expression twelve hours after injury. A) There is no effect of stretch-injury on $\alpha 5$ protein expression. B) Representative $\alpha 5$ western blot image. C) Stretch-injury does not alter the expression of $\beta 1$ protein expression. D) Representative $\beta 1$ western blot image. E) Gene expression of $\alpha 5$ does not change following injury. F) Stretch-injured microglia $\beta 1$ gene expression is unchanged following injury. Unpaired student's t-test. N=3. Bar represents standard deviation.

RGD-blocking peptide reduces media NO levels, iNOS expression and FAK phosphorylation.

Inhibiting integrin-binding with functional RGD blocking peptides alters microglia morphology and cellular function (140). In addition, stretch-injury to microglia cultured on Pronectin coated plates reduces NO levels and iNOS expression (177). To evaluate the involvement of the $\alpha 5\beta 1$ integrin in response to stretch-injury, 0.1mg/mL, 0.2mg/mL or 0.3mg/mL of a commercially available RGD blocking peptide was added to primary microglia cultured on Pronectin coated plates. For the RGD blocking study, we followed the Milner protocol (140) and evaluated the outcome measure at the forty-eight-

hour time point. Furthermore, we found that treatment with the RGD-blocking peptide did not significantly affect media NO levels or inflammatory associated gene expression twelve hours post-treatment (Supplementary figure 1 A & B; unpaired student t-test). Compared to untreated cells, all concentrations of the RGD peptide significantly reduced media levels of NO (Fig 11A; 0.1mg/mL $p=0.0127$, 0.2mg/mL $p=0.0025$ and 0.3mg/mL $p=0.0018$ one way ANOVA, Dunnett's multiple comparisons post-test). Evaluation of the enzyme responsible for microglial media NO, iNOS, was conducted using immunocytochemistry. Staining for iNOS showed that treatment with 0.2 mg/mL significantly reduced iNOS protein expression (Fig 11B; 0.2mg/mL $p=0.0460$ one way ANOVA, Dunnett's multiple comparisons post-test). Important to note is that the 0.3mg/mL treat displayed a strong but non-significant, downward trend, $p=0.0782$. From this data, the 0.2 mg/mL dose was chosen for subsequent blocking studies. Treatment with .2mg/mL RGD binding peptide significantly reduced FAK phosphorylation at tyrosine residue 397 forty-eight-hour post-treatment without affecting total FAK expression and significantly reduced the pFAK/FAK ratio (Fig 12 A & E; $p=0.0118$ and $p=0.0492$ unpaired student's t-test).

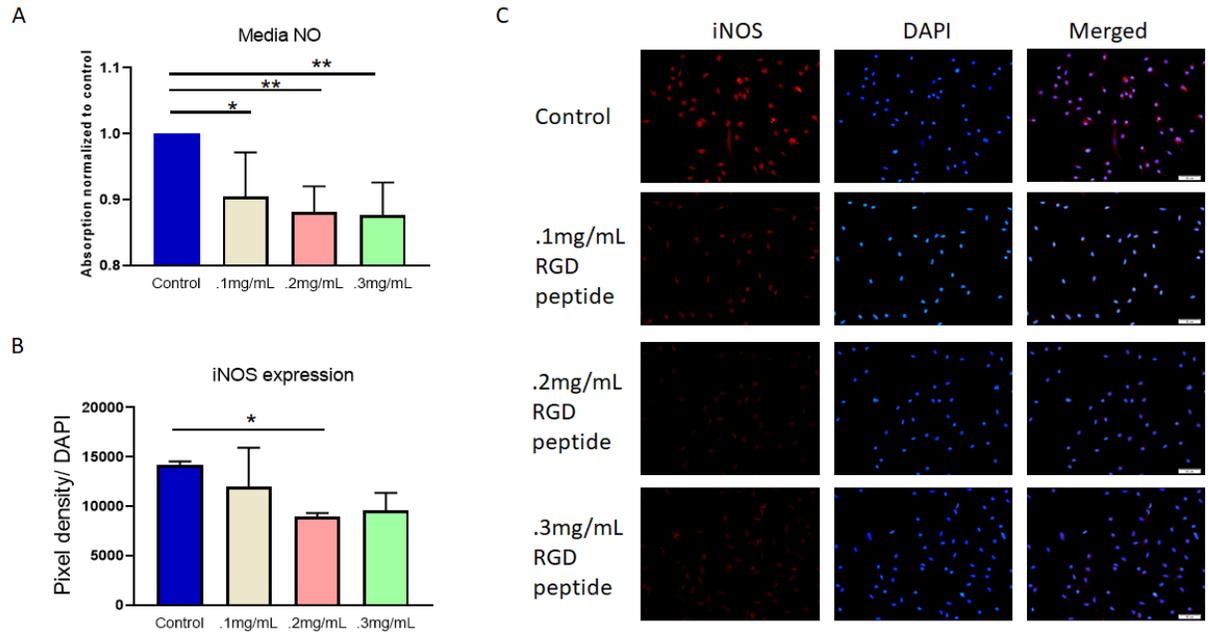


Figure 11: Treatment with .1mg/mL, .2mg/mL and .3mg/mL significantly reduced NO media levels forty eight hours after stretch-injury. Absorption values of the injured condition were normalized to controls (set as 1.0). B) iNOS expression is significantly downregulated forty-eight hours after treatment with .2mg/mL RGD peptide. C) Representative images of immunocytochemistry for iNOS expression forty-eight hours after treatment. All groups were compared using two-way ANOVA with Dunnett's post-test. * $p < 0.05$, ** $p < 0.01$. $N=3$ /group. Error bars represent \pm SD.

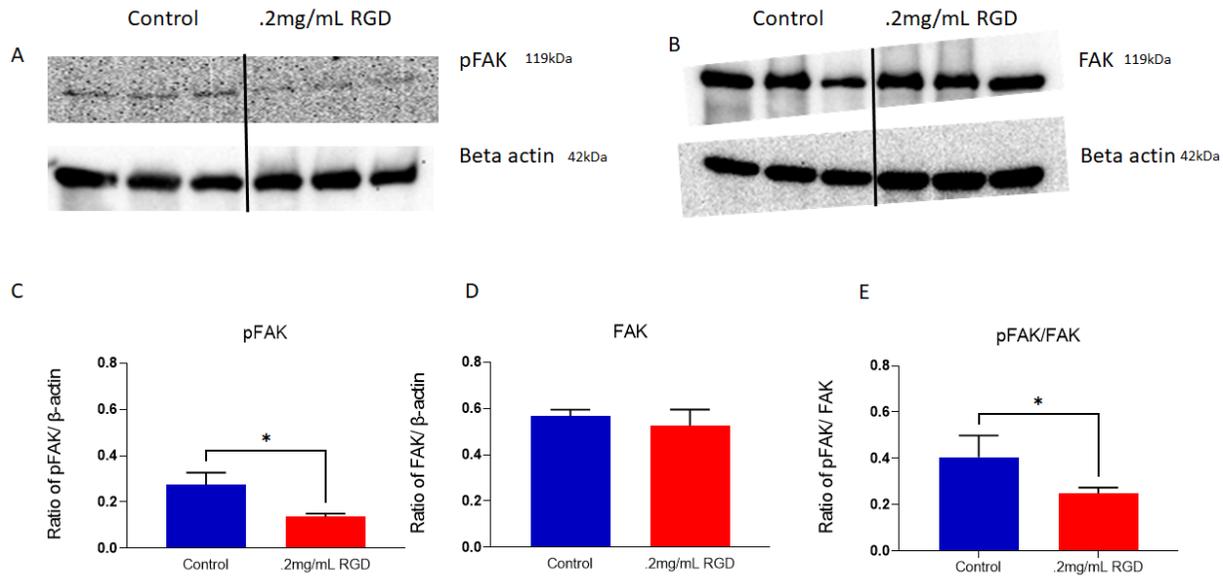
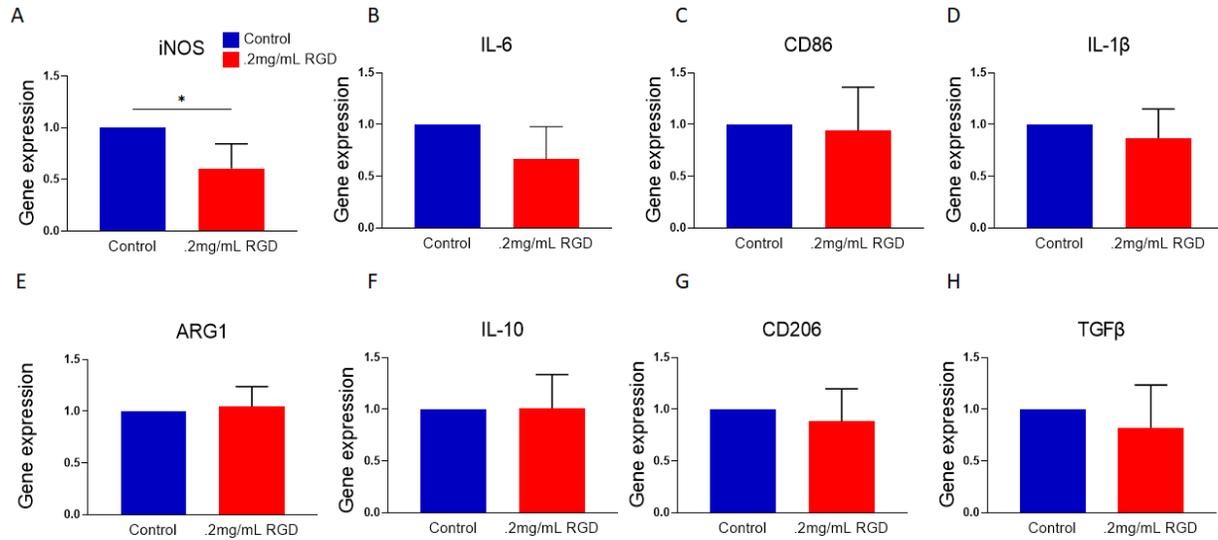


Figure 12. Treatment with .2mg/mL RGD peptide significantly decreases phosphorylation of tyrosine residue 397 forty-eight hours post-treatment. A) Representative images of pFAK western blot. B) Representative images of FAK

western blot. C) Blocking integrin-binding with .2mg/mL of an RGD peptide significantly decreases FAK phosphorylation forty-eight hours after treatment. D) Treatment does not alter FAK expression. E) The ratio of pFAK to total FAK has significantly decreased post-treatment at forty-eight hours. All groups were compared using a one-way ANOVA with Tukey's post-test. * $p < 0.05$. N=3/group. Error bars represent \pm SD.

Blocking integrin-binding with an RGD blocking peptide alters inflammatory gene expression.

We previously reported that stretch injury significantly alters microglial inflammatory associated gene expression (177). Using the 0.2mg/mL RGD peptide concentration, the same pro-inflammatory and anti-inflammatory associated genes were evaluated forty-eight hours after administration (140). Compared to untreated control cells, treatment with RGD (0.2 mg/mL) peptide significantly reduced iNOS gene expression (Fig 13D; $p=0.0457$ unpaired student's t-test). Anti-inflammatory associated genes Arg1, IL-10, CD206 and TGF- β and pro-inflammatory associated genes IL-6, CD86 and IL-1 β were unaffected following treatment (Fig 13 A-D, unpaired student's t-test and Fig 13 F-G, unpaired student's t-test, respectively). The results from the RGD blocking study suggest the $\alpha 5\beta 1$ integrin is involved in mediating that stretch-induced gene expression alteration.



Figures 13. RGD peptide treatment significantly down-regulated iNOS gene expression 48 hours after treatment. Treatment with .2mg/mL RGD peptide altered inflammatory associated gene expression at 48 hours post-treatment. Treatment decreased expression of pro-inflammatory associated gene iNOS. A) 48 hours after treatment. Gene expression of experimental groups normalized to controls set as 1.0. Treatment did not alter anti-inflammatory genes Arg1 (E), IL-10 (F), CD206 (G) and TGF β (H) or pro-inflammatory genes IL-6 (B), CD86 (C), and IL-1 β (D). N = 3/group. Points represent individual data points. Error bars represent \pm SD. Groups were compared using an unpaired t-test, * $p < 0.05$.

Migration is significantly impaired following the administration of an RGD blocking peptide.

Compared to non-injured cells, stretch-injured microglia cultured on Pronectin displayed migratory deficits on the cell exclusion assay at multiple post-injury time points (177). To assess the involvement of the $\alpha 5 \beta 1$ integrin in microglia migration, cells were treated with .2 mg/mL of the same RGD-blocking peptide and evaluated for migratory behavior using the cell exclusion zone assay. The results showed that RGD peptide treatment resulted in significantly fewer cells migrating into the exclusion zone than non-treated controls, at forty-eight and seventy-two hours after treatment (Figure 14B $p = 0.0407$ and $p = 0.0181$ two-way ANOVA with Sidak's multiple comparisons). The

effects on blocking $\alpha 5\beta 1$ integrin on microglia migration were identical to those of stretch-injury, suggesting that the $\alpha 5\beta 1$ integrin is involved in the migratory deficits following mechanical deformation.

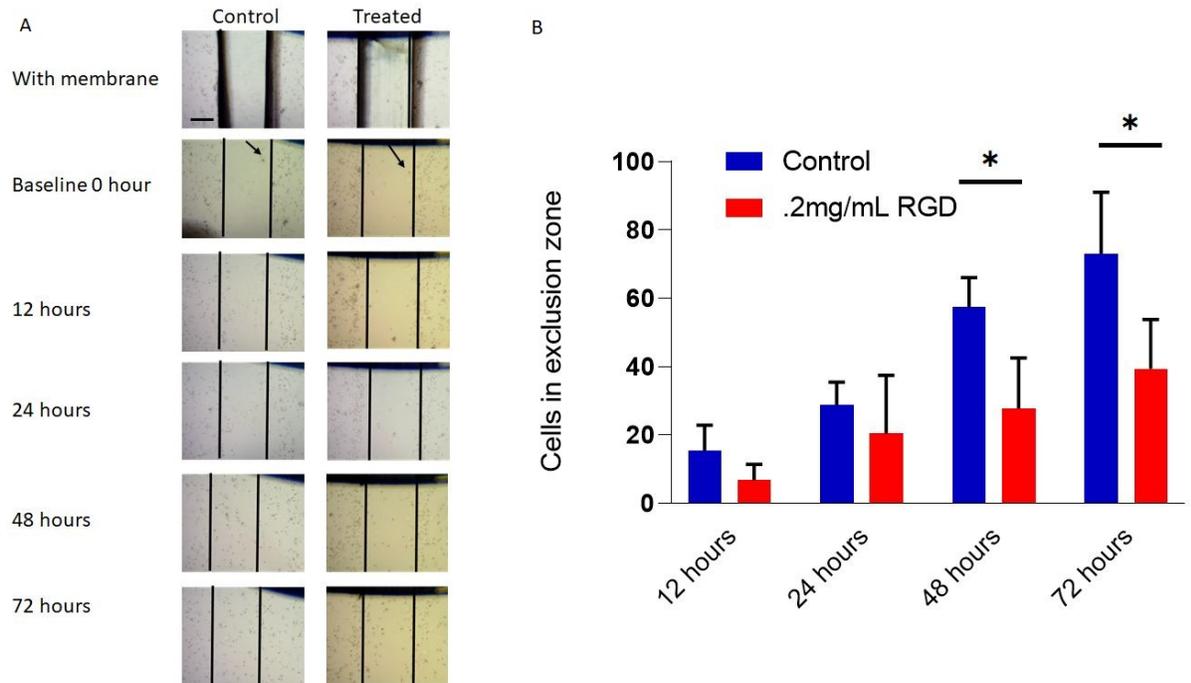


Figure 14. Migration is significantly decreased following RGD peptide treatment at 48 and 72 hours after injury. A) Representative phase-contrast micrographs of the cell exclusion zone assay. Black arrows indicate quantifiable cells. B) RGD peptide treatment significantly decreases the number of cells that migrate into the exclusion zone at 48 and 72 hours post-injury compared to the control group. N=3/group. Two-way ANOVA with Sidak's multiple comparison test, * $p < 0.05$. Bars represent mean \pm SD. Scale bar is set to 200 μ m.

Treatment with FAK activator rescues media NO levels, iNOS expression and FAK phosphorylation.

Following integrin ligation, FAK autophosphorylates and undergoes a conformational change that provides a binding site for structural and functional focal adhesion complex (FAC) associated proteins (74). After stretch-injury, FAK phosphorylation is significantly decreased (Figure 15C $p = 0.0491$ one-way ANOVA with

Tukey's post-test). At the same time, total FAK is unaffected, suggesting that injury-induced disruption of FAK activity is a potential site for pharmacological intervention to ameliorate the morphological and functional alterations; however, the ratio of pFAK to FAK was not statistically significant (Figure 15D $p=0.134$ one-way ANOVA with Tukey's post-test). Treatment with 20nM of a commercially available FAK activator, ZINC 40099027, six hours after injury, rescues the stretch-induced dephosphorylation of FAK 12 hours after injury (Figure 15C $p=0.0128$ one-way ANOVA with Tukey's post-test). Treatment alone does not significantly alter FAK phosphorylation or total FAK (Figure 15C one-way ANOVA with Tukey's post-test). Coinciding with the restoration of FAK phosphorylation is the restoration of the stretch-induced reduction of media NO. Treatment with 20 nM FAK activator, ZINC 40099027, immediately after an injury does not alter media NO levels (Figure 16C two-way ANOVA with Tukey's post-test). Treatment with the FAK activator (20 nM) does not significantly affect media NO when administered without stretch. These results show that injury reduces FAK phosphorylation and media NO twelve hours after injury, and restoring FAK phosphorylation with activator rescues media levels of NO (Figure 16C $p=0.0331$ two-way ANOVA). To determine if the effects of the FAK activator, ZINC 40099027, extend to iNOS expression, immunocytochemical analysis of iNOS was evaluated twelve hours after injury with cells treated with 20nM of the FAK activator six hours after injury. Treatment with 20 nM FAK activator, ZINC 40099027, significantly increased expression of iNOS compared to stretch-injured cells (Figure 16B $p=0.050$ one-way ANOVA with Tukey's post-test), whereas treatment with did not affect iNOS expression

compared to controls. The data are consistent with the media NO, suggesting that treatment with a FAK activator following stretch-injury.

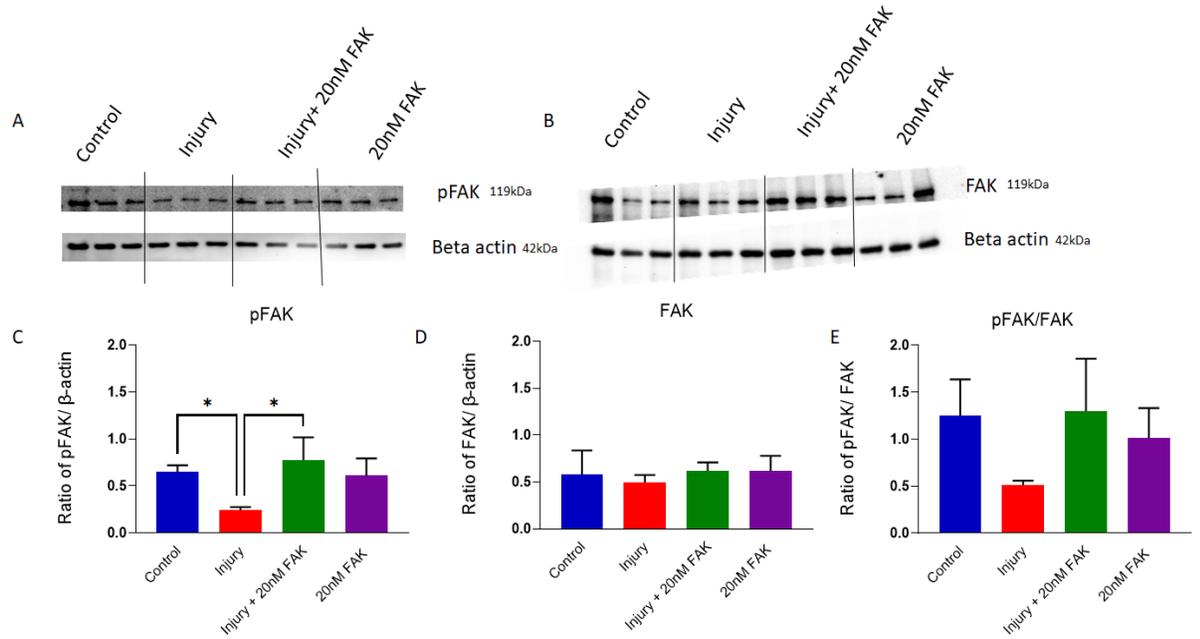


Figure 15. Six-hour post-injury treatment with 20 nM FAK activator rescues reduction in FAK phosphorylation. A) Representative western blot images for pFAK. B) Representative images for FAK. C) Stretch-injury significantly reduces FAK phosphorylation twelve hours post-injury and six-hour post-injury treatment with a FAK activator rescues FAK phosphorylation. Treatment only does not significantly alter FAK phosphorylation. D) FAK protein expression is unaffected by injury or treatment at twelve hours post-injury. E) The ratio of pFAK to total FAK is not significantly altered by injury, treatment or combination. However, there is a strong trend of injury decreasing the ratio and treatment restoring it. All groups were compared using one-way ANOVA with Tukey's post-test. * $p < 0.05$. $N=3$ /group. Error bars represent \pm SD.

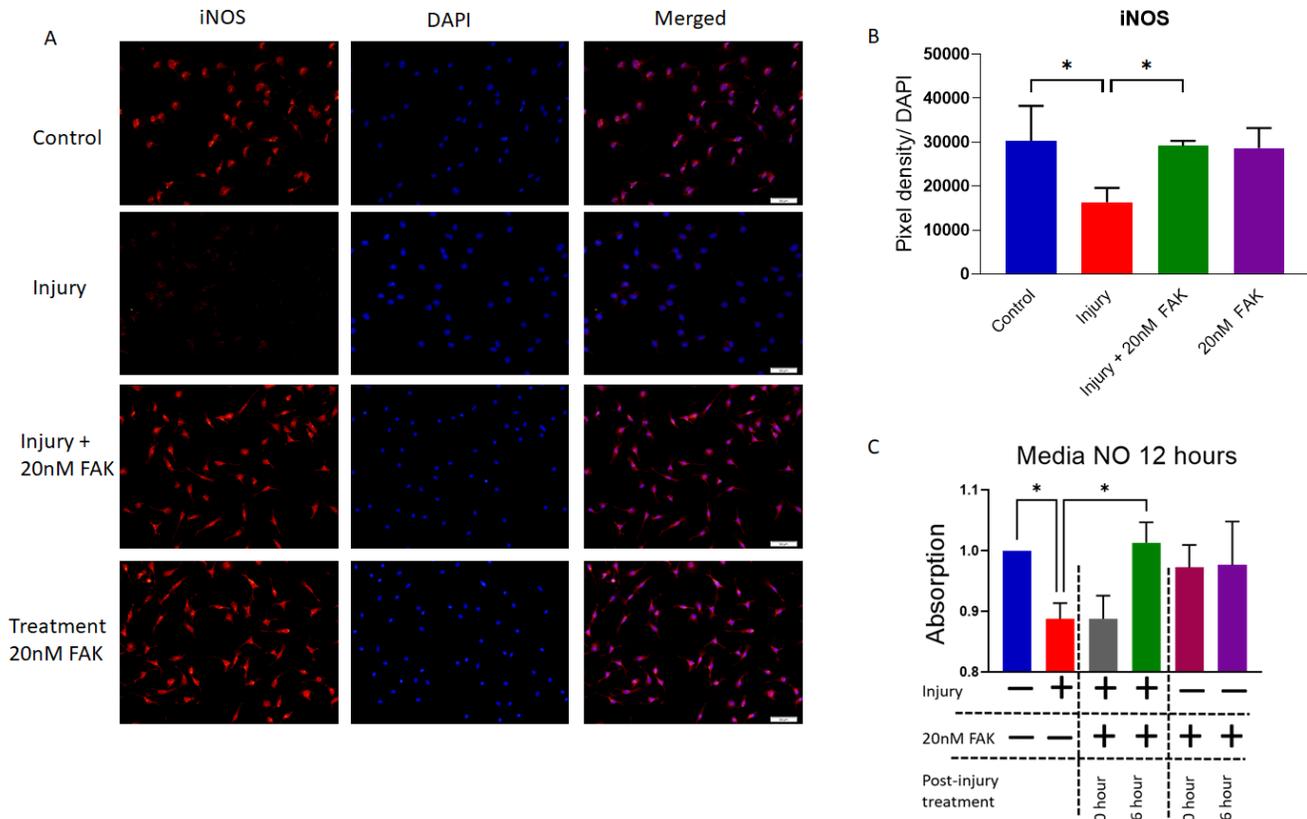


Figure 16. Treatment with a 20 nM FAK activator rescues the stretch-induced down-regulation of iNOS. A) Representative iNOS immunocytochemistry images. B) Stretch-injury significantly reduces iNOS expression 12 hours after injury compared to controls. Treatment with 20 nM FAK rescues the stretch-induced reduction in iNOS expression compared to injured cells twelve hours after injury. C) Stretch-injured cells display less NO media than controls, and treatment with 20 nM of a FAK activator six hours post-injury rescues the injury-induced decrease of NO media levels. FAK activator treatment alone did not alter media NO levels compared to control cells. Absorption values of the injured condition were normalized to controls (set as 1.0). All groups were compared using one-way ANOVA with Tukey's post-test. $*p < 0.05$. N=3/group. Error bars represent \pm SD.

Injury-induced morphological alterations are ameliorated with 20 nM FAK activator treatment.

Stretch-injured microglia display significantly increased cell area and decreased process length (177). When treated, injured cells were treated with the same 20 nM FAK activator, ZINC 40099027; after injury, cell area was returned to control levels (Fig 17B

p=0.0387 one-way ANOVA with Tukey's post-test). Process length was not significantly increased when treated with a FAK activator, ZINC 40099027; however, there was a trend towards increasing process length (Fig 17C p=0.09, one-way ANOVA with Tukey's post-test). The data presented show that treatment with a FAK activator, ZINC 40099027, restores FAK phosphorylation, rescuing the stretch-induced alterations in cell area and partially rescues the process length reduction. This demonstrates that disruption of FAK activity contributes to abnormal cellular morphology.

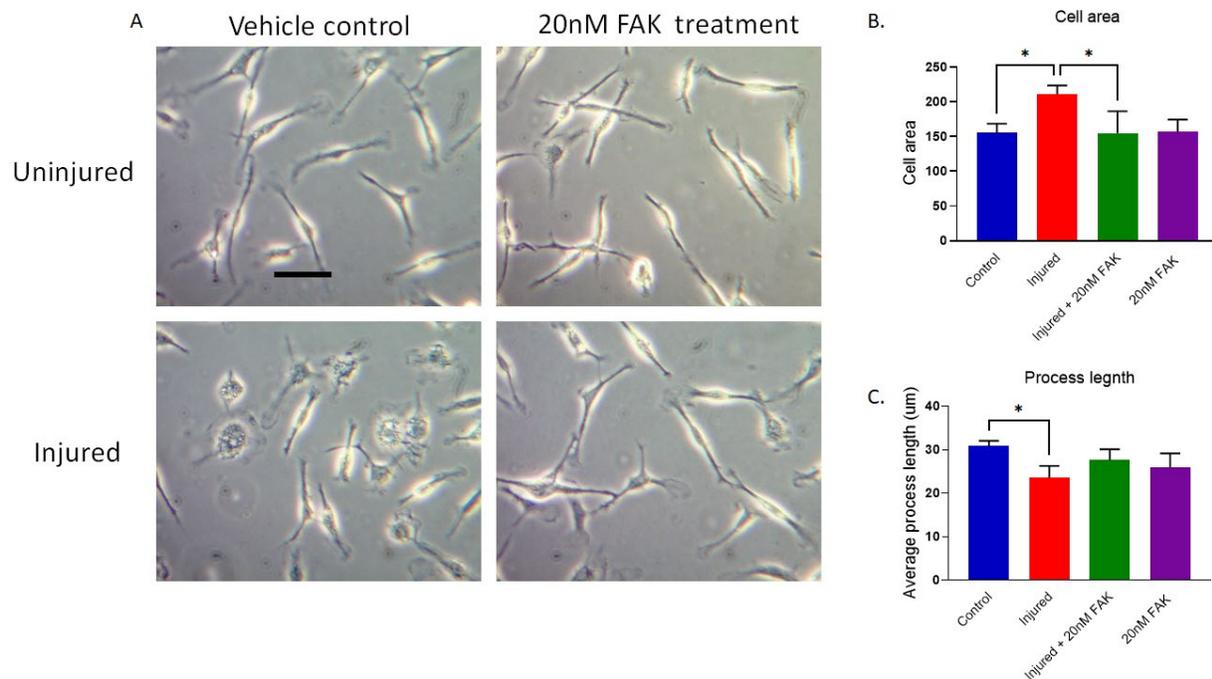


Figure 17. Treatment with a FAK activator, six hours after injury, restores stretch-injured morphological deficits. A) Representative phase-contrast microscopy images at 20x. Scale bar represents 50µm B) Cell diameter significantly increases after injury, and treatment with 20 nM FAK activator rescues the injury-induced increase. C) Stretch-injury significantly reduces average process length compared to controls. Treatment with a 20 nM FAK activator does not significantly increase process length following injury; however, there is a trend towards increasing process length. N=3/group. All groups were compared using a one-way ANOVA with Tukey's post-test, * p<0.05. Bars represent mean +/- SD.

Migration impairments following injury are ameliorated following treatment with FAK activator.

Migratory deficits coincided with a significant reduction in FAK phosphorylation following twelve hours of injury. Canonical phosphorylation of FAK is essential for properly integrating signaling pathways that control cellular migration (157). Furthermore, researchers found that inhibiting FAK phosphorylation significantly reduced microglial migration using a Transwell assay (37). Previous findings show stretch-injured microglia exhibit significant migratory impairments at forty-eight and seventy-two hours after injury (177). Treatment of stretch-injured cells with 20 nM of a FAK activator six hours after injury rescued the stretch-induced migratory deficits seventy-two hours after injury (Figure 18 B; $p=0.0069$ Two-way ANOVA with Tukey's multiple comparison test). Important to note is that forty-eight-hour did not reach statistical significance; however, there were strong trends for injury-induced migratory suppression and treatment rescuing migratory impairment (Figure 18 B; $p=0.0663$ Two-way ANOVA with Tukey's multiple comparison test). Taken together, the data show that restoration of FAK phosphorylation restores the injury-induced alteration in microglial migration.

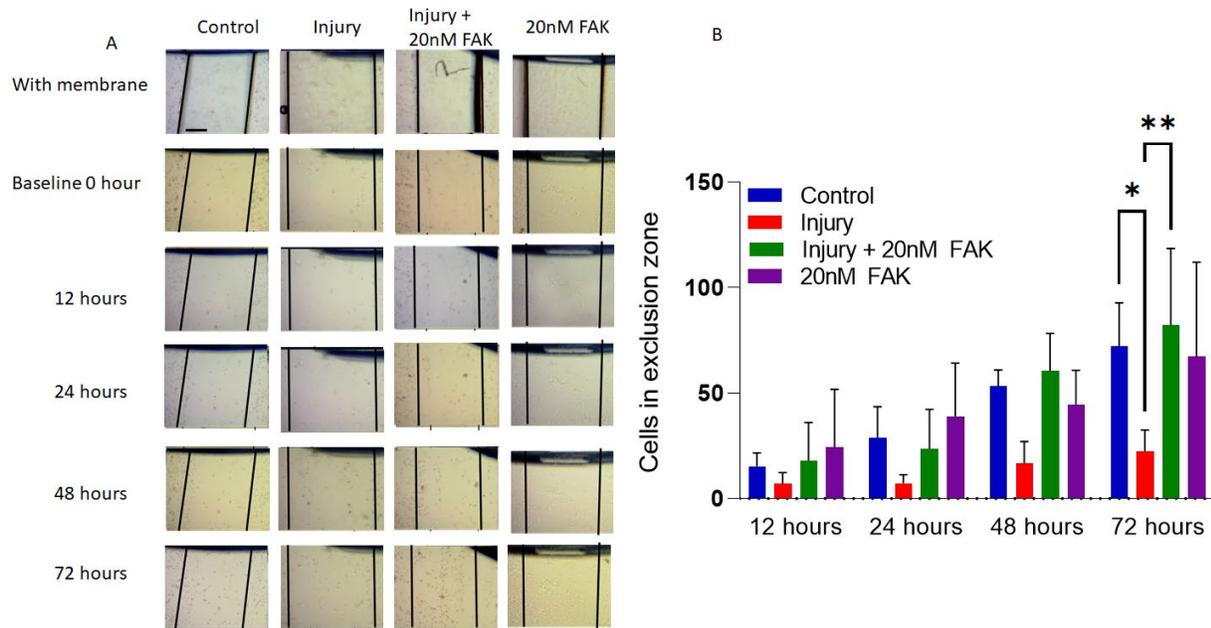


Figure 18. Treatment with the FAK activator rescues stretch-induced migratory deficits. A) Representative phase-contrast microscopy images of cell exclusion zone assay. B) Stretch-injury significantly reduces the number of cells in the exclusion zone 72 hours post-injury. Treatment with the FAK activator (20nM) ameliorates injury-induced reduction of cells migrating into the exclusion zone compared to controls. N=3/group. Two-way ANOVA with Tukey's multiple comparison test, * $p < 0.05$, ** $p < 0.01$. Bars represent mean \pm SD. Scale bar is 200 μ m.

Gene expression of stretch-injured microglia returns to control levels following treatment with the FAK activator.

Stretch injury significantly suppresses pro and inflammatory-associated gene transcripts twelve hours after injury (177). To determine an association between FAK phosphorylation and downstream inflammatory gene expression, stretch-injured cells were treated with the FAK activator (20 nM), ZINC 40099027, six hours after, and pro and anti-inflammatory genes were evaluated using RT-PCR twelve hours following injury. Following injury, pro-inflammatory associated gene IL-6 was significantly downregulated, consistent with a previous report (177), and treatment with the FAK

activator (20 nM) of a FAK activator, ZINC 40099027, restored its expression (Fig 19A; $p=0.0037$ one-way ANOVA with Tukey's post-test). Anti-inflammatory associated gene IL-10 was significantly reduced following stretch-injury; however, treatment with the FAK activator (20nM), ZINC 40099027, did not significantly alter its expression (Fig 19B; one-way ANOVA with Tukey's post-test). Treatment with the FAK activator (20nM) significantly increased the expression of anti-inflammatory associated gene Arg1 compared to the injured group (Fig 19C; $p=0.0491$ one-way ANOVA with Tukey's post-test). While not significant, Arg1 expression displayed a strong down-regulated trend following injury (Figure 19C; $p=0.067$ one-way ANOVA with Tukey's post-test). Neither stretch-injury nor treatment with the FAK activator (20nM), ZINC 40099027, affected the expression of associated pro-inflammatory genes IL-1 β , iNOS and CD86 or anti-inflammatory associated gene TGF- β or CD206 (Fig 19; D, F one-way ANOVA with Tukey's post-test and G and Fig 10; E and H, one-way ANOVA with Tukey's post-test, respectively). Taken together, the results show that FAK phosphorylation, post-injury treatment with the FAK activator, rescued the stretch-induced suppressed expression of pro and anti-associated inflammatory genes except for IL-10 gene expression.

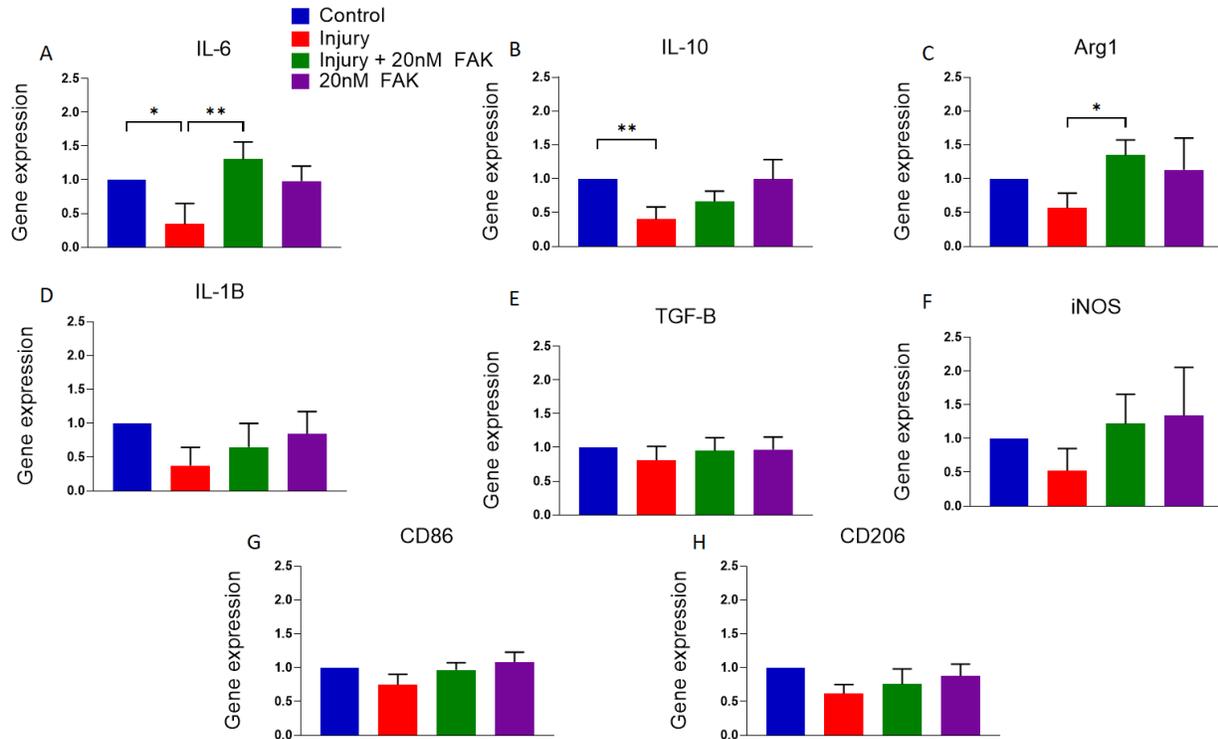


Figure 19. Treatment with FAK treatment rescues stretch-induced down-regulation of inflammatory gene expression. Stretch-injury significantly reduced pro-inflammatory and anti-inflammatory associated genes IL-6 (A) and IL-10 (B) expression, respectively. Notably, injured cells displayed a non-significant decreased expression of Arg1 (C). Injured cells treated with the FAK activator (20nM) restored the stretch-injured suppressed gene expression of IL-6 and Arg1. N=3/group. One-way ANOVA with Tukey's post-test. * $p < 0.05$, ** $p < 0.01$. Experimental groups are normalized to the control group and set at 1.0. For gene expression analysis, all experimental group changes are represented as fold changes compared to the control group. Error bars represent mean \pm SD.

DISCUSSION

Introduction

We have previously demonstrated that mechanical strain significantly alters microglial morphology and function twelve hours after injury (177). The work presented here suggests that the $\alpha 5 \beta 1$ integrin/FAK pathway is expressed in primary rat microglia and plays a role in the morphological and functional changes following injury. We found

that blocking integrin-binding using an RGD-peptide mimics the stretch-injured phenotype. RGD peptide-treated cells have significantly reduced FAK phosphorylation, media NO levels, iNOS gene and protein expression, and migration than vehicle-treated controls. Furthermore, we showed that stretch-injury and pharmacologically blocking the $\alpha 5\beta 1$ integrin significantly decreased FAK phosphorylation, a downstream FAK kinase of the $\alpha 5\beta 1$ integrin and was correlated with the effects of stretch-injury. We found that post-injury treatment with a small molecule activator of FAK, ZINC 40099027, rescued FAK phosphorylation, media NO levels, iNOS protein expression, inflammatory associated gene expression, altered morphology, and migratory deficits. Taken together, these results show that the $\alpha 5\beta 1$ integrin/FAK pathway contributes to the effects of stretch-injury on primary rat microglia.

Injury reduced FAK phosphorylation and NO production

Stretch-injured primary microglia have significantly reduced FAK phosphorylation, media levels of NO, and iNOS expression twelve hours after injury when cultured on Pronectin. This synthetic fibronectin substrate promotes integrin binding (177). The $\alpha 5\beta 1$ integrin mediates adhesion to fibronectin in microglia and multiple cell types (2; 86; 138; 186). Cellular adhesion is important to normal cellular processes, such as maintaining viability, morphology, migration, and immune function (187). Animal models of TBI (42), Parkinson's disease (PD) (83) and Alzheimer's disease (AD) (118) all show a relationship between integrin expression and microglial immune function, where activated microglia display increased $\alpha 5\beta 1$ integrin expression.

RGD-peptide treatment reduced FAK phosphorylation and NO production

Given these data and the literature, we targeted the binding of the $\alpha 5\beta 1$ integrin to Pronectin, a synthetic fibronectin analog, using a commercially available RGD peptide that inhibits $\alpha 5\beta 1$ integrin binding. We found that treatment significantly reduced FAK phosphorylation, media levels of NO, iNOS protein and gene expression, and inhibited migration. Researchers studying prion-induced microglia activation have highlighted the relationship between the $\alpha 5\beta 1$ integrin and NO production (31). They showed that cultured microglia were activated following treatment with a synthetic-prion with activated cells displaying a significant increase in NO media levels and iNOS protein expression. The increase was blocked in both by pretreatment with an $\alpha 5\beta 1$ integrin blocking antibody, demonstrating the relationship between the $\alpha 5\beta 1$ integrin and NO production. This relationship was further illustrated in a study by Chen Hai-Ying et al. (32) utilizing cultured rat bone marrow-derived mesenchymal stem cells (rBMSCs), which showed that overexpression of the $\alpha 5\beta 1$ led to a significant increase in culture media levels of NO levels compared to wild-type rBMSC controls. Interestingly, in the context of the TBI literature, our findings are contrary to the reports regarding microglial response following injury. In humans and animal models of experimental TBI, microglia are activated after they encounter factors released from the initial trauma (68; 77; 112; 116). The activated state is defined by morphological and functional changes that facilitate an immune response. Microglia transform from a small ramified cell body with multiple fine processes to a prominent amoeboid process-less phenotype during the activation process. Functionally, they upregulate the expression of genes and proteins for immune cell surface receptors, functional enzymes, cytokines/chemokines and phagocytic factors. The sterile *in vitro* evaluation of the primary injury may account for

these unexpected findings. Notwithstanding, our results contribute to the limited data found in the literature regarding the microglial $\alpha 5\beta 1$ /NO production pathway. We show that pharmacological treatment and mechanical injury disrupt integrin binding and reduce media levels of NO.

One issue is the discrepancy between the post-treatment time point evaluation in the RGD peptide blocking and stretch-injury studies. We chose to follow the Milner et al. (140) protocol for the blocking study, wherein RGD peptide administration required 48 hours to block integrin-binding effectively. Our pilot data showed that RGD administration failed to alter NO or gene expression at 12 hours post-treatment (Supplementary Fig. 1) but showed an effect at 48 hours post-treatment. We attributed the temporal kinetics of the blocking peptide to explain the temporal difference between stretch-injury and RGD peptide treatment outcomes.

Treatment with ZINC 40099027 (20 nM) restores FAK phosphorylation

Following integrin binding, FAK autophosphorylates at the tyrosine 397 residue to allow binding sites for structural proteins and enzymes; that provide a physical connection to the actin cytoskeleton and mediate downstream signaling, respectively (162; 212). Stretch injured cells showed a significant decrease in FAK phosphorylation at the tyrosine 397 residue; this was associated with morphological and functional deficits (Figure 6). Treatment with ZINC 40099027, a small molecule that leads to the phosphorylation of FAK at the 397 tyrosine residue, rescued the stretch-induced decrease in phosphorylation when administered six hours after injury. Consistent with previous studies, treatment did not significantly affect the phosphorylation of FAK in uninjured cells or the expression of total FAK (135; 161; 200). The activity of FAK, as evaluated

by the ratio of pFAK to total FAK, was not statistically different between the injured and control cells; however, there was a strong trend towards a stretch-induced decrease of FAK activity and a non-significant effect of treatment on restoring activity to un-injured levels; this can be attributed to the variability in the total FAK values.

Restoring FAK phosphorylation rescues NO production

Treatment with ZINC 40099027 (20 nM) abrogated the injury-induced decreases in media levels of NO and iNOS expression and did not affect either in uninjured cells. Basu et al. (8) evaluated the relationship between FAK activation and NO production in microglia utilizing BV2 microglia, an immortalized microglia cell line. They found that LPS significantly increased inflammation-associated gene expression for iNOS, TNF- α and IL-1 β , NO media levels and FAK phosphorylation. Furthermore, LPS-activated BV2 cells treated with a small cyclic peptide, LXW7, with a molecular structure similar to the RGD peptide that reduces FAK phosphorylation and used in our study, prevented the activation phenotype previously mentioned (91), demonstrating a relationship between microglial FAK phosphorylation and NO production. Moreover, examples from human studies show an association between FAK phosphorylation and NO production (194). Patients with vitiligo, a progressive depigmentation of the epidermis characterized by pathological melanocytes, present with skin lesions caused by pathological inflammation. A recent study showed that biopsied skin lesions from vitiligo patients had significantly higher expression of pFAK, iNOS and NO levels, suggesting an association between FAK phosphorylation, iNOS expression and NO production.

Gene expression and FAK activity are restored with the FAK activator, ZINC 40099027

Gene expression of pro-inflammatory cytokines, IL-6 and IL-10, is significantly decreased following a stretch-injury, and the associated anti-inflammatory gene, Arg-1, displays a substantial decrease in expression (177). We found that administration of ZINC 40099027 after injury significantly increased the expression of IL-6 and Arg-1 in injured cells compared to non-treated injured cells. This demonstrates that restoring FAK phosphorylation is associated with rescuing the injury-induced suppressed gene expression. The relationship between FAK phosphorylation and microglial gene expression was previously shown in a mouse model of facial nerve axotomy, wherein phosphorylated FAK and gene and protein expression of TNF- α and IL-1 β were significantly increased in activated microglia in the ipsilateral facial nucleus (8). Furthermore, *in vitro* experiments from the same study showed that cultured primary rat microglia stimulated with LPS had significantly increased FAK phosphorylation and inflammatory gene and protein expression of TNF- α and IL-1 β (215). Combined with data from the literature, these findings show that FAK phosphorylation contributes to mediating inflammatory associated gene expression, iNOS expression and media levels of NO. These findings are interesting since multiple processes, gene expression, NO production and morphology is altered in microglia following a TBI. Future studies will examine the individual pathways downstream of FAK responsible for the observed deficits. Furthermore, therapeutically modulating FAK in activated microglia in the TBI brain, either through the α 5 β 1 integrin or agents directly act on FAK phosphorylation, is a promising avenue to target dysfunctional states.

ZINC 40099027 restore normal morphology

Canonical FAK signaling contributes to normal cellular morphology (27; 155; 216). We have previously described morphological alterations following a stretch-injury, with injured cells displaying significant increases in cell area and decreases in average process length (177). We now show that administration of ZINC 40099027 after stretch injury significantly reduced the total cell area to control non-stretched-injured measures. Treatment did not considerably alter average process length following an injury; however, there was a non-significant trend toward increasing process length to controls. Disrupted FAK signaling and morphological alterations have been demonstrated in cultured mouse fibroblasts (179). FAK-knockout mouse fibroblasts display enlarged, rounded cell body morphologies with no processes when cultured on fibronectin, whereas wild-type cells display a pointed or stellate phenotype. This shows that FAK mediates the downstream signaling cascade for stabilizing the actin-cytoskeleton that occurs through the formation of ordered stress fiber bundles. When FAK is knocked down by siRNA in post-natal day three primary rat oligodendrocytes cultured on fibronectin, cells have a significantly larger network area than siRNA control cells. Furthermore, this phenotype was replicated when wild-type cells were treated with the FAK inhibitor, PF573228 (111). Our data and the literature demonstrate a relationship between FAK signaling and morphology. Contrary to our findings in cultured microglia, neuronal injury activates integrin-associated pathways, while as shown in our study, microglial injury inhibits a FAK integrin-associated pathway activation. A 2006 study found that stretch-injured primary cortical neurons cultured on fibronectin have significantly more focal swellings than injured cells cultured on poly-l-lysine (75). Neuronal focal swelling is a marker of Rho A-mediated cytoskeleton remodeling. The observed cytoskeleton alterations were

prevented with the immediate post-injury treatment of HA-1077, an inhibitor of downstream Rho A effector, ROCK. One explanation for the different responses to injury in microglial compared to neurons is the size and function of the cell types. Neurons are much larger, stationary, and adherent cells than the smaller, migratory microglia, resulting in greater integrins expressed on neurons than microglia. Additionally, because microglia are migratory cells, they have a higher turnover of integrin FACs and respond differently to supra-threshold mechanical forces. Future studies will investigate the role and activity of microglial actin-cytoskeleton kinase and effector proteins following injury to determine molecular targets to restore stretch-injured morphological deficits. While these findings counter what is reported in the literature, they contribute to the field's growing understanding of microglial morphology in the context of physical injury.

Migration is restored following treatment with ZINC 40099027

Stretch-injured microglia display migratory deficits on the cell exclusion zone assay at 48 and 72 hours post-injury (177). When uninjured cells were treated with the RGD blocking peptide, their migratory behavior was significantly reduced, compared to vehicle-treated controls, at forty-eight and seventy-two hours post-treatment. The $\alpha 5\beta 1$ integrin receptor mediates migration in retinal pigment epithelial (115), endothelial cells (41) and macrophages (2) and microglia (182). Using *ex vivo* mouse brain slices, Smolders et al. (182) visualized microglia during cortical development; they found that blocking the $\alpha 5\beta 1$ integrin receptor at embryonic day 13.5 significantly decreased microglial migratory behavior compared to controls. Evaluation of the $\alpha 5\beta 1$ integrin in microglia migration is not as well defined as peripheral macrophages in the literature. Compared to microglia, macrophages share similar embryonic origins, morphology and

function during an immune response (211). A mouse bone marrow-derived macrophage (BMM) study showed that treatment with an $\alpha 5$ integrin blocking antibody significantly decreased BMM invasion toward fibronectin in a Boyden chamber migration assay, demonstrating the inhibitory effect on haptotactic invasion by blocking the $\alpha 5\beta 1$ integrin (2). Our results contribute to the literature demonstrating that impaired $\alpha 5\beta 1$ integrin-binding alters migratory behavior and extend the literature by showing that shows the $\alpha 5\beta 1$ integrin mediates migration deficits on Pronectin following injury.

Summary:

Given that stretch-injury impairs migration (177) and decreases FAK activity, an important question is whether a pathway between FAK phosphorylation and migration exists. Recently, Rong et al. established that TREM2 mediated microglial migration, in response to $A\beta_{42}$, is mediated by FAK activation. They showed that primary mouse microglia from TREM2 knockouts significantly decreased FAK phosphorylation at tyrosine 397. At the same time, total FAK was unaffected, and these cells displayed significant deficits on a transwell migration assay compared to wild-type controls. Consistent with reports in the literature, we showed that restoration of FAK phosphorylation using ZINC 40099027 rescued the stretch-induced migratory deficits seventy-two hours after injury. Injured and treated cells had significantly more cells in the exclusion zone than injury-only cells. This is interesting because it shows that FAK activity is associated with morphological and migratory changes following injury, both of which are altered in the injured brain. Furthermore, the actin cytoskeleton dynamic mediates both of these processes. Future studies will explore the molecular mechanism that mediates these changes to identify a potential site for therapeutic targeting to

improve dysfunctional microglia response in the TBI brain. Taken together, our results demonstrate that impaired FAK activity is correlated with migratory deficits and re-phosphorylation of FAK abrogates the impairment.

Conclusions:

The findings presented here contribute to a growing body of literature evaluating the effects of mechanical injury on microglial viability, morphology, and function in the context of TBI. This work identified the $\alpha 5\beta 1$ /FAK pathway as a contributing pathway in stretch-induced morphological, functional, and gene expression alterations following injury. Pharmacologically blocking the $\alpha 5\beta 1$ integrin to Pronectin mimicked the stretch-injured phenotype with treated cells displaying significant iNOS protein and gene expression reductions, media NO levels, and impaired migration. Significant decreases in FAK phosphorylation accompany the stretch-injured phenotype. To this end, injured cells were treated with 20nM of ZINC 40099027 to restore FAK phosphorylation, restore FAK activity, rescued iNOS expression, NO media levels, morphological alterations, and migratory deficits gene expression. In conclusion, stretch-injury induced microglia morphological and functional deficiencies are associated with disruptions in $\alpha 5\beta 1$ /FAK signaling, specifically FAK phosphorylation, and re-phosphorylation of FAK alleviates the effects of an injury.

Chapter 4: Discussion

Introduction:

Current limitations in understanding chronic microglial activation after TBI may result from the incomplete understanding of the stimuli acting on microglia, specifically the physical injury that precedes activation. Previous research has focused exclusively on the secondary injury phase, with microglial activation modeled in cultured cells activated by treatment with an inflammogen (12; 100; 181). In contrast to these studies, we developed an *in vitro* model of microglial neurotrauma that replicates the temporal presentation of stimuli in the injured brain. Given the literature showing the ability of stretch-injury alone to induce cellular pathologies, we hypothesized that stretch-injury would alter microglia function, and our results confirm that microglial function is altered following a stretch-injury. We demonstrated that: 1) exposure to a stretch-injury altered multiple aspects of the inflammation process involved in response to a TBI, 2) injured cells retain normal responses to a secondary stimulus, LPS and 3) a novel integrin-mediated pathway is partially responsible for the effects of the injury.

Effects of injury on microglia verse other brain cells

The results from this work addressed a significant gap in the literature regarding microglial biology in the context of the injured brain. The data showed that injured cells remain viable like other brain cells but, in contrast, have a unique set of alterations in morphology and function. The majority of the research on the effects of the primary injury on other brain cell types is consistent with the presentation of pathophysiological markers observed in *in vivo* models of TBI. For example, stretch-injured primary rat astrocytes express a marker commonly observed in activated astrocytes, GFAP (113), and

display intracellular calcium disruptions (3). Primary rat neurons exposed to an *in vitro* injury have focal adhesion swellings that resemble cytoskeletal remodeling events seen in DAI (75). Lastly, endothelial cells have altered F-actin expression, suggestive of morphological changes after a single injury. Interestingly, our findings, excluding the morphology data, counter what is observed in microglia in the TBI brain. Activated microglia generate an immune response by migrating to the injury site, upregulating gene and protein expression of immune cell surface receptors and enzymes, cytokines/chemokines, and phagocytosis after a TBI. Our findings are significant, novel, and address a gap in the microglia field in the context of TBI. Furthermore, these results suggest that stretch-injured microglia are not classically ‘activated,’ like those observed in the TBI brain. However, the morphology data suggest they are activated but not in a traditional pro-inflammatory or anti-inflammatory state. Additional studies are needed to evaluate whether or not the effects of stretch-injury are observed during activation, as their homeostatic immune surveillance could be compromised, rendering the brain susceptible to aberrant protein aggregation and other harmful consequences.

Morphological changes in the absence of other markers of activation

A puzzling result was the alteration in morphology following an injury that mimicked a transition to an activated phenotype while presenting with functional changes that were opposite of activation (decreases in media NO, iNOS expression, and associated inflammatory genes). Traditionally, microglial activation involves the co-presentation of morphological changes and upregulation in the expression of immune enzymes, cell surface markers and cytokines and chemokines (10; 103). The findings showed an interesting microglial state previously unobserved in the literature. For

example, in the post mortem brains of American football players diagnosed with TBI-activated microglia present with a rounded morphology and expression of CD68 (34). Results from animal models of experimental models of TBI showed that microglia in injured animals are amoeboid and express significantly more iNOS and NOX2 than microglia from uninjured animals. This is important to the field because it shows that processes (iNOS expression, inflammatory associated gene expression, migration and morphology) involved in activation present counter to classical activation and are linked to FAK activation. This raises the possibility of identifying and selectively targeting or modifying pathways that are downstream of FAK to mediate dysfunctional or beneficial aspects of activation in the injury context.

Effects of substrate on microglial response

Our pilot studies showed that stretch-injury did not affect media NO or LDH levels when injured on Flexwell membranes coated with collagen I or IV, laminin, poly-d-lysine or uncoated membranes, demonstrating an effect of substrate on microglial morphology and function in the context of injury. The impact of the substrate on microglia morphology and function has been shown by work from Milner et al. (141), where cultured mouse microglia increased the expression of MHC class I and displayed an amoeboid phenotype when cultured on rigid plastic wells coated with fibronectin or vitronectin compared to hard plastic wells without coating. The morphological findings from Milner's study suggested that fibronectin activated microglia and is very interesting in light of our study. In contrast to the Milner study, our cells were cultured on Flexwell membranes coated with Pronectin, a synthetic substrate that mimics fibronectin. The Flexwell membrane is 2mm thick, soft, rubber polymer. Our cells presented

morphologically as small-bodied with thin ramified processes, counter to what Milner observed. A critical difference between our study and Milner's study was the substrate stiffness used in the experiments. Where Milner used hard plastic wells, we used a soft, flexible polymer membrane. A possible explanation for this discrepancy is the stiffness of the culture substrate. For example, a 2020 study that examined the effects of substrate stiffness on microglia morphology and basal level inflammatory state showed that primary rat microglia displayed marked morphological changes and higher basal level expression of anti-inflammatory associated proteins CD206, IGF-1 and vimentin when cultured on softer substrates compared to stiffer substrates (11). Soft-substrate cultured cells were less round and had longer processes compared to stiffer-substrate cultured cells. The data from the previously mentioned study showed that substrate stiffness significantly affected microglial morphology *in vitro*, where factors from other cells are absent, strongly suggesting that substrate stiffness influences microglia morphology and basal expression immune proteins. Substrate stiffness could explain the differential findings between our study and Milner's, where he concluded that fibronectin activated microglia, with increased MHC I and MMP-9 expression and classical amoeboid morphology. Additionally, our pilot study showed that, compared to other substrates, the Pronectin-cultured cells displayed significantly increased media NO and iNOS levels, suggestive of activation, but at the same time presented with a ramified morphology. These observations could translate to the *in vivo* setting where spatial expression of the ECM is regionally heterogenous and could promotes unique functional states based upon the environment (46).

$\alpha 5\beta 1$ integrin involvement in altered morphology and migration

As previously mentioned, the $\alpha 5\beta 1$ integrin mediates attachment to fibronectin in microglia and other cells types (41; 187). Contrary to our findings in cultured microglia, neuronal stretch-injury *activates* integrin-associated pathways, while in our study, injured microglia showed an inhibition of the FAK integrin-associated pathway. A 2006 study found that stretch-injured primary cortical neurons cultured on fibronectin have significantly more focal swellings than injured cells cultured on poly-l-lysine (75). Neuronal focal swellings are a marker of Rho A-mediated cytoskeleton remodeling. The observed cytoskeleton alterations were prevented with the immediate post-injury treatment of HA-1077, an inhibitor of downstream Rho A effector, ROCK. One explanation for the different responses to injury in microglial compared to neurons is the size and function of the cell types. Neurons are much larger, stationary, and adherent cells than the smaller, migratory microglia, resulting in greater integrins expressed on neurons than microglia. However, there are no studies comparing absolute integrin expression or binding affinity between neurons and microglia to date. Additionally, because microglia are migratory cells, they have a higher turnover of integrin FACs (138) and may respond differently to supra-threshold mechanical forces. The $\alpha 5\beta 1$ integrin/FAK pathway is necessary for mouse bone marrow-derived macrophages (BMM) haptotaxis towards fibronectin and chemotaxis towards M-CSF (2). There are similarities between our findings and the results of this study in the macrophages study, primarily the mediating effect of the $\alpha 5\beta 1$ integrin/FAK pathway on migration; however, the haptotaxis and chemotactic assays differ from our exclusion zone assay. The exclusion zone relies on the cells' natural propensity to spread and cultivate areas void of other cells. In contrast, the haptotaxis assay and chemotaxis assay utilizes substrate

stiffness and cytokine gradients to promote migration. Future studies will investigate the role and activity of microglial actin-cytoskeleton kinase and effector proteins following injury to determine molecular targets to restore stretch-injured morphological and migratory deficits. While these findings counter what is reported in the literature, they contribute to the field's growing understanding of microglial morphology in the context of physical injury.

$\alpha 5\beta 1$ integrin binding and inflammation

An exciting study evaluating the interaction between macrophage integrin binding and inflammation showed that human monocytic Thp-1 cells cultured on substrates without collagen I integrin ligands and stimulated with IL-4, a classical promoter of an anti-inflammatory state, cells were shifted towards a pro-inflammatory phenotype compared to stimulated cells cultured on substrates containing collagen I ligands (29). Furthermore, they identified the $\alpha 2\beta 1$ integrin as the mediating receptor responsible for the observed differences. These results suggested that preventing integrin signaling facilitated a transition to a pro-inflammatory state even in the presence of an agent that promotes differentiation towards an anti-inflammatory phenotype. Our study did not observe any results that showed a preference for a pro-inflammatory or anti-inflammatory response following the disruption of integrin binding. However, the study above evaluated a different integrin-ligand interaction than our study. Our pilot studies showed no effect of injury on media levels of NO when the cells were cultured on collagen I and IV and uncoated Flexwell membranes. However, we did see a significant increase in media NO levels in the Pronectin cultured cells compared to the other plating substrates.

Additionally, there were substantial increases in media NO levels in collagen I & IV cultured cells compared to uncoated membranes, suggesting an effect of culture substrate on basal level function. There was no difference in media NO levels between the collagen substrates. Interestingly, collagen I & IV culture cells had morphologies similar to those of the Pronectin cultured cells; however, this was a qualitative evaluation. Lastly, cells cultured on uncoated membranes had small rounded cells bodies with few to no processes. Taken together with the morphological findings, the media NO data showed that substrates affect basal level NO production. This is highlighted by the experiments that showed physical disrupting and pharmacological inhibiting integrin-binding reduced basal level NO production.

The FAK pathway and microglia function

The results from the second aim showed that the $\alpha 5\beta 1$ integrin/FAK pathway partially mediated the changes following stretch-injury, which is an exciting finding. Multiple processes involved in chronic microglia activation are downstream of the $\alpha 5\beta 1$ integrin, such as migration (182), morphological changes (140), cytokine/chemokine gene expression (31) and NO production (31). The potential of numerous processes under one pathway is therapeutically attractive. To date, the involvement of FAK activity on microglial function is not well defined. We reported that injury and pharmacological inhibition of FAK phosphorylation at the Y397 site alters morphology and suppresses multiple processes related to the immune response. There is one notable study that showed a relationship between FAK activity and microglial morphology and migration. Genetic gain of function mutations on the leucine-rich repeat kinase (LRRK2) gene, specifically G2019S, have received increased attention since it is found in sporadic cases

of Parkinson's disease (PD), where dysfunctional microglia response are commonly observed. Researchers showed that LRRK2 negatively regulates microglial FAK activity and is associated with retarded chemotactic motility and slower and ineffective migration following a stab wound injury in G2019S-LRRK2 transgenic (Tg) mice. A critical difference between this study and our own was the upstream pathway utilized; the study above used an ADP chemotactic assay to assess microglial migration, mediated by a purinergic receptor and not an integrin. However, the relationship between FAK phosphorylation at the Y397 residue and migratory deficits in microglia is consistent with our stretch-injury and RGD-blocking study results. Evaluating FAK activity in the context of chronic microglial activation could provide insight into the cellular pathophysiology of PD. Furthermore, there is a link between TBI and PD, primarily because TBI is a risk factor for PD (184). Stretch-injuries are prevalent in most TBIs, and chronic microglial activation is observed in both TBI and PD. Based on our findings and the literature, FAK signaling may become dysfunctional after a brain injury and promote atypical migration necessary for homeostatic immune surveillance essential for the clearance and containment of the injury site. This event could promote chronic microglia activation by a positive feedback loop where persistent inept clearance and production of neurotoxic factors generate persistent microgliosis and neurodegeneration.

Conclusions

In conclusion, we show that mechanical injury decreased FAK activity and was associated with reduced NO production, gene expression, migration and altered morphology (Figure 2). Disruption of basal level functioning of the production of

signaling factors such as NO could affect the behavior of cells in the injury context. This could leave the damaged site(s) or injury foci susceptible to further injury or propagation of other secondary injury processes. This interesting question was not fully addressed in our priming experiments, where we assessed media NO and LDH levels after injured cells were treated with LPS. Future studies will evaluate the outcome measures that affected stretch-injury in the same experimental design. As mentioned in paper 1 (177), the time point chosen to treat injured cells with LPS and the potency of LPS could account for the null findings. In addition, future efforts will explore the molecular deficits that mediate the decreased FAK phosphorylation, be it an alteration in integrin binding, reductions in secreted factors with an autocrine effect, or integrin activation status.

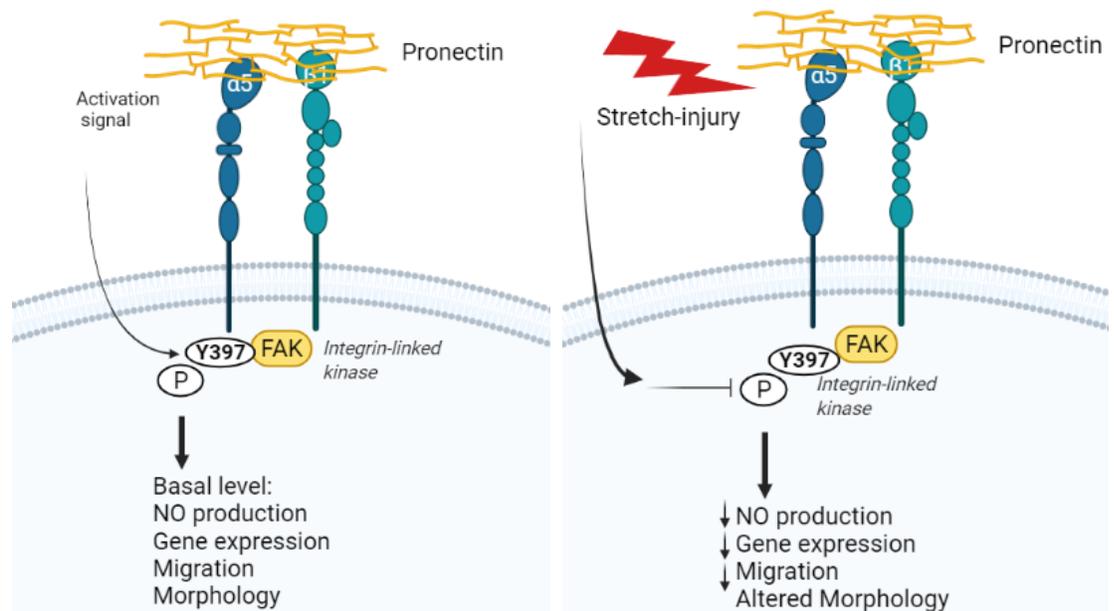


Figure 20. Normal integrin binding and Integrin signaling after injury. Binding activates intracellular FAK phosphorylation and facilitates canonical gene expression, NO production, migration and morphology. After a stretch-injury, FAK phosphorylation and gene expression, NO production and migration are decreased; additionally, morphology is altered.

Limitations and future directions

The results of this effort addressed an important gap in the field of TBI concerning the effects of the mechanical injury on microglia. The fundamental nature of the question made using traditional animal models of experimental TBI impossible, primarily because of the role microglia play following a TBI. We utilized a validated model of cellular neurotrauma that is well established in the literature. The model does not come without some limitations. The two-dimensional (2D) *in vitro* model utilizing a single culture substrate are two common translational limitations of *in vitro* models. Cells in the body and brain exist and function in a three-dimensional (3D) environment and interact with multiple ECM proteins and other cells differently than cells culture in a 2D setting. Furthermore, the composition of the ECM is heterogeneous and varies regionally and influences basal level morphology and function, which can alter the response to various stimuli. Future studies will address these issues by employing 3D matrix models containing multiple ECM proteins specific to the region of the brain being studied.

Our early pilot studies determined that the highest setting on the CIC II could generate a 20% stretch event, which significantly decreased media NO levels.

Researchers at the Army Research Laboratory (ARL) showed that the peak strain rate reached was 60 ms, with the event lasting 140 ms. Interestingly, in personal communication with Dr. Dileonardi, we used the same pressure and settings that caused morphological alterations in primary rat cultured neurons. The limitations of the device prevented us from exploring higher strain rates. Presumably, a threshold would cause the cells to detach from the membrane or cause cell death completely. When we evaluated the media for the presence of cells after injury, we found no difference between the injured and control group. Additionally, as determined by trypan blue staining, we did not observe a significant difference between the two groups in the number of dead cells. Given the migratory nature of microglia, there is a considerable turnover of FAC as cells move through the ECM (81). This turnover is a highly coordinated process of FAC assembly and disassembly as the leading edge of the cells progresses forward (148). Compared to the coordinated process of regular migration, we showed that injury disrupts FAK activity and inhibits normal downstream signaling and migration. It would be insightful to determine how complete detachment affects integrin expression and signaling; and how it compares to the findings of our injury-induced phenotype.

Pilot studies showed that glycolysis and oxidative phosphorylation markers were decreased in injured cells compared to non-injured cells. A decrease in global cellular metabolism could account for the nonspecific suppression of the inflammation-associated process. Interestingly, in the injured brain, chronically activated microglia show a propensity for glycolysis over oxidative phosphorylation (121). This is significant because the pentose phosphate pathway (PPP) parallels glycolysis and provides the enzyme NOX2 with NADPH to produce neurotoxic ROS and is associated with white

matter damage and neurodegeneration (42; 123). Future studies will evaluate how early injury-induced metabolic disruptions possibly contribute to the asymmetrical preference towards glycolysis in the injured state. Studies will use the Seahorse assay, which measures glycolysis and oxidative phosphorylation by assessing extracellular acidification and oxygen consumption media levels, respectively. Using RNA-Seq, we will evaluate differentially expressed genes (DEGs) that correlate with the metabolic changes found in the Seahorse and identify candidate proteins to target to modulate the metabolic states.

The findings from the post-injury LPS-activated cells experiment demonstrated that injured cells remain viable and respond similarly to non-injured cells. We expected that damaged cells that showed a significant decrease in NO media levels would have a similar reduction when treated with LPS compared to non-injured, LPS treated cells. The strength of LPS as an activator could contribute to this finding since the robust response to LPS may have masked the effect of a stretch-injury on NO media levels. LPS is found on the outer membrane of gram-negative bacteria and mimics an immune response to a bacterial infection. While it is not uncommon for patients with a TBI to develop nosocomial infections in the sub-acute and chronic periods (102), the presence of bacteria during the primary injury is less likely. To address this difference, other agents that are found after the direct damage that activates microglia, such as ATP (47) or glutamate (97), will be used to activate cells post-stretch-injury.

Conclusion

The central importance of this research effort lies in the characterization of the effects of physical forces acting on primary rat microglia and potentially identifying a

novel integrin that facilitates mechanotransduction which in turn mediates multiple aspects of microglia behavior. Given that chronic microglial activation is associated with worsening symptomology and neurodegeneration following a TBI, identifying relevant molecular pathway(s) for therapeutic modulation is essential. Some advancements in targeting specific microglial processes, such as NOX2 generated oxidative stress (20; 78), and promising results from animals studies using pharmacological agents, such as Apocynin (36; 60), highlight the contribution of microglial dysfunction to long-term effects of TBI. Despite these advances, experimental evidence suggests that multiple mechanisms underlie chronic microglial activation (51; 87), and more work is needed to characterize these mechanisms further. Incorporating the current findings into the literature will guide future studies investigating underlying mechanisms and therapeutic interventions geared towards ameliorating reactive microglial states in TBI.

REFERENCES

1. 2014. Delayed Increases in Microvascular Pathology after Experimental Traumatic Brain Injury Are Associated with Prolonged Inflammation, Blood–Brain Barrier Disruption, and Progressive White Matter Damage. *J Neurotrauma* 31:1180-93
2. Abshire MY, Thomas KS, Owen KA, Bouton AH. 2011. Macrophage motility requires distinct $\alpha 5\beta 1$ /FAK and $\alpha 4\beta 1$ /paxillin signaling events. *J Leukoc Biol* 89:251-7
3. Ahmed SM, Rzigalinski BA, Willoughby KA, Sitterding HA, Ellis EF. 2000. Stretch-Induced Injury Alters Mitochondrial Membrane Potential and Cellular ATP in Cultured Astrocytes and Neurons. *Journal of Neurochemistry* 74:1951-60
4. Alluri H, Wiggins-Dohlvik K, Davis ML, Huang JH, Tharakan B. 2015. Blood-brain barrier dysfunction following traumatic brain injury. *Metab Brain Dis* 30:1093-104
5. Andrews AM, Lutton EM, Merkel SF, Razmpour R, Ramirez SH. 2016. Mechanical Injury Induces Brain Endothelial-Derived Microvesicle Release: Implications for Cerebral Vascular Injury during Traumatic Brain Injury. *Front Cell Neurosci* 10
6. Au - Salvador E, Au - Neuhaus W, Au - Foerster C. 2013. Stretch in Brain Microvascular Endothelial Cells (cEND) as an In Vitro Traumatic Brain Injury Model of the Blood Brain Barrier. *JoVE*:e50928
7. Augustine C, Cepinkas G, Fraser DD. 2014. Traumatic injury elicits JNK-mediated human astrocyte retraction in vitro. *Neuroscience* 274:1-10
8. Basu A, Krady JK, Enterline JR, Levison SW. 2002. Transforming growth factor beta1 prevents IL-1beta-induced microglial activation, whereas TNFalpha- and IL-6-stimulated activation are not antagonized. *Glia* 40:109-20
9. Benson BA, Vercellotti GM, Dalmaso AP. 2015. IL-4 and IL-13 induce protection from complement and melittin in endothelial cells despite initial loss of cytoplasmic proteins: membrane resealing impairs quantifying cytotoxicity with the lactate dehydrogenase permeability assay. *Xenotransplantation* 22:295-301
10. Beynon SB, Walker FR. 2012. Microglial activation in the injured and healthy brain: What are we really talking about? Practical and theoretical issues associated with the measurement of changes in microglial morphology. *Neuroscience* 225:162-71
11. Blaschke SJ, Demir S, König A, Abraham J-A, Vay SU, et al. 2020. Substrate Elasticity Exerts Functional Effects on Primary Microglia. *Front Cell Neurosci* 14
12. Brabazon F, Bermudez S, Shaughnessy M, Khayrullina G, Byrnes KR. 2018. The effects of insulin on the inflammatory activity of BV2 microglia. *PLoS One* 13:e0201878
13. Brabazon F, Wilson CM, Jaiswal S, Reed J, Frey WHN, Byrnes KR. 2017. Intranasal insulin treatment of an experimental model of moderate traumatic brain injury. *J Cereb Blood Flow Metab* 37:3203-18
14. Brenner KA, Corbett SA, Schwarzbauer JE. 2000. Regulation of fibronectin matrix assembly by activated Ras in transformed cells. *Oncogene* 19:3156-63

15. Brettschneider J, Libon DJ, Toledo JB, Xie SX, McCluskey L, et al. 2012. Microglial activation and TDP-43 pathology correlate with executive dysfunction in amyotrophic lateral sclerosis. *Acta Neuropathol* 123:395-407
16. Brickell TA, Lange RT, French LM. 2014. Three-year outcome following moderate-to-severe TBI in U.S. military service members: a descriptive cross-sectional study. *Mil Med* 179:839-48
17. Brown AW, Moessner AM, Mandrekar J, Diehl NN, Leibson CL, Malec JF. 2011. A survey of very-long-term outcomes after traumatic brain injury among members of a population-based incident cohort. *J Neurotrauma* 28:167-76
18. Brown GC. 2007. Mechanisms of inflammatory neurodegeneration: iNOS and NADPH oxidase. *Biochem Soc Trans* 35:1119-21
19. Brown KM, Gillette TA, Ascoli GA. 2008. Quantifying neuronal size: summing up trees and splitting the branch difference. *Semin Cell Dev Biol* 19:485-93
20. Byrnes KR, Loane DJ, Stoica BA, Zhang J, Faden AI. 2012. Delayed mGluR5 activation limits neuroinflammation and neurodegeneration after traumatic brain injury. *J Neuroinflammation* 9:43
21. Byrnes KR, Stoica B, Loane DJ, Riccio A, Davis MI, Faden AI. 2009. Metabotropic glutamate receptor 5 activation inhibits microglial associated inflammation and neurotoxicity. *Glia* 57:550-60
22. Byrnes KR, Stoica B, Riccio A, Pajooohesh-Ganji A, Loane DJ, Faden AI. 2009. Activation of metabotropic glutamate receptor 5 improves recovery after spinal cord injury in rodents. *Ann Neurol* 66:63-74
23. Byrnes KR, Wilson CM, Brabazon F, von Leden R, Jurgens JS, et al. 2014. FDG-PET imaging in mild traumatic brain injury: a critical review. *Front Neuroenergetics* 5:13
24. Caldwell RW, Rodriguez PC, Toque HA, Narayanan SP, Caldwell RB. 2018. Arginase: A Multifaceted Enzyme Important in Health and Disease. *Physiol Rev* 98:641-65
25. Cao T, Thomas TC, Ziebell JM, Pauly JR, Lifshitz J. 2012. Morphological and genetic activation of microglia after diffuse traumatic brain injury in the rat. *Neuroscience* 225:65-75
26. Caplan HW, Cardenas F, Gudenkauf F, Zelnick P, Xue H, et al. 2020. Spatiotemporal Distribution of Microglia After Traumatic Brain Injury in Male Mice. *ASN Neuro* 12:1759091420911770
27. Castillo-Badillo JA, Gautam N. 2021. Optogenetic model reveals cell shape regulation through FAK and Fascin. *J Cell Sci*
28. Castro A, Bartos D, Kutas M, Weiss G. 1974. A new microcolumn for steroid separation in radioimmunoassay. *Clin Biochem* 7:64-7
29. Cha B-H, Shin SR, Leijten J, Li Y-C, Singh S, et al. 2017. Integrin-Mediated Interactions Control Macrophage Polarization in 3D Hydrogels. *Advanced Healthcare Materials* 6:1700289
30. Chamak B, Mallat M. 1991. Fibronectin and laminin regulate the in vitro differentiation of microglial cells. *Neuroscience* 45:513-27
31. Chang J, Yang L, Kouadir M, Peng Y, Zhang S, et al. 2012. Antibody-mediated inhibition of integrin $\alpha 5\beta 1$ blocks neurotoxic prion peptide PrP106-126-induced activation of BV2 microglia. *J Mol Neurosci* 48:248-52

32. Chen H-y, Pan L, Yang H-l, Xia P, Yu W-c, et al. 2018. Integrin alpha5beta1 suppresses rBMSCs anoikis and promotes nitric oxide production. *Biomedicine & Pharmacotherapy* 99:1-8
33. Chen T, Willoughby KA, Ellis EF. 2004. Group I metabotropic receptor antagonism blocks depletion of calcium stores and reduces potentiated capacitative calcium entry in strain-injured neurons and astrocytes. *J Neurotrauma* 21:271-81
34. Cherry JD, Tripodis Y, Alvarez VE, Huber B, Kiernan PT, et al. 2016. Microglial neuroinflammation contributes to tau accumulation in chronic traumatic encephalopathy. *Acta Neuropathol Commun* 4:112-
35. Chhor V, Le Charpentier T, Lebon S, Oré MV, Celador IL, et al. 2013. Characterization of phenotype markers and neuronotoxic potential of polarised primary microglia in vitro. *Brain Behav Immun* 32:70-85
36. Choi BY, Jang BG, Kim JH, Lee BE, Sohn M, et al. 2012. Prevention of traumatic brain injury-induced neuronal death by inhibition of NADPH oxidase activation. *Brain Res* 1481:49-58
37. Choi I, Kim B, Byun J-W, Baik SH, Huh YH, et al. 2015. LRRK2 G2019S mutation attenuates microglial motility by inhibiting focal adhesion kinase. *Nature Communications* 6:8255
38. Chuang DY, Simonyi A, Kotzbauer PT, Gu Z, Sun GY. 2015. Cytosolic phospholipase A2 plays a crucial role in ROS/NO signaling during microglial activation through the lipoxygenase pathway. *J Neuroinflammation* 12:199
39. Ciacci-Zanella J, Stone M, Henderson G, Jones C. 1999. The latency-related gene of bovine herpesvirus 1 inhibits programmed cell death. *J Virol* 73:9734-40
40. Colantonio A, Ratcliff G, Chase S, Kelsey S, Escobar M, Vernich L. 2004. Long-term outcomes after moderate to severe traumatic brain injury. *Disabil Rehabil* 26:253-61
41. Collo G, Pepper MS. 1999. Endothelial cell integrin alpha5beta1 expression is modulated by cytokines and during migration in vitro. *J Cell Sci* 112 (Pt 4):569-78
42. Cooney SJ, Bermudez-Sabogal SL, Byrnes KR. 2013. Cellular and temporal expression of NADPH oxidase (NOX) isoforms after brain injury. *J Neuroinflammation* 10:155
43. Coughlin JM, Wang Y, Munro CA, Ma S, Yue C, et al. 2015. Neuroinflammation and brain atrophy in former NFL players: An in vivo multimodal imaging pilot study. *Neurobiol Dis* 74:58-65
44. Cullen DK, Simon CM, LaPlaca MC. 2007. Strain rate-dependent induction of reactive astrogliosis and cell death in three-dimensional neuronal–astrocytic co-cultures. *Brain Res* 1158:103-15
45. Dalgard CL, Cole JT, Kean WS, Lucky JJ, Sukumar G, et al. 2012. The cytokine temporal profile in rat cortex after controlled cortical impact. *Front Mol Neurosci* 5:6
46. Dauth S, Grevesse T, Pantazopoulos H, Campbell PH, Maoz BM, et al. 2016. Extracellular matrix protein expression is brain region dependent. *J Comp Neurol* 524:1309-36

47. Davalos D, Grutzendler J, Yang G, Kim JV, Zuo Y, et al. 2005. ATP mediates rapid microglial response to local brain injury in vivo. *Nat Neurosci* 8:752-8
48. Davis BM, Salinas-Navarro M, Cordeiro MF, Moons L, De Groef L. 2017. Characterizing microglia activation: a spatial statistics approach to maximize information extraction. *Scientific Reports* 7:1576
49. Digiacomio G, Tusa I, Bacci M, Cipolleschi MG, Dello Sbarba P, Rovida E. 2017. Fibronectin induces macrophage migration through a SFK-FAK/CSF-1R pathway. *Cell Adh Migr* 11:327-37
50. DiSabato DJ, Quan N, Godbout JP. 2016. Neuroinflammation: the devil is in the details. *Journal of neurochemistry* 139 Suppl 2:136-53
51. Donat CK, Scott G, Gentleman SM, Sastre M. 2017. Microglial Activation in Traumatic Brain Injury. *Front Aging Neurosci* 9:208-
52. Dudiki T, Meller J, Mahajan G, Liu H, Zhevlakova I, et al. 2020. Microglia control vascular architecture via a TGF β 1 dependent paracrine mechanism linked to tissue mechanics. *Nature communications* 11:986-
53. Edwards KA, Pattinson CL, Guedes VA, Peyer J, Moore C, et al. 2020. Inflammatory Cytokines Associate With Neuroimaging After Acute Mild Traumatic Brain Injury. *Front Neurol* 11:348-
54. Ellis EF, McKinney JS, Willoughby KA, Liang S, Povlishock JT. 1995. A new model for rapid stretch-induced injury of cells in culture: characterization of the model using astrocytes. *J Neurotrauma* 12:325-39
55. Ellis EF, McKinney JS, Willoughby KA, Liang S, Povlishock JT. 1995. A new model for rapid stretch-induced injury of cells in culture: characterization of the model using astrocytes. *J Neurotrauma* 12:325-39
56. Erika A Matheis AJW, Meaghan Richardson, and Ann Mae DiLeonardi. 2020. Co-Cultures of Neurons and Astrocytes: Alterations to Morphology and Cell-Type Distribution. *CCDC Army Research Laboratory* 1:17
57. Faden AI, Demediuk P, Panter SS, Vink R. 1989. The role of excitatory amino acids and NMDA receptors in traumatic brain injury. *Science* 244:798-800
58. Faden AI, Wu J, Stoica BA, Loane DJ. 2016. Progressive inflammation-mediated neurodegeneration after traumatic brain or spinal cord injury. *British journal of pharmacology* 173:681-91
59. Fan Y, Chen Z, Pathak JL, Carneiro AMD, Chung CY. 2018. Differential Regulation of Adhesion and Phagocytosis of Resting and Activated Microglia by Dopamine. *Front Cell Neurosci* 12:309-
60. Feng Y, Cui C, Liu X, Wu Q, Hu F, et al. 2017. Protective Role of Apocynin via Suppression of Neuronal Autophagy and TLR4/NF- κ B Signaling Pathway in a Rat Model of Traumatic Brain Injury. *Neurochem Res* 42:3296-309
61. Fenn AM, Skendelas JP, Moussa DN, Muccigrosso MM, Popovich PG, et al. 2015. Methylene blue attenuates traumatic brain injury-associated neuroinflammation and acute depressive-like behavior in mice. *J Neurotrauma* 32:127-38
62. Fenn AM, Skendelas JP, Moussa DN, Muccigrosso MM, Popovich PG, et al. 2015. Methylene blue attenuates traumatic brain injury-associated neuroinflammation and acute depressive-like behavior in mice. *J Neurotrauma* 32:127-38

63. Franco-Bocanegra DK, McAuley C, Nicoll JAR, Boche D. 2019. Molecular Mechanisms of Microglial Motility: Changes in Ageing and Alzheimer's Disease. *Cells* 8:639
64. Föger P, Hefendehl JK, Veeraraghavalu K, Wendeln AC, Schlosser C, et al. 2017. Microglia turnover with aging and in an Alzheimer's model via long-term in vivo single-cell imaging. *Nat Neurosci* 20:1371-6
65. Gao T, Chen Z, Chen H, Yuan H, Wang Y, et al. 2018. Inhibition of HMGB1 mediates neuroprotection of traumatic brain injury by modulating the microglia/macrophage polarization. *Biochem Biophys Res Commun* 497:430-6
66. Ginhoux F, Garel S. 2018. The mysterious origins of microglia. *Nat Neurosci* 21:897-9
67. Gomez Perdiguero E, Klapproth K, Schulz C, Busch K, Azzoni E, et al. 2015. Tissue-resident macrophages originate from yolk-sac-derived erythro-myeloid progenitors. *Nature* 518:547-51
68. GRAEBER MB, BISE K, MEHRAEIN P. 1994. CR3/43, a marker for activated human microglia: application to diagnostic neuropathology. *Neuropathol Appl Neurobiol* 20:406-8
69. Grovola MR, Paleologos N, Brown DP, Tran N, Wofford KL, et al. Diverse changes in microglia morphology and axonal pathology during the course of 1 year after mild traumatic brain injury in pigs. *Brain Pathology* n/a:e12953
70. Günther M, Al Nimer F, Piehl F, Risling M, Mathiesen T. 2018. Susceptibility to Oxidative Stress Is Determined by Genetic Background in Neuronal Cell Cultures. *eNeuro* 5
71. Hagemeyer N, Hanft KM, Akriditou MA, Unger N, Park ES, et al. 2017. Microglia contribute to normal myelinogenesis and to oligodendrocyte progenitor maintenance during adulthood. *Acta Neuropathol* 134:441-58
72. Hailer NP, Jarhult JD, Nitsch R. 1996. Resting microglial cells in vitro: analysis of morphology and adhesion molecule expression in organotypic hippocampal slice cultures. *Glia* 18:319-31
73. Hashimoto D, Chow A, Noizat C, Teo P, Beasley MB, et al. 2013. Tissue-resident macrophages self-maintain locally throughout adult life with minimal contribution from circulating monocytes. *Immunity* 38:792-804
74. Heim JB, McDonald CA, Wyles SP, Sominidi-Damodaran S, Squirewell EJ, et al. 2018. FAK auto-phosphorylation site tyrosine 397 is required for development but dispensable for normal skin homeostasis. *PLoS One* 13:e0200558
75. Hemphill MA, Dabiri BE, Gabriele S, Kerscher L, Franck C, et al. 2011. A possible role for integrin signaling in diffuse axonal injury. *PLoS One* 6:e22899
76. Henry RJ, Doran SJ, Barrett JP, Meadows VE, Sabirzhanov B, et al. 2019. Inhibition of miR-155 Limits Neuroinflammation and Improves Functional Recovery After Experimental Traumatic Brain Injury in Mice. *Neurotherapeutics* 16:216-30
77. Henry RJ, Ritzel RM, Barrett JP, Doran SJ, Jiao Y, et al. 2020. Microglial Depletion with CSF1R Inhibitor During Chronic Phase of Experimental Traumatic Brain Injury Reduces Neurodegeneration and Neurological Deficits. *The Journal of Neuroscience* 40:2960-74

78. Henry RJ, Ritzel RM, Barrett JP, Doran SJ, Jiao Y, et al. 2020. Microglial Depletion with CSF1R Inhibitor During Chronic Phase of Experimental Traumatic Brain Injury Reduces Neurodegeneration and Neurological Deficits. *J Neurosci* 40:2960-74
79. Herzog C, Pons Garcia L, Keatinge M, Greenald D, Moritz C, et al. 2019. Rapid clearance of cellular debris by microglia limits secondary neuronal cell death after brain injury in vivo. *Development* 146
80. Hlavac N, VandeVord PJ. 2019. Astrocyte Mechano-Activation by High-Rate Overpressure Involves Alterations in Structural and Junctional Proteins. *Front Neurol* 10
81. Hood JD, Cheresch DA. 2002. Role of integrins in cell invasion and migration. *Nature Reviews Cancer* 2:91-100
82. Hornik TC, Vilalta A, Brown GC. 2016. Activated microglia cause reversible apoptosis of pheochromocytoma cells, inducing their cell death by phagocytosis. *Journal of Cell Science* 129:65-79
83. Hou L, Qu X, Qiu X, Huang R, Zhao X, Wang Q. 2020. Integrin CD11b mediates locus coeruleus noradrenergic neurodegeneration in a mouse Parkinson's disease model. *J Neuroinflammation* 17:148
84. Hsieh CL, Kim CC, Ryba BE, Niemi EC, Bando JK, et al. 2013. Traumatic brain injury induces macrophage subsets in the brain. *Eur J Immunol* 43:2010-22
85. Imai Y, Kohsaka S. 2002. Intracellular signaling in M-CSF-induced microglia activation: Role of Iba1. *Glia* 40:164-74
86. Izumi Y, Wakita S, Kanbara C, Nakai T, Akaike A, Kume T. 2017. Integrin $\alpha 5\beta 1$ expression on dopaminergic neurons is involved in dopaminergic neurite outgrowth on striatal neurons. *Scientific reports* 7:42111-
87. Izzy S, Liu Q, Fang Z, Lule S, Wu L, et al. 2019. Time-Dependent Changes in Microglia Transcriptional Networks Following Traumatic Brain Injury. *Front Cell Neurosci* 13
88. Izzy S, Liu Q, Fang Z, Lule S, Wu L, et al. 2019. Time-Dependent Changes in Microglia Transcriptional Networks Following Traumatic Brain Injury. *Front Cell Neurosci* 13:307-
89. Jayakumar AR, Rao KV, Panickar KS, Moriyama M, Reddy PV, Norenberg MD. 2008. Trauma-induced cell swelling in cultured astrocytes. *J Neuropathol Exp Neurol* 67:417-27
90. Ji J, Tyurina YY, Tang M, Feng W, Stolz DB, et al. 2012. Mitochondrial injury after mechanical stretch of cortical neurons in vitro: biomarkers of apoptosis and selective peroxidation of anionic phospholipids. *J Neurotrauma* 29:776-88
91. Jia J, Li C, Zhang T, Sun J, Peng S, et al. 2019. CeO₂@PAA-LXW7 Attenuates LPS-Induced Inflammation in BV2 Microglia. *Cellular and Molecular Neurobiology* 39:1125-37
92. Jin X, Ishii H, Bai Z, Itokazu T, Yamashita T. 2012. Temporal changes in cell marker expression and cellular infiltration in a controlled cortical impact model in adult male C57BL/6 mice. *PloS one* 7:e41892-e
93. Johnson VE, Stewart JE, Begbie FD, Trojanowski JQ, Smith DH, Stewart W. 2013. Inflammation and white matter degeneration persist for years after a single traumatic brain injury. *Brain* 136:28-42

94. Jones TR, Ruoslahti E, Schold SC, Bigner DD. 1982. Fibronectin and Glial Fibrillary Acidic Protein Expression in Normal Human Brain and Anaplastic Human Gliomas. *Cancer Research* 42:168-77
95. Kamm K, VanderKolk W, Lawrence C, Jonker M, Davis AT. 2006. The Effect of Traumatic Brain Injury Upon the Concentration and Expression of Interleukin-1 β and Interleukin-10 in the Rat. *Journal of Trauma and Acute Care Surgery* 60
96. Kao CQ, Goforth PB, Ellis EF, Satin LS. 2004. Potentiation of GABA(A) currents after mechanical injury of cortical neurons. *J Neurotrauma* 21:259-70
97. Katayama Y, Becker DP, Tamura T, Hovda DA. 1990. Massive increases in extracellular potassium and the indiscriminate release of glutamate following concussive brain injury. *J Neurosurg* 73:889-900
98. Keating CE, Cullen DK. 2021. Mechanosensation in traumatic brain injury. *Neurobiology of Disease* 148:105210
99. Kierdorf K, Erny D, Goldmann T, Sander V, Schulz C, et al. 2013. Microglia emerge from erythromyeloid precursors via Pu.1- and Irf8-dependent pathways. *Nat Neurosci* 16:273-80
100. Kloss CUA, Bohatschek M, Kreutzberg GW, Raivich G. 2001. Effect of Lipopolysaccharide on the Morphology and Integrin Immunoreactivity of Ramified Microglia in the Mouse Brain and in Cell Culture. *Experimental Neurology* 168:32-46
101. Kono R, Ikegaya Y, Koyama R. 2021. Phagocytic Glial Cells in Brain Homeostasis. *Cells* 10
102. Kourbeti IS, Vakis AF, Papadakis JA, Karabetsos DA, Bertias G, et al. 2012. Infections in traumatic brain injury patients. *Clinical Microbiology and Infection* 18:359-64
103. Kumar A, Alvarez-Croda D-M, Stoica BA, Faden AI, Loane DJ. 2016. Microglial/Macrophage Polarization Dynamics following Traumatic Brain Injury. *J Neurotrauma* 33:1732-50
104. Kumar A, Alvarez-Croda DM, Stoica BA, Faden AI, Loane DJ. 2016. Microglial/Macrophage Polarization Dynamics following Traumatic Brain Injury. *J Neurotrauma* 33:1732-50
105. Kumar A, Barrett JP, Alvarez-Croda D-M, Stoica BA, Faden AI, Loane DJ. 2016. NOX2 drives M1-like microglial/macrophage activation and neurodegeneration following experimental traumatic brain injury. *Brain, behavior, and immunity* 58:291-309
106. Kumar A, Henry RJ, Stoica BA, Loane DJ, Abulwerdi G, et al. 2019. Neutral Sphingomyelinase Inhibition Alleviates LPS-Induced Microglia Activation and Neuroinflammation after Experimental Traumatic Brain Injury. *J Pharmacol Exp Ther* 368:338-52
107. Kumar A, Stoica BA, Loane DJ, Yang M, Abulwerdi G, et al. 2017. Microglial-derived microparticles mediate neuroinflammation after traumatic brain injury. *J Neuroinflammation* 14:47-
108. Kumar A, Stoica BA, Sabirzhanov B, Burns MP, Faden AI, Loane DJ. 2013. Traumatic brain injury in aged animals increases lesion size and chronically alters microglial/macrophage classical and alternative activation states. *Neurobiology of aging* 34:1397-411

109. Kumar A, Stoica BA, Sabirzhanov B, Burns MP, Faden AI, Loane DJ. 2013. Traumatic brain injury in aged animals increases lesion size and chronically alters microglial/macrophage classical and alternative activation states. *Neurobiol Aging* 34:1397-411
110. Kuwar R, Rolfe A, Di L, Xu H, He L, et al. 2019. A novel small molecular NLRP3 inflammasome inhibitor alleviates neuroinflammatory response following traumatic brain injury. *J Neuroinflammation* 16:81
111. Lafrenaye AD, Fuss B. 2010. Focal adhesion kinase can play unique and opposing roles in regulating the morphology of differentiating oligodendrocytes. *J Neurochem* 115:269-82
112. Lafrenaye AD, Todani M, Walker SA, Povlishock JT. 2015. Microglia processes associate with diffusely injured axons following mild traumatic brain injury in the micro pig. *J Neuroinflammation* 12:186-
113. Levine J, Kwon E, Paez P, Yan W, Czerwiec G, et al. 2016. Traumatically injured astrocytes release a proteomic signature modulated by STAT3-dependent cell survival. *Glia* 64:668-94
114. Li Q, Barres BA. 2018. Microglia and macrophages in brain homeostasis and disease. *Nat Rev Immunol* 18:225-42
115. Li R, Maminishkis A, Zahn G, Vossmeier D, Miller SS. 2009. Integrin $\alpha 5 \beta 1$ Mediates Attachment, Migration, and Proliferation in Human Retinal Pigment Epithelium: Relevance for Proliferative Retinal Disease. *Investigative Ophthalmology & Visual Science* 50:5988-96
116. Lier J, Ondruschka B, Bechmann I, Dreßler J. 2020. Fast microglial activation after severe traumatic brain injuries. *Int J Legal Med* 134:2187-93
117. Liesi P, Kirkwood T, Vaheri A. 1986. Fibronectin is expressed by astrocytes cultured from embryonic and early postnatal rat brain. *Experimental Cell Research* 163:175-85
118. Lim J-E, Kou J, Song M, Pattanayak A, Jin J, et al. 2011. MyD88 deficiency ameliorates β -amyloidosis in an animal model of Alzheimer's disease. *Am J Pathol* 179:1095-103
119. Lim SH, Park E, You B, Jung Y, Park AR, et al. 2013. Neuronal synapse formation induced by microglia and interleukin 10. *PLoS One* 8:e81218
120. Ilić D, Furuta Y, Kanazawa S, Takeda N, Sobue K, et al. 1995. Reduced cell motility and enhanced focal adhesion contact formation in cells from FAK-deficient mice. *Nature* 377:539-44
121. Loane DJ, Kumar A. 2016. Microglia in the TBI brain: The good, the bad, and the dysregulated. *Experimental Neurology* 275:316-27
122. Loane DJ, Stoica BA, Byrnes KR, Jeong W, Faden AI. 2013. Activation of mGluR5 and inhibition of NADPH oxidase improves functional recovery after traumatic brain injury. *J Neurotrauma* 30:403-12
123. Loane DJ, Stoica BA, Byrnes KR, Jeong W, Faden AI. 2013. Activation of mGluR5 and inhibition of NADPH oxidase improves functional recovery after traumatic brain injury. *J Neurotrauma* 30:403-12
124. López-García I, Geró D, Szczesny B, Szoleczky P, Olah G, et al. 2018. Development of a stretch-induced neurotrauma model for medium-throughput

- screening in vitro: identification of rifampicin as a neuroprotectant. *Br J Pharmacol* 175:284-300
125. López-García I, Gerő D, Szczesny B, Szoleczky P, Olah G, et al. 2018. Development of a stretch-induced neurotrauma model for medium-throughput screening in vitro: identification of rifampicin as a neuroprotectant. *British Journal of Pharmacology* 175:284-300
126. Lu Y-B, Franze K, Seifert G, Steinhäuser C, Kirchhoff F, et al. 2006. Viscoelastic properties of individual glial cells and neurons in the CNS. *Proceedings of the National Academy of Sciences* 103:17759-64
127. Lucke-Wold BP, Logsdon AF, Turner RC, Huber JD, Rosen CL. 2017. Endoplasmic Reticulum Stress Modulation as a Target for Ameliorating Effects of Blast Induced Traumatic Brain Injury. *J Neurotrauma* 34:S62-s70
128. Maas AI, Stocchetti N, Bullock R. 2008. Moderate and severe traumatic brain injury in adults. *Lancet Neurol* 7:728-41
129. Mao H, Lu L, Bian K, Clausen F, Colgan N, Gilchrist M. 2018. Biomechanical analysis of fluid percussion model of brain injury. *Journal of Biomechanics* 77:228-32
130. McKinney JS, Willoughby KA, Liang S, Ellis EF. 1996. Stretch-induced injury of cultured neuronal, glial, and endothelial cells. Effect of polyethylene glycol-conjugated superoxide dismutase. *Stroke* 27:934-40
131. McNamara EH, Grillakis AA, Tucker LB, McCabe JT. 2020. The closed-head impact model of engineered rotational acceleration (CHIMERA) as an application for traumatic brain injury pre-clinical research: A status report. *Experimental Neurology* 333:113409
132. McWhorter FY, Wang T, Nguyen P, Chung T, Liu WF. 2013. Modulation of macrophage phenotype by cell shape. *Proc Natl Acad Sci U S A* 110:17253-8
133. Meaney D, Olvey S, Gennarelli T. 2011. Biomechanical basis of traumatic brain injury. *Youmans & Winn Neurological Surgery* 4:2755-64
134. Meller J, Chen Z, Dudiki T, Cull RM, Murtazina R, et al. 2017. Integrin-Kindlin3 requirements for microglial motility in vivo are distinct from those for macrophages. *JCI Insight* 2:e93002
135. Meng XN, Jin Y, Yu Y, Bai J, Liu GY, et al. 2009. Characterisation of fibronectin-mediated FAK signalling pathways in lung cancer cell migration and invasion. *Br J Cancer* 101:327-34
136. Miller WJ, Leventhal I, Scarsella D, Haydon PG, Janmey P, Meaney DF. 2009. Mechanically induced reactive gliosis causes ATP-mediated alterations in astrocyte stiffness. *J Neurotrauma* 26:789-97
137. Milner R. 2009. Microglial expression of alphavbeta3 and alphavbeta5 integrins is regulated by cytokines and the extracellular matrix: beta5 integrin null microglia show no defects in adhesion or MMP-9 expression on vitronectin. *Glia* 57:714-23
138. Milner R, Campbell IL. 2002. The integrin family of cell adhesion molecules has multiple functions within the CNS. *J Neurosci Res* 69:286-91
139. Milner R, Campbell IL. 2003. The Extracellular Matrix and Cytokines Regulate Microglial Integrin Expression and Activation. *The Journal of Immunology* 170:3850-8

140. Milner R, Crocker SJ, Hung S, Wang X, Frausto RF, del Zoppo GJ. 2007. Fibronectin- and vitronectin-induced microglial activation and matrix metalloproteinase-9 expression is mediated by integrins $\alpha_5\beta_1$ and $\alpha_v\beta_5$. *J Immunol* 178:8158-67
141. Milner R, Crocker SJ, Hung S, Wang X, Frausto RF, del Zoppo GJ. 2007. Fibronectin- and Vitronectin-Induced Microglial Activation and Matrix Metalloproteinase-9 Expression Is Mediated by Integrins $\alpha_5\beta_1$ and $\alpha_v\beta_5$. *The Journal of Immunology* 178:8158-67
142. Mitra SK, Hanson DA, Schlaepfer DD. 2005. Focal adhesion kinase: in command and control of cell motility. *Nature Reviews Molecular Cell Biology* 6:56-68
143. Moore SW, Roca-Cusachs P, Sheetz MP. 2010. Stretchy Proteins on Stretchy Substrates: The Important Elements of Integrin-Mediated Rigidity Sensing. *Developmental Cell* 19:194-206
144. Moreno-Layseca P, Streuli CH. 2014. Signalling pathways linking integrins with cell cycle progression. *Matrix Biology* 34:144-53
145. Morganti JM, Riparip L-K, Rosi S. 2016. Call Off the Dog(ma): M1/M2 Polarization Is Concurrent following Traumatic Brain Injury. *PLOS ONE* 11:e0148001
146. Muhamed I, Chowdhury F, Maruthamuthu V. 2017. Biophysical Tools to Study Cellular Mechanotransduction. *Bioengineering (Basel)* 4:12
147. Murphy JM, Jeong K, Rodriguez YAR, Kim J-H, Ahn E-YE, Lim S-TS. 2019. FAK and Pyk2 activity promote TNF- α and IL-1 β -mediated pro-inflammatory gene expression and vascular inflammation. *Scientific Reports* 9:7617
148. Nagano M, Hoshino D, Koshikawa N, Akizawa T, Seiki M. 2012. Turnover of Focal Adhesions and Cancer Cell Migration. *International Journal of Cell Biology* 2012:310616
149. Namjoshi DR, Cheng WH, Bashir A, Wilkinson A, Stukas S, et al. 2017. Defining the biomechanical and biological threshold of murine mild traumatic brain injury using CHIMERA (Closed Head Impact Model of Engineered Rotational Acceleration). *Experimental Neurology* 292:80-91
150. Nasr IW, Chun Y, Kannan S. 2019. Neuroimmune responses in the developing brain following traumatic brain injury. *Experimental Neurology* 320:112957
151. Nguyen PT, Dorman LC, Pan S, Vainchtein ID, Han RT, et al. 2020. Microglial Remodeling of the Extracellular Matrix Promotes Synapse Plasticity. *Cell* 182:388-403.e15
152. Ohsawa K, Imai Y, Kanazawa H, Sasaki Y, Kohsaka S. 2000. Involvement of Iba1 in membrane ruffling and phagocytosis of macrophages/microglia. *Journal of Cell Science* 113:3073-84
153. Ohsawa K, Imai Y, Sasaki Y, Kohsaka S. 2004. Microglia/macrophage-specific protein Iba1 binds to fimbrin and enhances its actin-bundling activity. *J Neurochem* 88:844-56
154. Ommaya A, Goldsmith W, Thibault L. 2002. Biomechanics and neuropathology of adult and paediatric head injury. *British journal of neurosurgery* 16:220-42

155. Ozgun A, Erkok-Biradlı FZ, Bulut O, Garipcan B. 2021. Substrate stiffness effects on SH-SY5Y: The dichotomy of morphology and neuronal behavior. *J Biomed Mater Res B Appl Biomater* 109:92-101
156. Parkhurst CN, Yang G, Ninan I, Savas JN, Yates JR, 3rd, et al. 2013. Microglia promote learning-dependent synapse formation through brain-derived neurotrophic factor. *Cell* 155:1596-609
157. Parsons JT, Martin KH, Slack JK, Taylor JM, Weed SA. 2000. Focal adhesion kinase: a regulator of focal adhesion dynamics and cell movement. *Oncogene* 19:5606-13
158. Perry VH, Nicoll JA, Holmes C. 2010. Microglia in neurodegenerative disease. *Nat Rev Neurol* 6:193-201
159. Qu WS, Liu JL, Li CY, Li X, Xie MJ, et al. 2015. Rapidly activated epidermal growth factor receptor mediates lipopolysaccharide-triggered migration of microglia. *Neurochem Int* 90:85-92
160. Ramlackhansingh AF, Brooks DJ, Greenwood RJ, Bose SK, Turkheimer FE, et al. 2011. Inflammation after trauma: microglial activation and traumatic brain injury. *Ann Neurol* 70:374-83
161. Rigracciolo DC, Santolla MF, Lappano R, Vivacqua A, Cirillo F, et al. 2019. Focal adhesion kinase (FAK) activation by estrogens involves GPER in triple-negative breast cancer cells. *Journal of Experimental & Clinical Cancer Research* 38:58
162. Rong Z, Cheng B, Zhong L, Ye X, Li X, et al. 2020. Activation of FAK/Rac1/Cdc42-GTPase signaling ameliorates impaired microglial migration response to A β 42 in triggering receptor expressed on myeloid cells 2 loss-of-function murine models. *The FASEB Journal* 34:10984-97
163. Rong Z, Cheng B, Zhong L, Ye X, Li X, et al. 2020. Activation of FAK/Rac1/Cdc42-GTPase signaling ameliorates impaired microglial migration response to A β (42) in triggering receptor expressed on myeloid cells 2 loss-of-function murine models. *Faseb j* 34:10984-97
164. Russo MV, McGavern DB. 2015. Immune Surveillance of the CNS following Infection and Injury. *Trends Immunol* 36:637-50
165. Rzigalinski BA, Weber JT, Willoughby KA, Ellis EF. 1998. Intracellular free calcium dynamics in stretch-injured astrocytes. *J Neurochem* 70:2377-85
166. Rzigalinski BA WJ, Willoughby KA, Liang S, Woodward JJ, Ellis EF. 1998. Glutamate release and enhanced receptor sensitivity in stretch-injured neurons. *J Neurotrauma* 15:894
167. Sabet AA, Christoforou E, Zatlın B, Genin GM, Bayly PV. 2008. Deformation of the human brain induced by mild angular head acceleration. *Journal of Biomechanics* 41:307-15
168. Salvador E, Burek M, Förster CY. 2015. Stretch and/or oxygen glucose deprivation (OGD) in an in vitro traumatic brain injury (TBI) model induces calcium alteration and inflammatory cascade. *Front Cell Neurosci* 9:323-
169. Salvador E, Neuhaus W, Foerster C. 2013. Stretch in brain microvascular endothelial cells (cEND) as an in vitro traumatic brain injury model of the blood brain barrier. *J Vis Exp*:e50928-e

170. Santos AR, Corredor RG, Obeso BA, Trakhtenberg EF, Wang Y, et al. 2012. β 1 integrin-focal adhesion kinase (FAK) signaling modulates retinal ganglion cell (RGC) survival. *PLoS One* 7:e48332
171. Sauaia A, Moore FA, Moore EE, Moser KS, Brennan R, et al. 1995. Epidemiology of Trauma Deaths: A Reassessment. *Journal of Trauma and Acute Care Surgery* 38
172. Saykally JN, Hatic H, Keeley KL, Jain SC, Ravindranath V, Citron BA. 2017. Withania somnifera Extract Protects Model Neurons from In Vitro Traumatic Injury. *Cell Transplant* 26:1193-201
173. Schafer DP, Heller CT, Gunner G, Heller M, Gordon C, et al. 2016. Microglia contribute to circuit defects in Mecp2 null mice independent of microglia-specific loss of Mecp2 expression. *Elife* 5
174. Schimmel SJ, Acosta S, Lozano D. 2017. Neuroinflammation in traumatic brain injury: A chronic response to an acute injury. *Brain Circ* 3:135-42
175. Scott G, Hellyer PJ, Ramlackhansingh AF, Brooks DJ, Matthews PM, Sharp DJ. 2015. Thalamic inflammation after brain trauma is associated with thalamo-cortical white matter damage. *J Neuroinflammation* 12:224-
176. Sevenich L. 2018. Brain-Resident Microglia and Blood-Borne Macrophages Orchestrate Central Nervous System Inflammation in Neurodegenerative Disorders and Brain Cancer. *Front Immunol* 9:697-
177. Shaughness M, Byrnes K. 2021. Assessment of the Effects of Stretch-Injury on Primary Rat Microglia. *Mol Neurobiol*
178. Shin N, Kim HG, Shin HJ, Kim S, Kwon HH, et al. 2019. Uncoupled Endothelial Nitric Oxide Synthase Enhances p-Tau in Chronic Traumatic Encephalopathy Mouse Model. *Antioxid Redox Signal* 30:1601-20
179. Sieg DJ, Hauck CR, Schlaepfer DD. 1999. Required role of focal adhesion kinase (FAK) for integrin-stimulated cell migration. *J Cell Sci* 112 (Pt 16):2677-91
180. Singer AJ, Clark RAF. 1999. Cutaneous Wound Healing. *New England Journal of Medicine* 341:738-46
181. Slepko N, Levi G. 1996. Progressive activation of adult microglial cells in vitro. *Glia* 16:241-6
182. Smolders SM, Swinnen N, Kessels S, Arnauts K, Smolders S, et al. 2017. Age-specific function of α 5 β 1 integrin in microglial migration during early colonization of the developing mouse cortex. *Glia* 65:1072-88
183. Stein M, Keshav S, Harris N, Gordon S. 1992. Interleukin 4 potently enhances murine macrophage mannose receptor activity: a marker of alternative immunologic macrophage activation. *J Exp Med* 176:287-92
184. Stern MB. 1991. Head trauma as a risk factor for Parkinson's disease. *Movement Disorders* 6:95-7
185. Stopper L, Bălșeanu TA, Cătălin B, Rogoveanu OC, Mogoantă L, Scheller A. 2018. Microglia morphology in the physiological and diseased brain - from fixed tissue to in vivo conditions. *Rom J Morphol Embryol* 59:7-12
186. Strohmeyer N, Bharadwaj M, Costell M, Fässler R, Müller DJ. 2017. Fibronectin-bound α 5 β 1 integrins sense load and signal to reinforce adhesion in less than a second. *Nat Mater* 16:1262-70

187. Stupack DG, Cheresh DA. 2002. Get a ligand, get a life: integrins, signaling and cell survival. *J Cell Sci* 115:3729-38
188. Tamashiro TT, Dalgard CL, Byrnes KR. 2012. Primary microglia isolation from mixed glial cell cultures of neonatal rat brain tissue. *J Vis Exp*:e3814-e
189. Tan HP, Guo Q, Hua G, Chen JX, Liang JC. 2018. Inhibition of endoplasmic reticulum stress alleviates secondary injury after traumatic brain injury. *Neural Regen Res* 13:827-36
190. Tate CC, García AJ, LaPlaca MC. 2007. Plasma fibronectin is neuroprotective following traumatic brain injury. *Experimental Neurology* 207:13-22
191. Tavalin SJ, Ellis EF, Satin LS. 1995. Mechanical perturbation of cultured cortical neurons reveals a stretch-induced delayed depolarization. *J Neurophysiol* 74:2767-73
192. Tchanchou F, Zhang Y. 2013. Selective inhibition of alpha/beta-hydrolase domain 6 attenuates neurodegeneration, alleviates blood brain barrier breakdown, and improves functional recovery in a mouse model of traumatic brain injury. *J Neurotrauma* 30:565-79
193. Turtzo LC, Lescher J, Janes L, Dean DD, Budde MD, Frank JA. 2014. Macrophagic and microglial responses after focal traumatic brain injury in the female rat. *J Neuroinflammation* 11:82-
194. Vaccaro M, Irrera N, Cutroneo G, Rizzo G, Vaccaro F, et al. 2017. Differential Expression of Nitric Oxide Synthase Isoforms nNOS and iNOS in Patients with Non-Segmental Generalized Vitiligo. *Int J Mol Sci* 18:2533
195. Vainchtein ID, Molofsky AV. 2020. Astrocytes and Microglia: In Sickness and in Health. *Trends Neurosci* 43:144-54
196. Villalba N, Sackheim AM, Nunez IA, Hill-Eubanks DC, Nelson MT, et al. 2017. Traumatic Brain Injury Causes Endothelial Dysfunction in the Systemic Microcirculation through Arginase-1-Dependent Uncoupling of Endothelial Nitric Oxide Synthase. *J Neurotrauma* 34:192-203
197. Villapol S, Loane DJ, Burns MP. 2017. Sexual dimorphism in the inflammatory response to traumatic brain injury. *Glia* 65:1423-38
198. Waltzman D, Haarbauer-Krupa J, Daugherty J, Thomas K, Sarmiento K. 2020. State-Level Numbers and Rates of Traumatic Brain Injury-Related Emergency Department Visits, Hospitalizations, and Deaths by Sex, 2014. *The Journal of Head Trauma Rehabilitation* 35
199. Wang G, Zhang J, Hu X, Zhang L, Mao L, et al. 2013. Microglia/macrophage polarization dynamics in white matter after traumatic brain injury. *J Cereb Blood Flow Metab* 33:1864-74
200. Wang Q, More SK, Vomhof-DeKrey EE, Golovko MY, Basson MD. 2019. Small molecule FAK activator promotes human intestinal epithelial monolayer wound closure and mouse ulcer healing. *Scientific Reports* 9:14669
201. Wanner IB. 2012. An in vitro trauma model to study rodent and human astrocyte reactivity. *Methods Mol Biol* 814:189-219
202. Webb DJ, Donais K, Whitmore LA, Thomas SM, Turner CE, et al. 2004. FAK–Src signalling through paxillin, ERK and MLCK regulates adhesion disassembly. *Nature Cell Biology* 6:154-61

203. Weber JT, Rzigalinski BA, Willoughby KA, Moore SF, Ellis EF. 1999. Alterations in calcium-mediated signal transduction after traumatic injury of cortical neurons. *Cell Calcium* 26:289-99
204. Werner C, Engelhard K. 2007. Pathophysiology of traumatic brain injury. *Br J Anaesth* 99:4-9
205. Willoughby KA, Kleindienst A, Müller C, Chen T, Muir JK, Ellis EF. 2004. S100B protein is released by in vitro trauma and reduces delayed neuronal injury. *J Neurochem* 91:1284-91
206. Wlodarczyk A, Holtman IR, Krueger M, Yogev N, Bruttger J, et al. 2017. A novel microglial subset plays a key role in myelinogenesis in developing brain. *Embo j* 36:3292-308
207. Xu Z, Liu Y, Yang D, Yuan F, Ding J, et al. 2017. Sesamin protects SH-SY5Y cells against mechanical stretch injury and promoting cell survival. *BMC Neurosci* 18:57-
208. Yao Y, Xu X-H, Jin L. 2019. Macrophage Polarization in Physiological and Pathological Pregnancy. *Front Immunol* 10
209. Yauger YJ, Bermudez S, Moritz KE, Glaser E, Stoica B, Byrnes KR. 2019. Iron accentuated reactive oxygen species release by NADPH oxidase in activated microglia contributes to oxidative stress in vitro. *J Neuroinflammation* 16:41
210. Yi S, Jiang X, Tang X, Li Y, Xiao C, et al. 2020. IL-4 and IL-10 promotes phagocytic activity of microglia by up-regulation of TREM2. *Cytotechnology*
211. Yin J, Valin KL, Dixon ML, Leavenworth JW. 2017. The Role of Microglia and Macrophages in CNS Homeostasis, Autoimmunity, and Cancer. *Journal of Immunology Research* 2017:5150678
212. Yu H, Gao M, Ma Y, Wang L, Shen Y, Liu X. 2018. Inhibition of cell migration by focal adhesion kinase: Time-dependent difference in integrin-induced signaling between endothelial and hepatoblastoma cells. *Int J Mol Med* 41:2573-88
213. Yu J, Zhang Y, Ma H, Zeng R, Liu R, et al. 2020. Epitranscriptomic profiling of N6-methyladenosine-related RNA methylation in rat cerebral cortex following traumatic brain injury. *Mol Brain* 13:11
214. Zaidel-Bar R, Cohen M, Addadi L, Geiger B. 2004. Hierarchical assembly of cell-matrix adhesion complexes. *Biochem Soc Trans* 32:416-20
215. Zhu L, Su Q, Jie X, Liu A, Wang H, et al. 2016. NG2 expression in microglial cells affects the expression of neurotrophic and proinflammatory factors by regulating FAK phosphorylation. *Scientific Reports* 6:27983
216. Zhu NW, Perks CM, Burd AR, Holly JM. 1999. Changes in the levels of integrin and focal adhesion kinase (FAK) in human melanoma cells following 532 nm laser treatment. *Int J Cancer* 82:353-8
217. Ziaja M, Pyka J, Machowska A, Maslanka A, Plonka PM. 2007. Nitric oxide spin-trapping and NADPH-diaphorase activity in mature rat brain after injury. *J Neurotrauma* 24:1845-54